UNIVERSITÀ DEGLI STUDI DI SALERNO

DIPARTIMENTO DI CHIMICA E BIOLOGIA
"ADOLFO ZAMBELLI"
DOTTORATO DI RICERCA IN CHIMICA

XIV CICLO (Nuova serie)

# *FLUORESCENCE-BASED SENSORS FOR THE DETECTION OF BIOLOGICALLY AND ENVIRONMENTALLY RELEVANT MOLECULES*

***Silvia Mirra***

TUTOR
*Prof. Claudio Pellecchia*

CO-TUTORS
*Dott.ssa Mina Mazzeo*
*Prof. Gerard Canters*

COORDINATORE
*Prof. Gaetano Guerra*

2013-2016

*Ai miei genitori.*

# Table of Contents

## List of abbreviations

| | |
|---|---|
| d | duplet |
| dfgH | diphenhylglyoxime anion |
| DFT | Density Functional Theory |
| dmgH | dimethylglyoxime anion |
| ESI-MS | Electrospray Ionization Mass Spectrometry |
| Et | Ethyl |
| FRET | Förster Resonance Energy Transfer |
| GSH | Glutathione |
| HEPES | 4-(2-hydroxyethyl)-1-piperazineethanesulfonic acid |
| KPi | Potassium Phosphate |
| L-Cys | L-Cysteine |
| LMCT | Ligand-to-Metal Charge Transfer |
| m | multiplet |
| mins. | Minutes |
| Mt-S | Metal-sulfide |
| o.d. | outside diameter |
| PET | Photoinduced Electron Transfer |
| Ph | Phenyl |
| PPIX | Protoporphyrin IX |
| Py | Pyridine, pyrene |
| q | Quartet |
| rt. | Room temperature |
| s | Singlet |
| SR | Switching Ratio |
| t | Triplet |

| | |
|---|---|
| TLC | Thin-Layer Chromatography |
| TRIS | Tris(hydroxymethyl)aminomethane |
| UV | Ultraviolet |

# Chapter 1: Introduction

Hydrogen sulfide ($H_2S$) is a colorless and flammable gas with a characteristic odor of rotten eggs. Ambient air $H_2S$ comes from two different sources. Natural sources include bacteria, decomposition of organic matters, volcanic gases, natural gas and undersea vents. Industrial sources are petroleum refinery, rayon manufacturing, paper and pulp mill industry.[1] Its danger for human body is because of its reducibility and high lipid solubility even at low levels. It is usually regarded as both an environmental and industrial pollutant.

## 1.1 Physiological Implications

Exposure to this gas can trigger eye and respiratory tract irritation, whereas inhalation of excess of $H_2S$ can result in loss of consciousness, respiratory failure, cardiac arrest, and, in extreme cases, death.[2] Therefore, for centuries, hydrogen sulfide ($H_2S$) has been viewed primarily as a noxious chemical species.[3] More recent studies have broadened its traditional view as a noxious chemical species and patently established $H_2S$ as an essential physiological mediator and cellular signalling species.[4] It acts as the third endogenously generated gaseous signaling compound with

[1] E. T. Kato Jr., C. M. P. Yoshida, A. B. Reis, I. S. Melo, T. T. Franco, *Polym. Int.* **2011**, *60*, 951.

[2] J. R. Reiffenstein, W. C. Hulbert, S. H. Roth, *Annu. Rev. Pharmacol. Toxicol.* **1992**, *32*, 109.

[3] (*a*) V. S. Lin, C. J. Chang, *Curr. Opin. Chem. Biol.* **2012**, *16*, 595; (b) R. P. Smith, *Can. Med. Assoc. J.* **1978**, *118*, 775; (*c*) R. P. Smith, *Am. Sci*. **2010**, *98*, 6.

[4] (*a*) L. Li, P. K. Moore, *Trends Pharmacol. Sci.* **2008**, *29*, 84; (*b*) L. Li, P. K. Moore, *Biochem. Soc. Trans.* **2007**, *35*, 1138; (*c*) *R.* Wang, *Physiol. Rev.* **2012**, *92*, 791.

cytoprotective properties; the other two are the well-known gasotransmitters NO and CO. In mammalian systems, $H_2S$ is produced from cysteine and homocysteine by the enzymes cystathionine beta-synthase (CBS), cystathionine gamma-lyase (CSE) and 3-mercaptopyruvate sulfurtransferase (CAT/MST) (**Figure 1.1a**).[5]

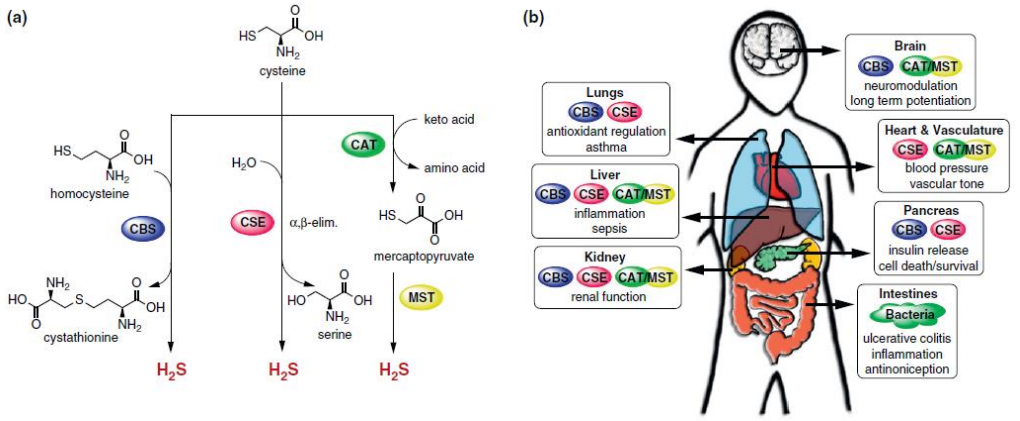


**Figure 1.1.** Biology of $H_2S$ in the human body. **(a)** Major biochemical pathways for $H_2S$ production. Cystathionine β-synthase (CBS) and cystathionine γ-lyase (CSE), are hemeproteins found in the cytoplasm and synthesize $H_2S$. CBS primarily catalyzes the formation of cystathionine from homocysteine and cysteine, whereas CSE facilitates the α,β-elimination of cysteine by water, producing serine and $H_2S$. Cysteine aminotransferase (CAT) and mercaptopyruvate sulfur transferase (MST), enzymes localized in the cytoplasm and mitochondria have also been identified as sources of $H_2S$. CAT acts upon keto acids and cysteine to yield mercaptopyruvate, from which $H_2S$ is released by MST. **(b)** Selected physiological effects and biological roles of $H_2S$ in the human body and enzymes responsible for $H_2S$ production in various tissue types.

CBS is mostly found in the brain, nervous system, and liver, while CSE is predominantly found in the vasculature and liver and MST can be found in the brain and vasculature. However, all these enzymes are distribuited across many tissues and are often jointly

[5] C. Q. Chen, H. Xin, Y. Z. Zhu, *Acta Pharmacol. Sin.* **2007**, *28*, 1709.

present (**Figure 1.1b**). Apart from enzymatic synthesis pathways, endogenous production of $H_2S$ can also occur through other non-enzymatic processes that are less well understood. Non-enzymatic production of $H_2S$ occurs through glucose,[6] glutathione, inorganic polysulfides (present in garlic)[7] and elemental sulfur. $H_2S$ is engaged in a number of physiological and pathological processes, such as cardiovascular protection, hypertension, relaxation, proliferation, apoptosis and inflammation processes. Previous reports have shown that cystathionine β-synthase gene, is overexpressed in Down's syndrome.[8] Inadequate levels of $H_2S$ are connected with Alzheimer's disease and impaired cognitive ability; excessive $H_2S$ production may be responsible for the pathogenesis of other diseases such as diabetes. These preliminary studies have clearly established $H_2S$ as an essential physiological mediator and cellular signaling species,[9] but our understanding of $H_2S$ chemistry and its far-ranging contributions to physiology and pathology is still mostly unknown.[10] The complex biological roles of $H_2S$ and potential therapeutic implications constitute a challenging motivation for devising new ways to monitor its production, trafficking, and consumption in living systems.

[6] D. G. Searcy, S. H. Lee, *j. Exp. Zool.* **1998**, *282*, 310.
[7] A. J. Cooper, *Annu. Rev. Biochem.* **1983**, *52*, 187.
[8] P. Kamoun, M. C. Belardinelli, A. Chabli, K. Lallouchi, B. Chadefaux-Vekemans, *Am. J. Med. Genet. A.* **2003**, *116A*, 310.
[9] Li L., Rose P., Moore P. K., *Annu. Rev. Pharmacol. Toxicol.* **2011**, *51*, 169.
[10] J. Liu, Y. Q. Sun, J. Zhang, T. Yang, J. Cao, L. Zhang, W. Guo, *Chemistry* **2013**, *19*, 4717.

## 1.2 Conventional Methods for $H_2S$ Detection

The determination of the physiological concentrations of $H_2S$ in specific tissue and in circulation is of crucial importance for determining the impact of $H_2S$ on a given physiological function. This allows us to correlate $H_2S$ levels with specific pathophysiological alterations, to examine physiological roles of $H_2S$ under *in vitro* conditions at organ, tissue, and cellular levels and to guide pharmacological and therapeutic administrations of $H_2S$ donors. Conflicting data exist on the $H_2S$ concentration in the tissues and blood of healthy subjects, with values ranging from 10-300 μM at values of two orders of magnitude lower. This discrepancy of data seems to be linked to the different methods used, with formation of numerous artifacts due to instability of the sulphides, the high volatility and the great susceptibility to oxidation of $H_2S$. In addition, many papers do not distinguish between free $H_2S$ and sulphides acid-labile and no acid-labile sulfides. With the p$K_{a1}$ ~ 7.0 and the p$K_{a2}$ > 17, there is essentially no $S^{2-}$ in biological tissues, almost the same amounts of $H_2S$ and $HS^-$ within the cell, and approximately a 20% $H_2S$ and 80% $HS^-$ in extracellular fluid and plasma at 37 °C and pH 7.4.[11]

Current literature reports several measurement techniques for $H_2S$ such as spectrophotometry,[12] chromatography,[13] and electrochemical

[11] A. H. Nielsen, J. Vollertsen, T. Hvitved-Jacobsen, *Water Environ. Res.* **2006**, *78*, 275.

[12] (*a*) E. A. Guenther, K. S. Johnson, K. H. Coale, *Anal. Chem.* **2001**, *73*, 3481; (*b*) E. Fisher, *Chem. Ber.* **1883**, *16*, 2234; (*c*) J.K. Fogo, M. Popowsky, *Anal. Chem.* **1949**, *21*, 732.

techniques[14] that detect forms of sulfide from different non-biological and biological sources like sewage, marine water, urine, feces, blood, serum, tissue and breath.[15] These methods generally require cell lysis or destructive tissue preparation and yield a wide range of measured values for biological $H_2S$ concentrations. Although these techniques can garner useful information from biological samples, the real-time visualization of $H_2S$ in living intact specimens remains a significant challenge (**Table 1.1**).[16]

| Measurement method | Advantages | Disadvantages |
|---|---|---|
| Spectrophotometry | • Widely used<br>• Less expensive | • Long experimental time (1.5 days)<br>• Bulky sample<br>• Invasive<br>• *In-vitro* |
| Chromatography | • Accurate detection<br>• Separates $H_2S$ from mixtures of chemical substances | • Expensive for the first setup<br>• Bulky sample<br>• Invasive<br>• *In-vitro* |
| Sulfide ion-specific electrode | • Low cost for initial setup<br>• Popular in serum/plasma measurement | • Needs to be calibrated before every measurement<br>• Calibration procedure is complicated<br>• Large amount of sample<br>• Desulfurization of the samples<br>• *In- vitro* |

**Table 1.1.** Comparison of the current methods for $H_2S$ measurement.

[13] (*a*) J. Furne, A. Saeed, M. D. Levitt, *Am. J. Physiol. Regul. Integr. Comp. Physiol.* **2008**, *295*, R1479; (*b*) A. Tangerman, *J. Chromatogr.* **2009**, *B 877*, 3366.
[14] N. S. Lawrence, J. Davis, R. G. Compton, *Talanta* **2000**, *52*, 771.
[15] T. Ubuka, T. Abe, R. Kajikawa, K. Morino, *J. Chromatogr. B. Biomed. Sci. Appl.* **2001**, *757*, 31.
[16] T. Ubuka, *Journal of Chromatography* **2002**, *B 781*, 227.

## 1.3 Fluorescent Molecular Probes

Recently, fluorescence-based systems for $H_2S$ detection have been proposed as selective probes for biological applications.[17] Reaction-based fluorescent probes offer the potential for sensitivity, selectivity, ease to application, biological compatibility and high signal-to-noise ratio, all of which enable the real-time visualization of $H_2S$ in living, intact specimens. As such, fluorescent molecular probes provide an attractive approach for the detection of $H_2S$ because of their molecular biocompatibility, cell permeability and high sensitivity. This reaction-based probes react chemoselectively with hydrogen sulfide to put in place a signal-producing molecular transformation. Reactions with $H_2S$ switch a probe from a non-fluorescent to a highly fluorescent molecule and this provide a sensitive optical signal (**Figure 1.2**), allowing visualization of biological molecules in real time using fluorescence microscopy.

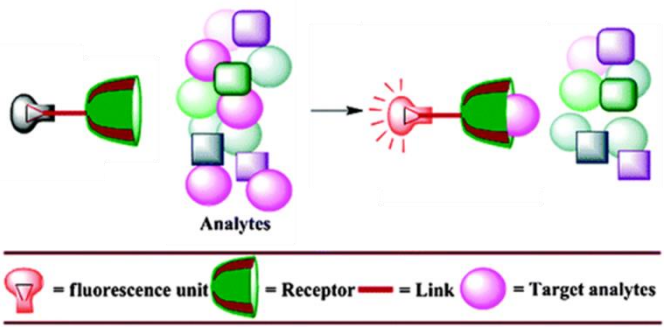


**Figura 1.2.** Schematic representation of fluorescent sensor.

[17] (*a*) T. Chen, Y. Zheng, Z. Xu, M. Zhao, Y. Xu, J. Cui, *Tetrahedron Lett.* **2013**, *54*, 2980; (*b*) M. Tropiano, S. Faulkner, *Chem. Commun.* **2014**, *50*, 4696; (*c*) I. Takashima, M. Kinoshita, R. Kawagoe, S. Nakagawa, M. Sugimoto, I. Hamachi, A. Ojida, *Chemistry* **2014**, *20*, 2184.

Existing fluorescence-based probes implemented so far have been subdivided into four different categories (depending on the reaction mechanism by which analyte recognition occurs): (i) azide-to-amine reduction;[18] (ii) nucleophilic addition;[19] (iii) copper displacement;[20] and (iv) nitro-to-amine reduction[21] (**Figure 1.3**). All the sensors belonging to the above categories make use of organic molecules that change their fluorescence intensity when interacting with $H_2S$. $H_2S$ is an effective reducing and displays enhanced nucleophilicity compared to other thiols, likely due to its small size and lower $pK_a$. Sensors belonging to category (iii) constitute an exception since in this case the molecule acting as the recognition element is a metal complex. Here, recognition builds on the displacement of the metal from the fluorophore's environment to generally produce fluorescence turn-on changes via $H_2S$ mediated precipitation of Mt–S.[22] Despite all the advantages of the above mentioned probes (e.g. high selectivity and sensitivity), some shortcomings typically involve slow response, irreversibility and poor water solubility.

---

[18] (*a*) K. Zheng, W. Lin, L. Tan, *Org. Biomol. Chem.* **2012**, *10*, 9683; (*b*) Z. Wu, Z. Li, L. Yang, J. Han, S. Han, *Chem. Commun.* **2012**, *48*, 10120.

[19] (*a*) C. Liu, B. Peng, S. Li, C. M. Park, A. R. Whorton, M. Xian, *Org. Lett.* **2012**, *14*, 2184; (*b*) Y. Zhao, X. Zhu, H. Kan, W. Wang, B. Zhu, B. Du, X. Zhang, *Analyst* **2012**, *137*, 5576.

[20] (*a*) F. Hou, L. Huang, P. Xi, J. Cheng, X. Zhao, G. Xie, Y. Shi, F. Cheng, X. Yao, D. Bai, Z. Zeng, *Inorg. Chem.* **2012**, *51*, 2454; (*b*) M. Q. Wang, K. Li, J. T. Hou, M. Y. Wu, Z. Huang, X. Q. Yu, *J. Org. Chem.* **2012**, *77*, 8350.

[21] (*a*) M. Y. Wu, K. Li, J. T. Hou, Z. Huang, X. Q. Yu, *Org. Biomol. Chem.* **2012**, *10*, 8342; (*b*) W. Xuan, R. Pan, Y. Cao, K. Liu, W. Wang, *Chem. Commun.* **2012**, *48*, 10669.

[22] (*a*) L. E. Santos-Figueroa, C. de la Torre, S. El Sayed, F. Sancenon, R. Martinez-Manez, A. M. Costero, S. Gil, M. Parra, *Eur. J. Inorg. Chem.* **2014**, 41–45; (*b*) Z. Ye, X. An, B. Song, W. Zhang, Z. Dai, J. Yuan, *Dalton Trans.* **2014**, *43*, 13055.

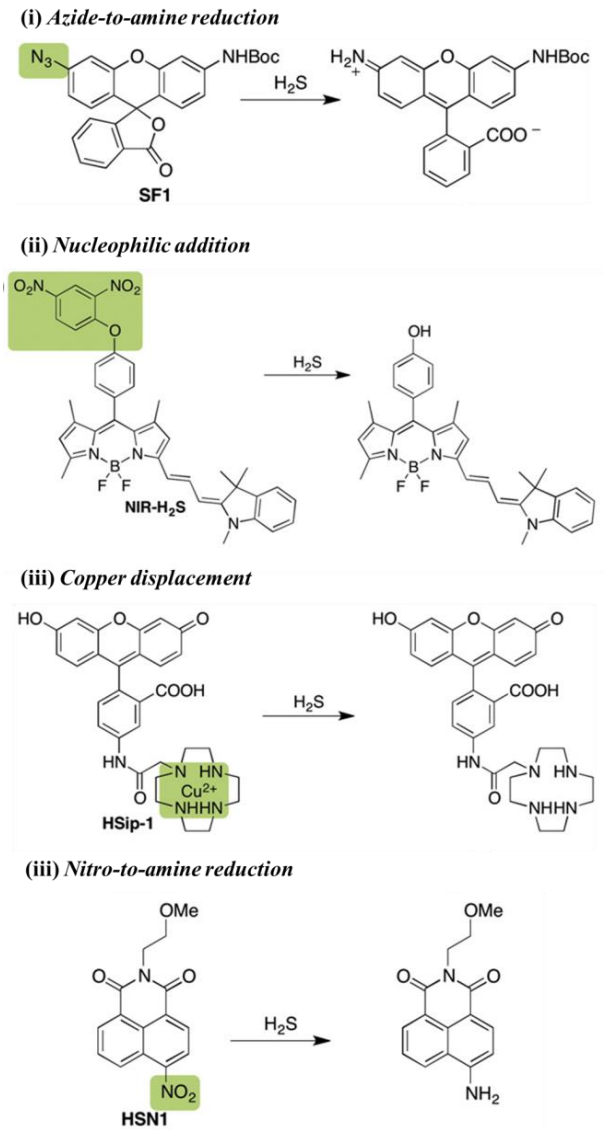


**Figura 1.3.** (i) Fluorescent probe SF1 is based on the $H_2S$-mediated reduction of an aryl azide to an aryl amine; (ii) dinitrophenyl ethers are suitable electrophilic triggers for fluorescent $H_2S$ probes and display selectivity for $H_2S$ versus a panel of other biological nucleophiles; (iii) fluorescent sulfide sensor based on copper sulfide precipitation; (iv) the nitro-functionalized probe HSN1 undergoes selective reduction to an amine upon reaction with $H_2S$ with greater thiol cross reactivity than the analogous azide probe.

In the end, a key challenge for selective detection of $H_2S$ within the cellular milieu is the comparatively high concentrations of biological sulfur species such as glutathione as well as cysteine residues.

## 1.4 Aim of the Thesis

In my opinion a limitation of the fluorescent sensors developed so far is the irreversibility of the reaction by which $H_2S$ recognition occurs, which renders the devices not reusable. With a coordinative-based approach one may, in principle, be able to remove $H_2S$ from the metal center of the sensor and ensure a reversible $H_2S$ binding process. This would be advantageous for practical sensing applications allowing reusability of the sensing device. Knowing this, I try to improve $H_2S$ sensors focusing on designing new complexes, which could work by a coordinative-based approach.

## 1.5 Reference List

1. E. T. Kato Jr., C. M. P. Yoshida, A. B. Reis, I. S. Melo, T. T. Franco, *Polym. Int.* **2011**, *60*, 951.

2. J. R. Reiffenstein, W. C. Hulbert, S. H. Roth, *Annu. Rev. Pharmacol. Toxicol.* **1992**, *32*, 109.

3. (*a*) V. S. Lin, C. J. Chang, *Curr. Opin. Chem. Biol.* **2012**, *16*, 595; (*b*) R. P. Smith, *Can. Med. Assoc. J.* **1978**, *118*, 775; (*c*) R. P. Smith, *Am. Sci.* **2010**, *98*, 6.

4. (*a*) L. Li, P. K. Moore, *Trends Pharmacol. Sci.* **2008**, *29*, 84; (*b*) L. Li, P. K. Moore, *Biochem. Soc. Trans.* **2007**, *35*, 1138; (*c*) *R.* Wang, *Physiol. Rev.* **2012**, *92*, 791.

5. C. Q. Chen, H. Xin, Y. Z. Zhu, *Acta Pharmacol. Sin.* **2007**, *28*, 1709.

6. D. G. Searcy, S. H. Lee, *j. Exp. Zool.* **1998**, *282*, 310.

7. A. J. Cooper, *Annu. Rev. Biochem.* **1983**, *52*, 187.

8. P. Kamoun, M. C. Belardinelli, A. Chabli, K. Lallouchi, B. Chadefaux-Vekemans, *Am. J. Med. Genet. A.*, **2003**, *116A*, 310.

9. Li L., Rose P., Moore P. K., *Annu. Rev. Pharmacol. Toxicol.* **2011**, *51*, 169.

10. J. Liu, Y. Q. Sun, J. Zhang, T. Yang, J. Cao, L. Zhang, W. Guo, *Chemistry* **2013**, *19*, 4717.

11. A. H. Nielsen, J. Vollertsen, T. Hvitved-Jacobsen, *Water Environ. Res.* **2006**, *78*, 275.

12. (*a*) E. A. Guenther, K. S. Johnson, K. H. Coale, *Anal. Chem.* **2001**, *73*, 3481; (*b*) E. Fisher, *Chem. Ber.* **1883**, *16*, 2234; (*c*) J.K. Fogo, M. Popowsky, *Anal. Chem.* **1949**, *21*, 732.

13. J. Furne, A. Saeed, M. D. Levitt, *Am. J. Physiol. Regul. Integr. Comp. Physiol.* **2008**, *295*, R1479; (*b*) A. Tangerman, *J. Chromatogr.* **2009**, *B 877*, 3366.

14. N. S. Lawrence, J. Davis, R. G. Compton, *Talanta* **2000**, *52*, 771.

15. T. Ubuka, T. Abe, R. Kajikawa, K. Morino, *J. Chromatogr. B. Biomed. Sci. Appl.*, **2001**, *757*, 31.

16. T. Ubuka, *Journal of Chromatography B*, 2002, 781, 227.

17. (*a*) T. Chen, Y. Zheng, Z. Xu, M. Zhao, Y. Xu, J. Cui, *Tetrahedron Lett.* **2013**, *54*, 2980; (*b*) M. Tropiano, S. Faulkner, *Chem. Commun.* **2014**, *50*, 4696; (*c*) I. Takashima, M. Kinoshita, R. Kawagoe, S. Nakagawa, M. Sugimoto, I. Hamachi, A. Ojida, *Chemistry* **2014**, *20*, 2184.

18. (*a*) K. Zheng, W. Lin, L. Tan, *Org. Biomol. Chem.* **2012**, *10*, 9683; (*b*) Z. Wu, Z. Li, L. Yang, J. Han, S. Han, *Chem. Commun.* **2012**, *48*, 10120.

19. (*a*) C. Liu, B. Peng, S. Li, C. M. Park, A. R. Whorton, M. Xian, *Org. Lett.* **2012**, *14*, 2184; (*b*) Y. Zhao, X. Zhu, H. Kan, W. Wang, B. Zhu, B. Du, X. Zhang, *Analyst* **2012**, *137*, 5576.

20. (*a*) F. Hou, L. Huang, P. Xi, J. Cheng, X. Zhao, G. Xie, Y. Shi, F. Cheng, X. Yao, D. Bai, Z. Zeng, *Inorg. Chem.* **2012**, *51*, 2454; (*b*) M. Q. Wang, K. Li, J. T. Hou, M. Y. Wu, Z. Huang, X. Q. Yu, *J. Org. Chem.* **2012**, *77*, 8350.

21. (*a*) M. Y. Wu, K. Li, J. T. Hou, Z. Huang, X. Q. Yu, *Org. Biomol. Chem.* **2012**, *10*, 8342; (*b*) W. Xuan, R. Pan, Y. Cao, K. Liu, W. Wang, *Chem. Commun.* **2012**, *48*, 10669.

22. (*a*) L. E. Santos-Figueroa, C. de la Torre, S. El Sayed, F. Sancenon, R. Martinez-Manez, A. M. Costero, S. Gil, M. Parra, *Eur. J. Inorg. Chem.* **2014**, 41–45; (*b*) Z. Ye, X. An, B. Song, W. Zhang, Z. Dai, J. Yuan, *Dalton Trans.* **2014**, *43*, 13055.

# Chapter 2: Cobaloximes as selective tools for $H_2S$ sensing

## 2.1. Introduction

In the human organism hydrogen sulfide can diffuse between blood and tissues or within cells and can be combined with metalloproteins,[1] e.g. hemoglobin, methemoglobin, hematin, and cysteine residues leading to the formation of persulfides or sulfhydrated proteins.[2] An important metal-containing and redox-active species present in the human organism is cobalamin (**Figure 2.1**), the cofactor of several coenzyme-B12-dependent enzymes.

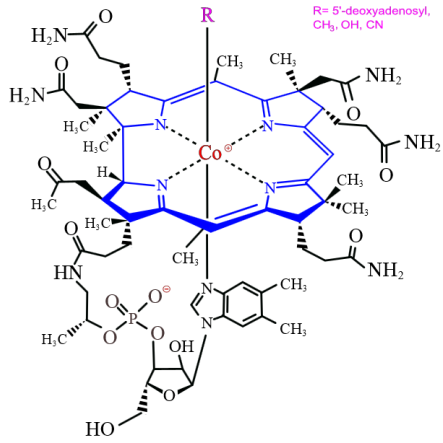


**Figure 2.1.** Structure of B12-Cobalamin.

In spite of the controversy about its interaction with hydrogen sulfide, recent studies highlighted that cobalamin constitutes a valid approach to affect endogenous $H_2S$ concentration in clinical conditions (e.g.

[1] (*a*) X. Bailly, S. J. Vinogradov, *J. Inorg. Biochem.* **2005**, *99*, 142; (*b*) R. E. Weber, S. N. Vinogradov, *Physiol. Rev.* **2001**, *81*, 569.
[2] (*a*) A. K. Mustafa, M. M. Gadalla, N. Sen, S. Kim, W. Mu, S. K. Gazi, R. K. Barrow, G. Yang, R. Wang, S. H. Snyder, *Sci Signal* **2009**, *2*, ra72; (*b*) B. D. Paul, S. H. Snyder, *Nat. Rev. Mol. Cell. Biol.* **2012**, *13*, 499.

wherein systemic inflammation or ipoxia is present).[3] In particular cobalamin has been reported to be able to enhance the natural ability of the plasma and supernatant of tissues to complex $H_2S$.

Knowing that vitamin B12 is involved in the $H_2S$ transport,[4] I decided to use vitamin's models: cobaloximes [5] (Co(III) complexes of bis(dimethylglyoximate), **Figure 2.2**) to implement $H_2S$ sensors.

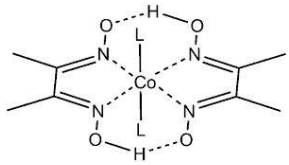


**Figure 2.2.** Structure of a generic cobaloxime $[Co(dmgH)_2L_2]$.

These complexes are water soluble and easily synthesized. Both these conditions are highly desirable when implementing a sensing device.

## 2.2. Results and Discussion

### 2.2.1. $[Co(dmgH)_2(CH_2CH_3)(py)]$

In the first year has been investigated the reaction of hydrogen sulfide with different alkyl cobaloximes. The first that has been examined is the simplest, already known $[Co(dmgH)_2(CH_2CH_3)(py)]$ (**1**) (dmgH = dimethylglyoximate anion). This complex can be prepared converting a preformed chlorocobaloxime to a Co(I) species that, in

[3] (*a*) A. Van de Louw, P. Haouzi, *Critical Care* **2012**, *16*, R178; (*b*) A. Van de Louw, P. Haouzi, *Antioxid.Redox.Signal.* **2013**, *19*, 510.
[4] A. Van de Louw, P. Haouzi, *ANTIOXIDANTS & REDOX SIGNALING* **2012**, *00*, 1.
[5] (*a*) P. J. Toscano, L. G. Marzilli, *Prog. Inorg. Chem.* **1984**, *31*, 105. (*b*) N. Bresciani-Pahor, M. Forcolin, L. G. Marzilli, L. Randaccio, M. F. Summers, P. J. Toscano, *Coord. Chem. Rev.* **1985**, *63*, 1.

basic conditions, has significant anionic character to react with the electrophilic ethyl iodide (**Scheme 2.1**).[6]

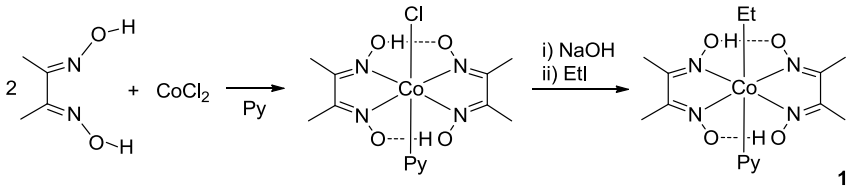


**Scheme 2.1.** Synthesis of $[Co(dmgH)_2(CH_2CH_3)(py)]$ (**1**).

### 2.2.1.1. NMR Studies

In the first instance, the reaction of complex **1** potassium hydrosulfide (KSH) was studied using NMR spectroscopy (**Figure 2.3)**. It was previously reported that in coordinating solvents cobaloximes undergo solvolysis reactions in which the pyridine ligand is displaced by a molecule of solvent.[7] Accordingly, in the $^1$H NMR spectrum of **1** recorded in $D_2O$, two sets of resonances were detected indicating the presence of the solvated and pyridine-coordinated species. The addition of one equivalent of KSH to the NMR sample of **1** in $D_2O$ instantaneously led to the appearance of a new pattern of resonances. In particular in the aliphatic region of the spectrum, in addition to the signals due to the ethyl groups of **1** and the corresponding solvated species, a new $A_3X_2$ pattern was detected (**Figure 2.3b**), whereas in the aromatic region, the signals of the pyridine bound to the cobalt atom were flanked by the signal of the free pyridine.

[6] B. D. Gupta, K. Qanungo, *J. Organomet. Chem.* **1997**, *543*, 125.
[7] (*a*) K. L. Brown, D. Lyles, M. Pencovici, R. G. Kallen, *J. Am. Chem. Soc.* **1975**, *97*, 7338; (*b*) K. L. Brown, A. W. Awtrey, *Inorg. Chem.* **1978**, *17*, 111.

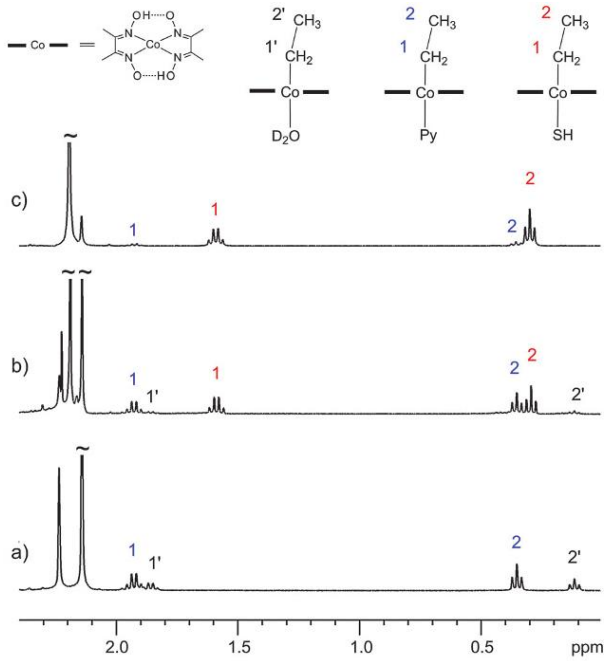


**Figure 2.3.** Aliphatic region of the $^{1}$H NMR spectrum of [Co(dmgH)$_2$(CH$_2$CH$_3$)(py)] (**1**) before (**a**) and after the addition of 1 (**b**) and 3 (**c**) equivalents of KSH ([**1**] = 34.5 mM, D$_2$O, rt, 400 MHz).

The coupling patterns between different signals were determined by a COSY experiment (**Figure 2.4**). By adding increasing equivalents of KSH, the amount of pyridine-bound and solvated species decreased, at the same time the amount of the new species increased. The reaction was completed when 5 equivalents of KSH were added to the NMR tube.

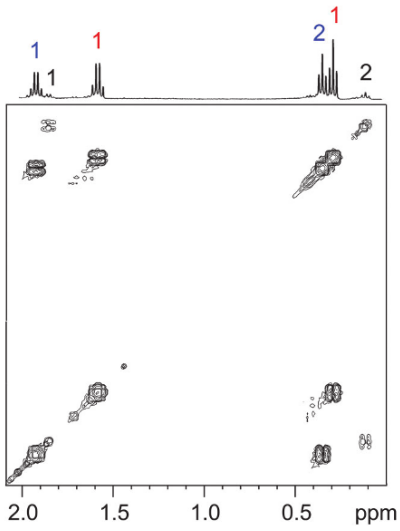


**Figure 2.4.** COSY spectrum of a mixture of **1** and KSH in a 1/1 molar ratio ([**1**] = 34.5 mM, $D_2O$, rt, 400 MHz). The assignment of the resonance is shown in **Figure 2.2**.

The oxime-proton in the cobaloxime has an acidic character, so it can be removed in alkaline solution. To exclude the possibility that the new species observed in the NMR spectrum comes from the deprotonation of cobaloxime by the $HS^-$ anion, the reaction was repeated with a solution of NaOH. Upon addition of increasing amounts of NaOH to a solution of **1** a drift of the resonances of the solvated species was observed. No evidence for the formation of the new species was found. It is reasonable to assume that the addition of KSH leads to the selective substitution of the axial ligand to form the corresponding hydrosulfide adduct. To assess whether the substitution reaction is carried out by $HS^-$ or $H_2S$, DFT calculations were performed. In the first instance both possible adducts of **1**, namely $Co(dmgH)_2(CH_2CH_3)(H_2S)$ and $[Co(dmgH)_2(CH_2CH_3)(HS)]^-$, were successfully optimized. In each species, the geometry of the Co atom is best described as a distorted octahedron with ligand-cobalt

bond distances very similar to those observed in the X-ray structure of **1**.[8] In the $H_2S$-adduct, the Co-S bond length of 2.45 Å compares favourably with the metal-sulfur bond lengths observed in the X-ray structures of $H_2S$ adducts reported in the literature, all of which are ruthenium(II) complexes.[9] The S-H bonds are slightly polarized as reflected by the increase of the bond length from 1.33 Å[10] in gaseous $H_2S$ to 1,36 Å in the coordinated $H_2S$. In the $HS^-$-adduct, the $HS^-$ anion is located at 2.40 Å from the metal centre. This bond distance is slightly longer than the M-S bond distance in metal complexes with bridging $SH^-$ groups – this bond distance ranges between 2.34 and 2.38 Å in the cluster $[Co_3(\mu_3\text{-}S)\text{-}(\mu_3\text{-}SH)_2\text{-}(\mu\text{-}PEt_2)(PHEt_2)_6][ClO_4]_2$[11] and between 2.33 and 2.36 Å in the cationic iron complex $[Fe_2(\mu\text{-}SH)_3(triphos)_2]$ [triphos = bis-(2-diphenylphosphinoethyl)phenylphosphine].[12] Even though the $H_2S$-adduct is predicted to be stable, its formation starting from the pyridine-adduct **1**, is not favoured, As a matter of fact the substitution reaction of pyridine by $H_2S$ (reaction (1)) was predicted to be endoergonic by 54.8 kJ $mol^{-1}$. $HS^-$ is an electron pair donor more

[8] (*a*) P. J. Toscano, G. Marzilli, *Prog. Inorg. Chem.* **1984**, *31*, 105; (*b*) N. Bresciani-Pahor, M. Forcolin, L. G. Marzilli, L. Randaccio, M. F. Summers, P. J. Toscano, *Coord. Chem. Rev.* **1985**, *63*, 1.

[9] (*a*) S. L. Chatwin, R. A. Diggle, R. F. Jazzar, S. A. MacGregor, M. F. Mahon, M. K. Whittlesey, *Inorg. Chem.* **2003**, *42*, 7695; (*b*) D. C. Mudalige, E. S. Ma, S. J. Rettig, B. R. James, W. C. Cullen, *Inorg. Chem.* **1997**, *36*, 5426; (*c*) D. Sellman, P. Lechner, F. Knoch, M. Moll, *J. Am. Chem. Soc.* **1992**, *114*, 922.

[10] T. H. Edwards, N. K. Moncur, L. E. Snyder, *J. Chem. Phys.* **1967**, *46*, 2139.

[11] C. A. Ghilardi, S. Midollini, A. Orlandini, G. Scapacci, *J. Chem. Soc., Dalton Trans.* **1992**, 2909.

[12] M. di Vaira, S. Midollini, L. Sacconi, *Inorg. Chem.* **1979**, *18*, 3466.

effective than $H_2S$, the substitution of pyridine by the hydrogen sulfide anion (reaction (2)) was predicted to be exergonic by -15.1 kJ $mol^{-1}$.

$Co(dmgH)_2(Et)(py) + H_2S \rightarrow Co(dmgH)_2(Et)(H_2S) + py$ (1)

$Co(dmgH)_2(Et)(py) + HS^- \rightarrow Co(dmgH)_2(Et)(HS)^- + py$ (2)

Analogous results were obtained if the solvated species, $Co(dmgH)_2(CH_2CH_3)(H_2O)$, was considered as the starting reagent – the substitution of $H_2O$ by $H_2S$ (reaction (3)) was predicted to be endergonic by 25.5 kJ $mol^{-1}$ while the substitution of $H_2O$ by $HS^-$ (reaction (4)) was predicted to be exergonic by -33.9 kJ $mol^{-1}$.

$Co(dmgH)_2(Et)(H_2O) + H_2S \rightarrow Co(dmgH)_2(Et)(H_2S) + H_2O$ (3)

$Co(dmgH)_2(Et)( H_2O) + HS^- \rightarrow Co(dmgH)_2(Et)(HS)^- + H_2O$ (4)

The substitution of the axial ligand of **1** should be promoted only by the $HS^-$ anion; this finding is consistent with the results of a recent study on the different reactivity of $HS^-$ and $H_2S$ species toward metal centers in which it was shown that zinc(II) and cobalt(II) phtalocyanine complexes react whit $HS^-$ but not whit $H_2S$.[13] In order to verify if **1** and the hydrosulfide-bound complex $[Co(dmgH)_2(CH_2CH_3)(SH)]^-$ (**2**) are in equilibrium, a $^1H$-$^1H$ EXSY experiment was perfomed on a solution containing the complexes **1** and **2** in equimolar amounts. In the corresponding spectrum positive

[13] M. D. Hartle, S. K. Sommer, S. R. Dietrich, M. D. Pluth, *Inorg. Chem.* **2014**, *53*, 7800.

cross-peaks correlating complex **1** (the pyridine-bound complex and the solvated one) with complex **2** were clearly odserved (**Figure 2.5**).

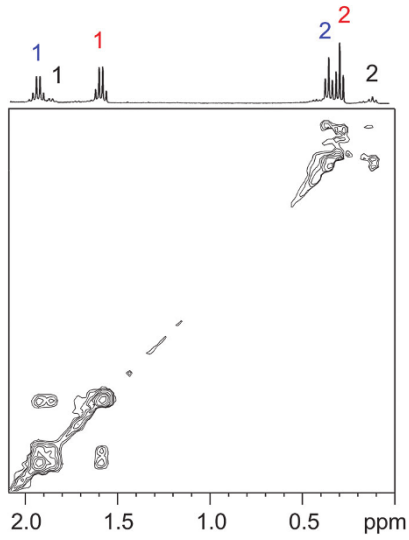


**Figure 2.5.** EXSY spectrum of a mixture of **1** and KSH in a 1/1 molar ratio ($D_2O$, rt, 400 MHz). The assignment of the resonance is shown in **Figure 2.2**.

This indicates that species actually are in the slow exchange regime as depicted in **Scheme 2.2**.

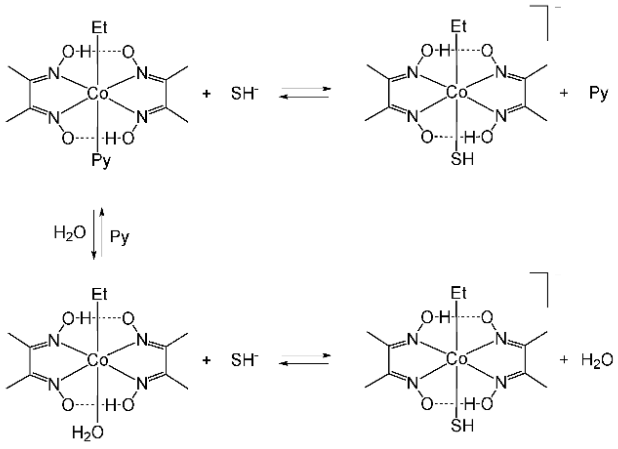


**Scheme 2.2.** Substitution of the axial ligand by $SH^-$.

With these results, the synthesis of the hydroulfido-complex $K[Co(dmgH)_2(CH_2CH_3)(SH)]$ (**2**) was attempted on a preparative scale. The treatment of complex **1** with 10 equivalents of KSH in a water-methanol solution at room temperature afforded an orange powder, the $^1H$ NMR spectrum of which was perfectly superimposable with that observed for the species generated *in situ* (**Figure2.6**). In addition a broad singolet was detected at 2.5 ppm that can be attributed to the resonance of the $HS^-$ group on the basis of literature data.[14]

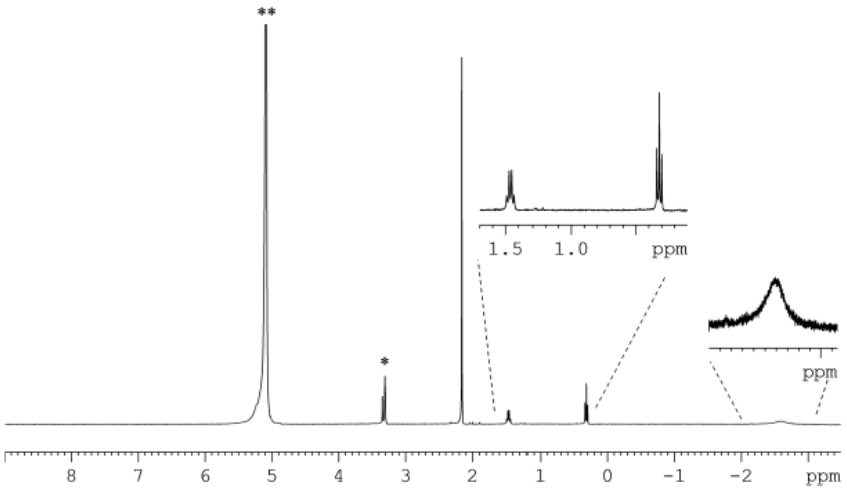


**Figure 2.6.** $^1H$ NMR spectrum of $K[Co(dmgH)_2(CH_2CH_3)(SH)]$ (**2**) in methanol-$d_4$ (rt, 400 MHz).

[14] A. Müller, E. Diemann, in *Comprehensive coordination chemistry*, ed. G. Wilkinson, R. D. Gillard, J. A. McCleverty, Pergamon Press, Oxford, UK, **1987**, ch. 161, vol *2*.

### 2.2.1.2. Crystal Structure

Despite several attempts, we could not obtain single crystals of **2** suitable for X-ray structure analysis. In one of the crystallization tests, an unexpected trisulfido-bridged dinuclear complex $K_2[Co_2(dmgH)_2(CH_2CH_3)_2(\mu\text{-}S_3)]$ (**3**) was isolated and structurally characterized (**Figure 2.7**). The crystal were produced by the direct reaction of **1** with KSH in MeOH/$Et_2O$ over two weeks. In this species two cobaloxime units are axially bridged together with a trisulfide anion ($S_3^{2-}$).

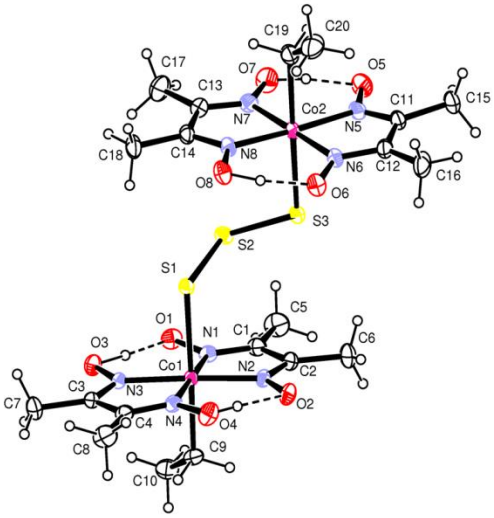


**Figure 2.7.** ORTEP xiew of the anionic complex $[Co_2(dmgH)_4(CH_2CH_3)_2(\mu\text{-}S_3)]^{2-}$ with the thermal ellipsoids at 30% probability.

The geometry around each Co atom is a distorted octahedron with four nitrogens of the dimethylglyoximato ligands in the equatorial plane and a sulphur atom of the trisulfide moiety and an ethyl group axially coordinated. The Co1 and Co2 atoms deviate from the equatorial planes formed by the four nitrogen atoms by only

0.0222(2) and 0.0308(2) Å, towards the S1 and S3 sulphur atoms, respectively. For the Co1 cobaloxime unit, the chelate rings defined by N1, N2, C1, C2 and N3, N4, C3, C4 atoms are bent by 1.23(7) and 4.55(8)° with respect the equatorial plane towards the S1 atom, while for the Co2 cobaloxime unit the corresponding bent angles are 5.58(9) and 0.99(7)° towards the S3 atom. The two coordination basal planes are almost parallel forming a dihedral angle of 8.96(6)°. The Co1-S1 and Co2-S3 bond distances of 2.3902(5) and 2.3757(5) Å, respectively can be compared with Co-S distance of 2.342(2) Å observed in a Co-$(dmgH)_2$ complex having an ethanethiolate group in axial position trans to a $CH_3$ group.[15] This complex displays very short O-H···O intramolecular hydrogen bonds with O···O distances in the range 2.474(2)-2.516(2) Å, typical for this kind of compounds. Both potassium cations are hexa-coordinated: K1 by three oxygens of the dimethylglyoximato ligands, two sulfur atoms and a water molecule, while K2 is coordinated by two oxygens of the dimethylglyoximato ligands, a sulfur atom and three water molecules. All the other structural parameters are in good agreement with those observed for other similar complexes.

Solutions of hydrogen sulfide are unstable; in the presence of atmospheric oxygen, $HS^-$ is slowly converted into a complicated mixture of several partially oxidized sulfur species such as elemental sulfur, sulfite, thiosulfate, tetrathionate, sulfate and polysulfides ions.[16] It was also reported that the oxidation of $HS^-$ to polysulfides

[15] S. M. Polson, L. Hansen, L. G. Marzilli, *Inorg. Chem.* **1997**, *36*, 307.

[16] (*a*) K. Y. Chen, J. C. Morris, *Environ. Sci. Technol.* **1972**, *6*, 529; (*b*) D. J. O'Brien, F. B. Birkner, *Environ. Sci. Technol.* **1977**, *11*, 1114.

can be promoted by traces of metals.[17] To determine whether the formation of the $S_3^{2-}$ anion was catalyzed by complex **1**, we carried out a reaction in water with a **1**/KSH molar ratio of 1/50 at room temperature under aerobic conditions and analyzed the product mixtures sampled from the reactor at certain reaction times.[18] It is worth noting that freshly prepared solutions of KSH or other $H_2S$ donors commonly contain low quantities of the $S_2^{2-}$ anion.[19] In my experiments its amount slowly increased over the days, whereas the $S_3^{2-}$ anion was detected only after four days of reaction. The same polysulfide distributions were found in a solution of KSH used as a blank. We can reasonably assume that the formation of the trisulfide anion found in **3** is not mediated by the cobalt complex **1**.

#### 2.2.1.3. ESI-MS studies

In the negative ion ESI-MS spectrum two ions at *m/z* 351.5 and 322.4 are consistent with the coordinated $HS^-$ anions $[Co(dmgH)_2(CH_2CH_3)(SH)]^-$ and $[Co(dmgH)_2(SH)]^-$ (**Figure 2.8**).

[17] (*a*) M. R: Hoffmann, B. C. Lim, *Environ. Sci. Technol.* **1979**, *13*, 1406; (*b*) A. P. Hong, S. D. Boyce, M. R. Hoffmann, *Environ. Sci. Technol.* **1989**, *23*, 533; (*c*) S. M. Chen, S. W. Chiu, *J. Mol. Catal. A: Chem.* **2001**, *166*, 243.

[18] I. Filipponen, A. Guerra, A. Hai, L. A. Lucia, D. S. Argyropoulos, *Ind. Eng. Chem. Res.* **2006**, *45*, 7388; (*b*) D. S. Argyropoulos, Y. Hou, R. Ganesaratnam, D. N. Harpp, K. Koda, *Holzforschung*, **2005**, *59*, 124.

[19] (*a*) M. N. Hughes, M. N. Centelles, K. P. Moore, *Free Radical Biol. Med.* **2009**, *47*, 1346; (*b*) J. I. Toothey, *Anal. Biochem.* **2011**, *413*, 1; (*c*) R. Greiner, Z. Pálinkás, K. Bäsell, D. Becher, H. Antelmann, P. Nagy, T. P. Dick, *Antioxid. Redox Signaling* **2013**, *19*, 1749.

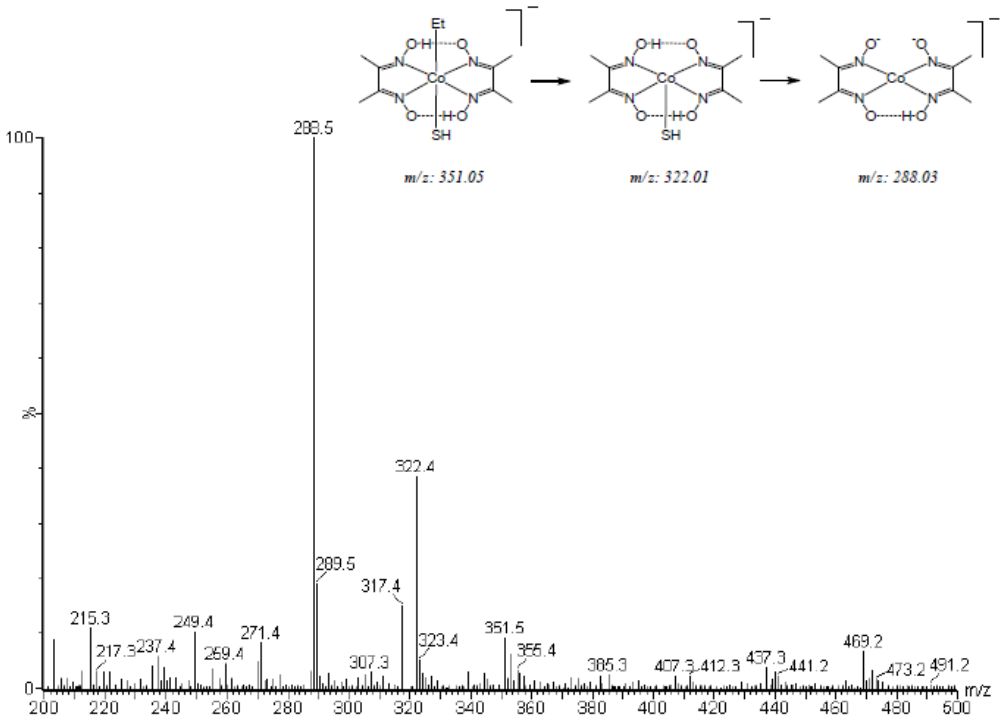


**Figure 2.8.** Electrospray mass spectra (negative-ion mode) of K[Co(dmgH)$_2$(CH$_2$CH$_3$)(SH)] (**2**) in methanol.

### 2.2.1.4. Optical Studies

Optical sensors are a type of chemical sensors which act on the basis of changes in the optical properties. Optical properties are changed because of the interaction between the analyte and the receptor. Aimed to test the principal usability of the system as an optical sensor, in the first instance the $H_2S$ binding to the ethyl-cobaloxime complex has been studied by UV-visible spectroscopy. In such way it was possible to determine at which wavelengths the maximum change in the absorbance occurs. Thus, the fluorescence spectra were detected at this wavelength. When KSH (a commonly employed $H_2S$ donor) was added to a MilliQ water solution of the ethyl-cobaloxime

complex, the absorption spectrum significantly changed. Specifically, while the absorption spectrum of the free complex exhibits a band at 230 nm and three less intense bands centered at 285, 398 and 450 nm, $H_2S$ addition quenches the 398 nm band and leads to the appearance of a new band centered at 330 nm (that can be assigned to S → Co(III) ligand-to-metal charge transfer (LMCT) transition on the basis of analogy with other Co(III) complexes)[20] whereas the 230 nm band becomes consistently more intense (**Figure 2.9**)

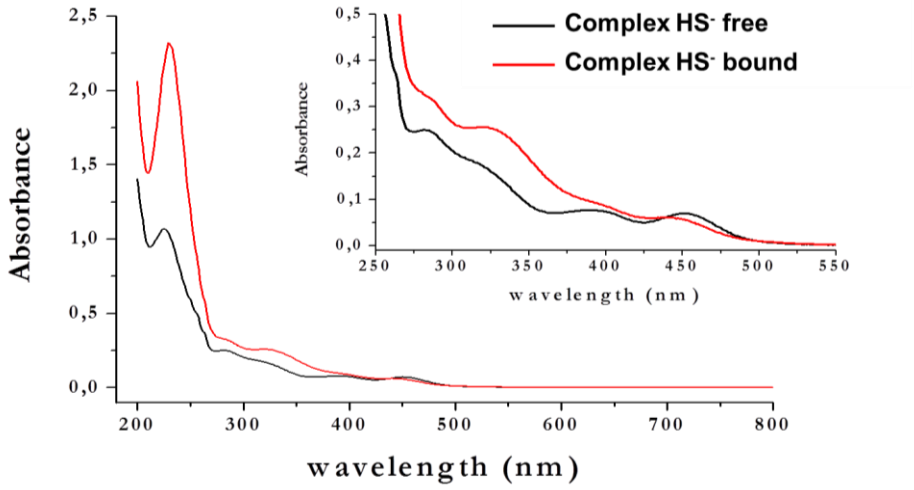


**Figure 2.9.** Electronic absorption spectra of $[Co(dmgH)_2(CH_2CH_3)(py)]$ (**1**) (rt, black line, 3.2 x $10^{-5}$ M, $H_2O$) and after addition of KSH (rt, red line, 3.2 x $10^{-5}$ M, $H_2O$).

To assess whether the absorption spectrum of the ethyl-pyridine complex varies with the concentration of the analyte, UV-vis spectra of the system were recovered after the addition of increasing amounts

[20] (*a*) K. L. Brown, R. G. Kallen, *J. Am. Chem. Soc.* **1972**, *94*, 1894; (*b*) G. Pellizer, G. R. Tauszik, G. Costa, *J. Chem. Soc., Dalton Trans.* **1973**, 317; (*c*) T. C. Higgs, D. Ji, R. S. Czernuszewicz, B. F. Matzanke, V. Schunemann, A. X. Trautwein, M. Helliwell, W. Ramirez, C. Carrano, J. *Inorg. Chem.* **1998**, *37*, 2383.

of KSH solution. **Figure 2.10** shows that there is a clear dependence of the absorption spectrum of the ethyl-pyridine complex on the KSH concentration (from 3.2 x $10^{-5}$ M to 1.0 x $10^{-3}$ M).

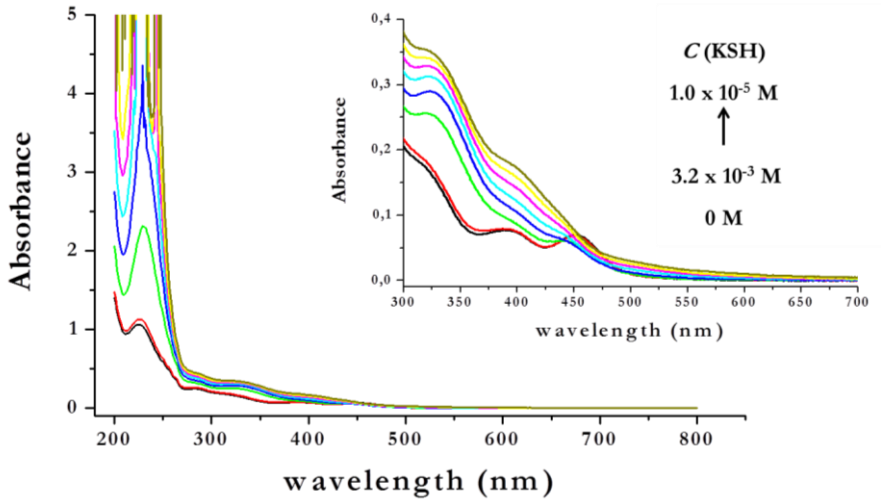


**Figure 2.10.** Electronic absorption spectra of [Co(dmgH)$_2$($CH_2CH_3$)(py)] (**1**) (rt, 3.2 x $10^{-5}$ M, $H_2O$) upon addition of increasing concentrations of KHS (from 3.2 x $10^{-5}$ M to 1.0 x $10^{-3}$ M).

The same spectrum is acquired for the adduct obtained on a preparative scale (**Figure 2.11**).

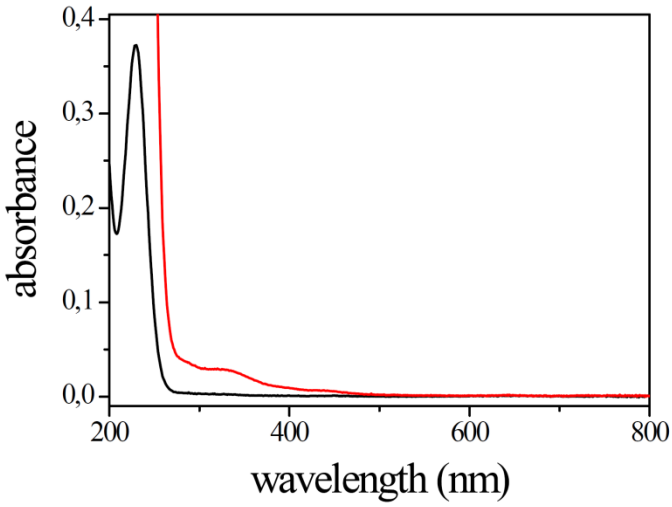


**Figure 2.11.** Electronic absorption spectra of K[Co(dmgH)$_2$(CH$_2$CH$_3$)(SH)] (**2**) (rt, 3.2 x $10^{-5}$ mM black line, 3.2 x $10^{-4}$ mM red line, $H_2O$).

To obtain an indication on the selectivity of the construct, the absorption spectrum of the system was checked in the presence of biologically relevant and potentially competing thiols. In the presence of either GSH or L-cys or $Na_2S_2O_3$ or NaSCN no significant shifts could be observed (**Figure 2.12**). These findings clearly evidence the high selectivity of the system over other biologically related species.

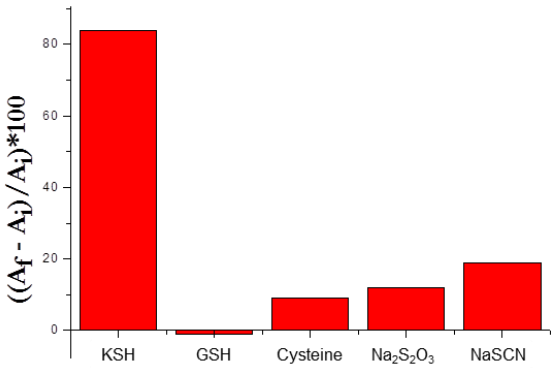

**Figure 2.12.** Relative Absorbance at 330 nm of [Co(dmgH)$_2$(CH$_2$CH$_3$)(py)] (**1**) (3.2 x 10$^{-5}$ M) in the presence of KSH (3.2 x 10$^{-4}$ M), glutathione (GSH), cysteine, $S_2O_3^{2-}$, $SCN^-$ (3.2 x 10$^{-4}$ M) in an aqueous solution.

To exclude that the modification of the absorption spectrum of the ethyl-pyridine complex in the presence of increasing amounts of KSH could be only due to the changing of the pH of the sample solution, we measured the UV-vis spectrum of the system in the presence of an excess of NaOH or HCOOH. No changes could be observed (**Figure 2.13**).

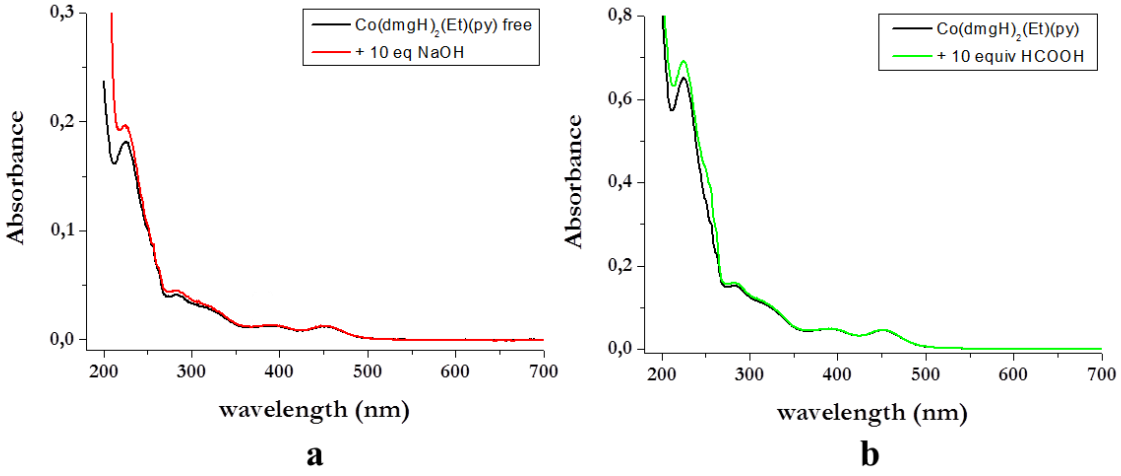


**Figure 2.13.** Electronic absorption spectra of [Co(dmgH)$_2$(CH$_2$CH$_3$)(py)] (**1**) (rt, black line, 3.2 x 10$^{-5}$ M, H$_2$O) and after addition of (**a**) NaOH (rt, red line, 3.2 x 10$^{-4}$ M, H$_2$O) and (**b**) HCOOH (rt, green line, 3.2 x 10$^{-4}$ M, H$_2$O).

Despite the great potential of complex **1** as $H_2S$ sensor (e.g. water solubility, high selectivity for $H_2S$ over several biologically relevant thiols, easy of synthesis) the lack of a consistent fluorescence response on the KSH concentration constitutes a limitation of the present system. Therefore it has been thought of modifying the framework of complex **1** to implement a fluorescent $H_2S$ sensor.

### 2.2.2. [Co(dfgH)$_2$(CH$_2$CH$_3$)(py)] and [Co(dmgH)$_2$(ph)(py)]

Then, making appropriate modifications, other two complexes were synthetized. In the first case we chose to replace the equatorial dimethylglyoxime ligand with another which contained potentially fluorescent groups, such as the diphenylglyoxime, thus obtaining complex **4 (**[Co(dfgH)$_2$(CH$_2$CH$_3$)(py)]). In the second case one of the axial ligands has been modified, replacing the ethylenic moiety with a phenyl, obtaining the formation of the complex **5 (**[Co(dmgH)$_2$(ph)(py)]). Complexes **4** and **5** were prepared in good yields (75% for complex **4** and 46%) by following synthetic procedures similar to that of complex **1** (**Scheme 2.3**).

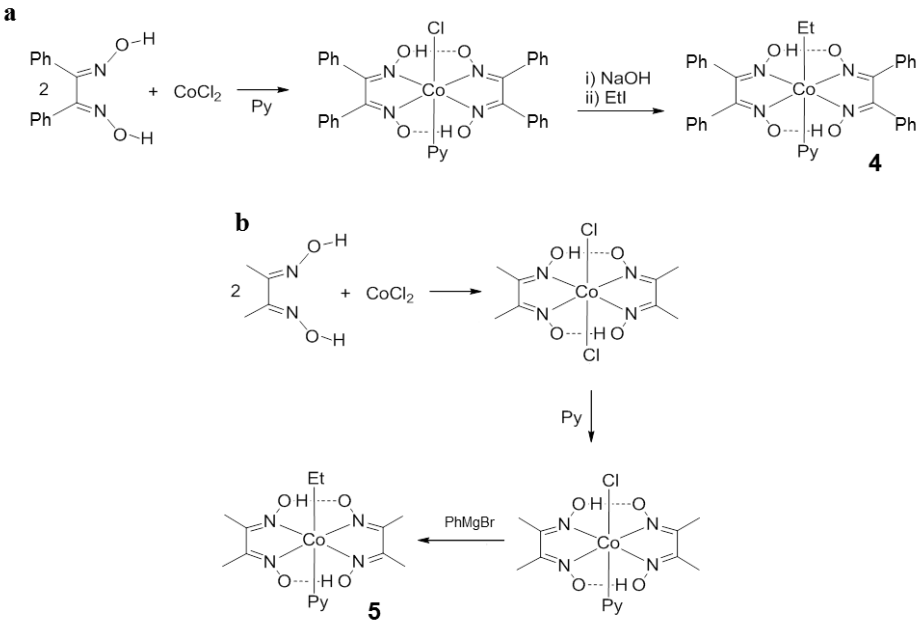


**Scheme 2.3. (a)** Synthesis of [Co(dfgH)$_2$(CH$_2$CH$_3$)(py)] (**1**); **(b)** Synthesis of [Co(dmgH)$_2$(C$_6$H$_5$)(py)].

Slow cooling of saturated methanol solutions of complex **4** yielded single crystals suitable for X-ray diffraction (**Figure 2.14**).

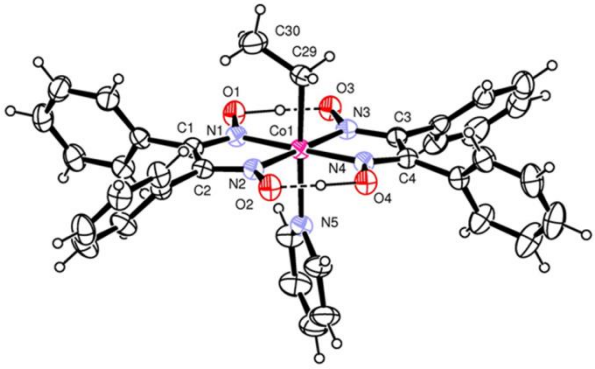


**Figure 2.14.** ORTEP xiew of the anionic complex $[Co(dfgH)_2(CH_2CH_3)\ (py)]$.

$H_2S$ binding to complex **4** was first assessed by UV/Vis spectroscopy. Adding KSH to a methanolic solution of **4** a clear change of the initial spectrum was observed. **Figure 2.15** shows a typical UV/Vis spectrum of a solution containing $1.5 \cdot 10^{-5}$ M of $[Co(dfgH)_2(CH_2CH_3)(py)]$ in which the increase of the band at 280 nm is particularly evident.

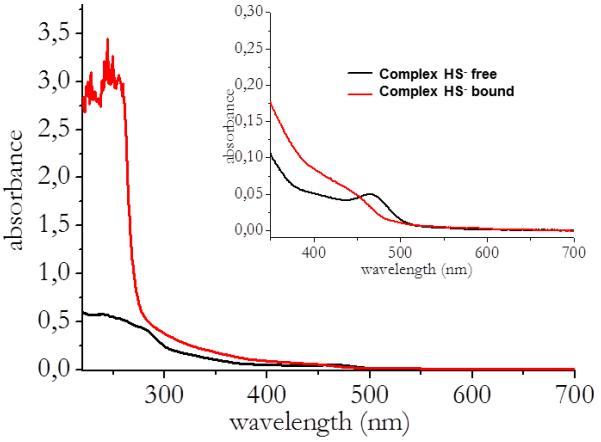

**Figure 2.15.** Electronic absorption spectra of $[Co(dfgH)_2(CH_2CH_3)(py)]$ (**4**) (rt, black line, $1.5 \cdot 10^{-5}$ M, MeOH) and after addition of KSH (rt, red line, $7.5 \cdot 10^{-5}$ M, MeOH).

Pronounced changes were observed also in the fluorescence response. Exciting the wavelength at which we observe the maximum variation in absorption (280 nm), addition of KSH to a methanol solution of complex **4** resulted in a consistent quenching of the fluorescence intensity (SR ~ 50% ; see **Figure 2.16**).

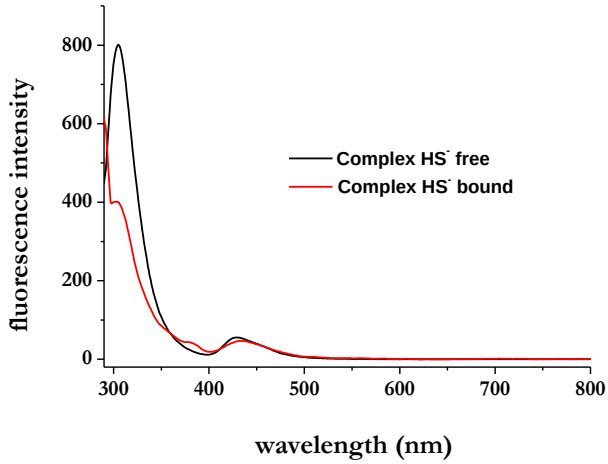


**Figure 2.16.** Emission spectra of $[Co(dfgH)_2(CH_2CH_3)(py)]$ (**4**) ($\lambda_{exc}$ = 280 nm) before and after addition of an excess of KSH.

When increasing amounts of KSH were added and the fluorescence intensities were monitored, a progressive quenching was observed (**Figure 2.17**).

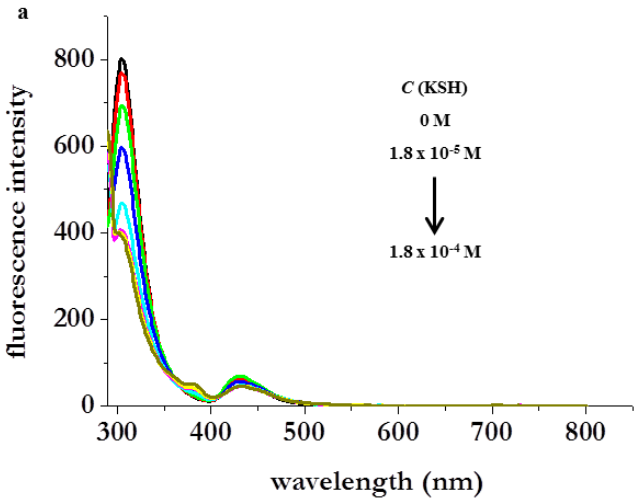


**Figure 2.17.** Emission spectra of $[Co(dfgH)_2(CH_2CH_3)(py)]$ (**4**) ($\lambda_{exc}$ = 280 nm, rt, 3.9 x $10^{-6}$ M, MeOH) upon addition of increasing concentrations of KHS (from 1.8 x $10^{-5}$ M to 1.8 x $10^{-4}$ M).

**W**hen the fluorescence intensity values were plotted against the KSH concentrations, a linear fit was observed (**Figure 2.18**).

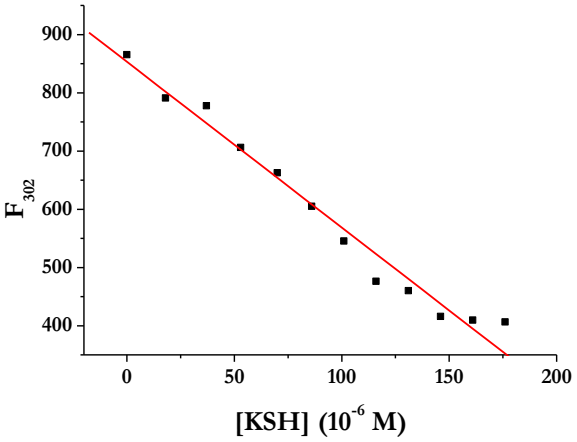


**Figure 2.18.** The relationship between the fluorescence intensity ($\lambda_{em}$ = 302 nm) and the KSH concentrations.

To gain insight in the binding mode of $H_2S$ to complex **4** $^1$H NMR experiment was taken. The $^1$H NMR spectrum of **4** recorded in $CD_3OD$ shows two sets of resonances, for the solvated and pyridine-coordinated species (black spectra,below). The addition of one equivalent of KSH to the NMR sample of **1** in $CD_3OD$ led to the appearance of a new pattern of resonances (red spectra, above). In particular in the aliphatic region of the spectrum, in place of the signals due to the ethyl groups of **4** and the corresponding solvated species, a new $A_3X_2$ pattern was detected (**Figure 2.19**).

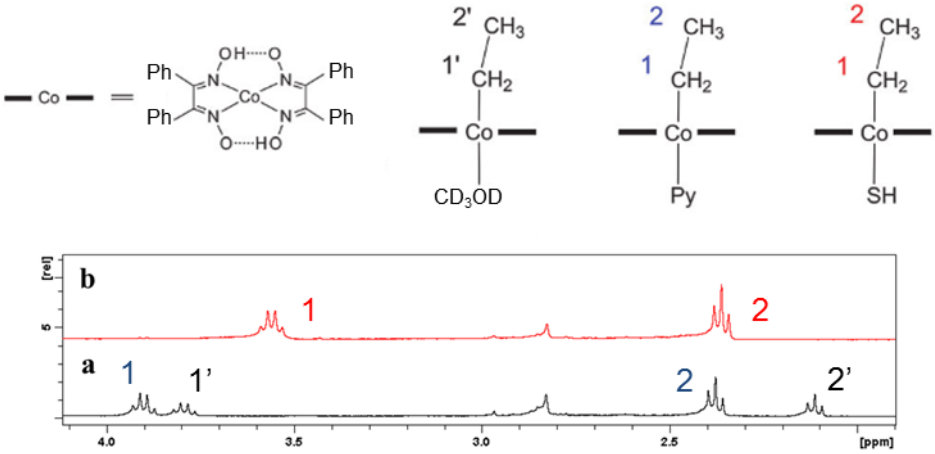


**Figure 2.19.** Aliphatic region of the $^1$H NMR spectrum of $[Co(dfgH)_2(CH_2CH_3)(py)]$ (**4**) before (**a**) and after the addition of 1 (**b**) equivalent of KSH ([**4**] = $7.7 \cdot 10^{-6}$ M, $CD_3OD$, rt, 400 MHz).

Differently than in the case of complex **4** for complex **5** was possible to obtain a KSH-dependent fluorescence response in Milli-Q water solution. Again a fluorescence quenching (SR ~ 40%) was observed when adding an excess of KSH to complex **5** (**Figure 2.20**), even if lower than that obtained with the complex **4**.

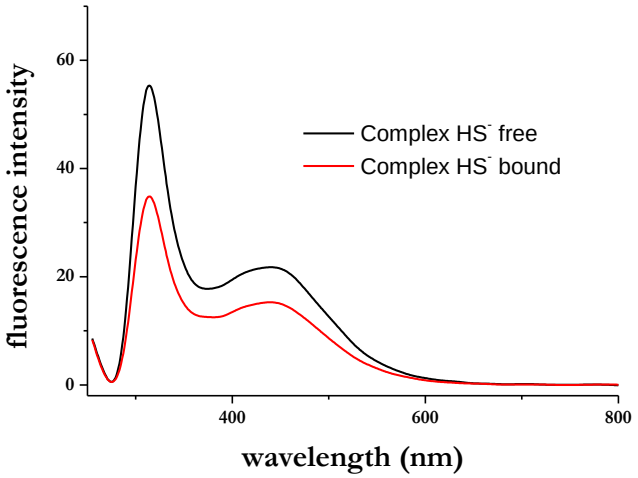


**Figure 2.20.** Emission spectra of [Co(dmgH)$_2$(ph)(py)] (**4**) ($\lambda_{exc}$ = 314 nm) before and after addition of an excess of KSH.

Also with this complex, when increasing amounts of KSH were added, a progressive quenching of fluorescence was observed (**Figure 2.21**).

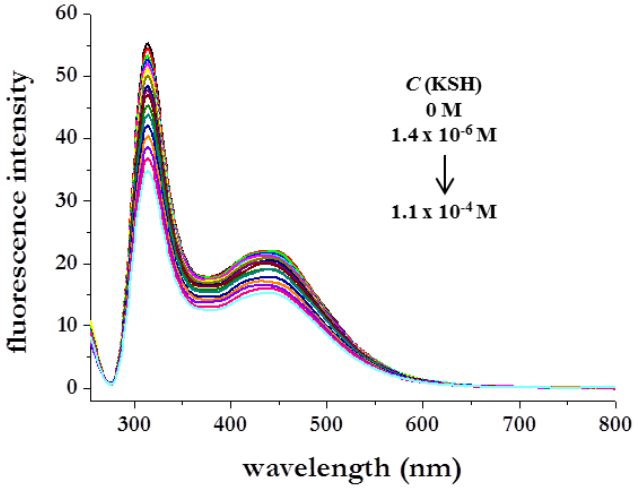


**Figure 2.21.** Emission spectra of [Co(dmgH)$_2$(ph)(py)] (**4**) ($\lambda_{exc}$ = 250 nm, rt, 2.7 x $10^{-6}$ M, $H_2O$) upon addition of increasing concentrations of KHS (from 1.4 x $10^{-6}$ M to 1.1 x $10^{-4}$ M).

For both complex **4** and complex **5** in the presence of either L-cysteine or glutathione, was observed SRs significantly lower than those found with KSH (**Figure 2.22**).

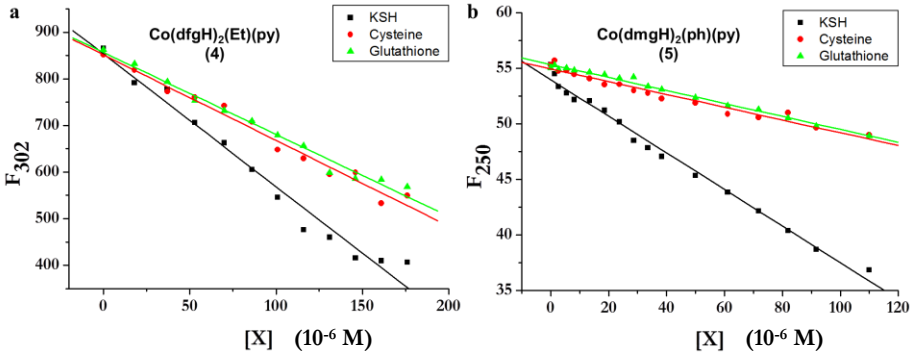


**Figure 2.22.** The relationship between the fluorescence intensity ((**a**) [**4**] = $3.9 \cdot 10^{-6}$ M, $\lambda_{em}$ = 302 nm; (**b**) [**5**] = $2.7 \cdot 10^{-6}$ M, $\lambda_{em}$ = 250 nm); and the concentrations of KSH, cysteine, glutathione ((**a**) from $1.8 \cdot 10^{-5}$ M to $1.8 \cdot 10^{-4}$ M, (**b**) from $1.4 \cdot 10^{-6}$ M to $1.1 \cdot 10^{-4}$ M).

### 2.2.3. Conclusions

In summary the potential of a family of model complexes of Vitamin B12 has been investigated as $H_2S$ sensors in aqueous solution. Clear evidence that complex **1** can be successfully used for the optical detection of $H_2S$ has been provided. High selectivity of the devised construct over potentially competing thiols and other biologically related species has been also shown. To gain further insights in the mechanism of recognition of $H_2S$ mono-dimensional and bi-dimensional NMR experiments were performed. DFT calculations shed further light on the binding mechanism of $H_2S$ to the title complex. However, the main limit of the complex **1** is the lack of fluorescence response. Efforts to modify the skeleton of the devised

construct to translate the absorption information into fluorescence information led to two new fluorescent $H_2S$ sensor (complex **4** and complex **5**). In particular complex **5** works successfully in water. However, these complexes show a turn-off fluorescence response, that is not the most satisfactory for our purpose. Indeed, energy transfer, collisional quenching and photobleaching can also led to a fluorescence turn-off.

## 2.3. Reference List


1. (*a*) X. Bailly, S. J. Vinogradov, *J. Inorg. Biochem.* **2005**, *99*, 142; (*b*) R. E. Weber, S. N. Vinogradov, *Physiol. Rev.* **2001**, *81*, 569.

2. (*a*) A. K. Mustafa, M. M. Gadalla, N. Sen, S. Kim, W. Mu, S. K. Gazi, R. K. Barrow, G. Yang, R. Wang, S. H. Snyder, *Sci Signal* **2009**, *2*, ra72; (*b*) B. D. Paul, S. H. Snyder, *Nat. Rev. Mol. Cell. Biol.* **2012**, *13*, 499.

3. (*a*) A. Van de Louw, P. Haouzi, *Critical Care* **2012**, *16*, R178; (*b*) A. Van de Louw, P. Haouzi, *Antioxid.Redox.Signal.* **2013**, *19*, 510.

4. A. Van de Louw, P. Haouzi, *ANTIOXIDANTS & REDOX SIGNALING* **2012**, *00*, 1.

5. (*a*) P. J. Toscano, L. G. Marzilli, *Prog. Inorg. Chem.* **1984**, *31*, 105; (*b*) N. Bresciani-Pahor, M. Forcolin, L. G. Marzilli, L. Randaccio, M. F. Summers, P. J. Toscano, *Coord. Chem. Rev.* **1985**, *63*, 1.

6. B. D. Gupta, K. Qanungo, *J. Organomet. Chem.* **1997**, *543*, 125.

7. (*a*) K. L. Brown, D. Lyles, M. Pencovici, R. G. Kallen, *J. Am. Chem. Soc.* **1975**, *97*, 7338; (*b*) K. L. Brown, A. W. Awtrey, *Inorg. Chem.* **1978**, *17*, 111.

8. (*a*) P. J. Toscano, G. Marzilli, *Prog. Inorg. Chem.* **1984**, *31*, 105; (*b*) N. Bresciani-Pahor, M. Forcolin, L. G. Marzilli, L. Randaccio, M. F. Summers, P. J. Toscano, *Coord. Chem. Rev.* **1985**, *63*, 1.

9. (*a*) S. L. Chatwin, R. A. Diggle, R. F. Jazzar, S. A. MacGregor, M. F. Mahon, M. K. Whittlesey, *Inorg. Chem.* **2003**, *42*, 7695; (*b*) D. C. Mudalige, E. S. Ma, S. J. Rettig, B. R. James, W. C. Cullen, *Inorg. Chem.* **1997**, *36*, 5426; (*c*) D. Sellman, P. Lechner, F. Knoch, M. Moll, *J. Am. Chem. Soc.* **1992**, *114*, 922.

10. T. H. Edwards, N. K. Moncur, L. E. Snyder, *J. Chem. Phys.* **1967**, *46*, 2139.

11. C. A. Ghilardi, S. Midollini, A. Orlandini, G. Scapacci, *J. Chem. Soc., Dalton Trans.* **1992**, 2909.

12. M. di Vaira, S. Midollini, L. Sacconi, *Inorg. Chem.* **1979**, *18*, 3466.

13. M. D. Hartle, S. K. Sommer, S. R. Dietrich, M. D. Pluth, *Inorg. Chem.* **2014**, *53*, 7800.

14. A. Müller, E. Diemann, in *Comprehensive coordination chemistry*, ed. G. Wilkinson, R. D. Gillard, J. A. McCleverty, Pergamon Press, Oxford, UK, **1987**, ch. 161, vol *2*.

15. S. M. Polson, L. Hansen, L. G. Marzilli, *Inorg. Chem.* **1997**, *36*, 307.

16. (*a*) K. L. Brown, R. G. Kallen, *J. Am. Chem. Soc.* **1972**, *94*, 1894; (*b*) G. Pellizer, G. R. Tauszik, G. Costa, *J. Chem. Soc., Dalton Trans.* **1973**, 317; (*c*) T. C. Higgs, D. Ji, R. S. Czernuszewicz, B. F. Matzanke, V. Schunemann, A. X. Trautwein, M. Helliwell, W. Ramirez, C. Carrano, J. *Inorg. Chem.* **1998**, *37*, 2383.

17. M. Frisch, G. W. Trucks, H. B. Schlegel, G. E. Scuseria, M. A. Robb, J. R. Cheeseman, G. Scalmani, V. Barone, B. Mennucci, G. A. Petersson, H. Nakatsuji, M. Caricato, X. Li, H. P. Hratchian, A. F. Izmaylov, J. Bloino, G. Zheng, J. L. Sonnenberg, M. Hada,

M. Ehara, K. Toyota, R. Fukuda, J. Hasegawa, M. Ishida, T. Nakajima, Y. Honda, O. Kitao, H. Nakai, T. Vreven, J. A. Montgomery Jr., J. E. Peralta, F. Ogliaro, M. Berpark, J. J. Heyd, E. Brothers, K. N. Kudin, V. N. Staroverov, R. Kobayashi, J. Normand, K. Raghavachari, A. Rendell, J. C. Burant, S. S. Iyengar, J. Tomasi, M. Cossi, N. Rega, J. M. Millam, M. Klene, J. E. Knox, J. B. Cross, V. Bakken, C. Adamo, J. Jaramillo, R. Gomperts, R. E. Stratmann, O. Yazyev, A. J. Austin, R. Cammi, C. Pomelli, J. W. Ochterski, R. L. Martin, K. Morokuma, V. G. Zakrzewski, G. A. Voth, P. Salvador, J. J. Dannenberg, S. Dapprich, A. D. Daniels, O. Farkas, J. B. Foresman, J. V. Ortiz, J. Cioslowski, D. J. Fox, *Gaussian 09, revision A.02*, Gaussian, Inc., Wallingford, CT, **2009**.

18. A. D. Becke, *Phys. Rev. A: At., Mol., Opt. Phys.* **1988**, *38*, 3098.

19. (*a*) J. P. Perdew, *Phys. Rev. B: Condens. Matter, Mater. Phys.* **1986**, *33*, 8822; (*b*) J. P. Perdew, *Phys. Rev. B: Condens. Matter Mater. Phys.* **1986**, *34*, 7406.

20. J. Tomasi, B. Mennucci, R. Cammi, *Chem. Rev.* **2005**, *105*, 2999.

21. The solvent-corrected Gibbs free energies = gas-phase Gibbs free enrgies + (solvent-phase electronic energies – gas-phase electronic energies).

22. Z. Otwinowski, W. Minor, in *Methods in Enzymology, Part A*, ed. C. W. Carter and R. M. Sweet, Academic Press, London, **1997**, *276*, 307.

23. R. H. Blessing, *Acta Crystallogr., Sect. A: Found. Crystallogr.* **1995**, *51*, 33.

24. A. Altomare, M. C. Burla, M. Camalli, G. L. Cascarano, C. Giacovazzo, A. Guagliardi, A. G. Moliterni, G. Polidori, R. Spagna, *J. Appl. Crystallogr.* **1999**, *32*, 115.

25. G. M. Sheldrick, SHELX-97, *Program for Crystal Structure Refinement*, University of Gottingen, Germany, **1997**.

26. M. Nardelli, *J. Appl. Crystallogr.* **1995**, *28*, 659.

27. L. J. Farrugia, *J. Appl. Crystallogr.* **1999**, *32*, 837.

# Chapter 3: A Copper Porphyrin for Sensing $H_2S$ in Aqueous Solution via a "Coordinative-Based" Approach

## 3.1. Introduction

It is well known that $H_2S$ can bind to heme proteins, inducing different responses that in turn modulate its cytotoxic and cytoprotective activities.[1] In a previous work of my research group was devised as a fluorescent $H_2S$ sensor by exploiting a coordination-based approach makes use of a heme protein. In particular, was employed myoglobin from horse skeletal muscle (Mb).[2] A limitation of the Mb monitoring system was the low fluorescence enhancement in the presence of an excess of $H_2S$. Furthermore, with the addition of $H_2S$, Mb($Fe^{3+}$) was reduced to the ferrous from. Thus a mixture of Mb($Fe^{3+}$)–$H_2S$, Mb($Fe^{2+}$)–$H_2S$, and Mb($Fe^{2+}$) occurred in the cuvette samples that were measured. A similar reduction was observed by Scheidt et al. for the hydrosulfide ($HS^-$) coordination in iron porphyrinates.[3] Aiming at overcoming some of the limitations of this Mb-based $H_2S$ sensing system was used cobalt containing peptide deformylase (Co–PDF) for implementation in a $H_2S$ sensor by the same coordinative-based approach.[4] The Co–PDF system operates as

[1] R. Pietri, A. Lewis, R. G. Leon, G. Casabona, L. Kiger, S. R. Yeh, S. Fernandez-Alberti, M. C. Marden, C. L. Cadilla, J. Lopez-Garriga, *Biochemistry* **2009**, *48*, 4881.

[2] M. Strianese, F. De Martino, C. Pellecchia, G. Ruggiero, S. D'Auria, *Protein Pept. Lett.* **2011**, *18*, 282.

[3] J. W. Pavlik, B. C. Noll, A. G. Oliver, C. E. Schulz, W. R. Scheidt, *Inorg. Chem.* **2010**, *49*, 1017.

[4] M. Strianese, G. J. Palm, S. Milione, O. Kuhl, W. Hinrichs, C. Pellecchia, *Inorg. Chem.* **2012**, *51*, 11220.

a "turn-off" devise, which is a limitation for real applications (**Figure 3.1**).

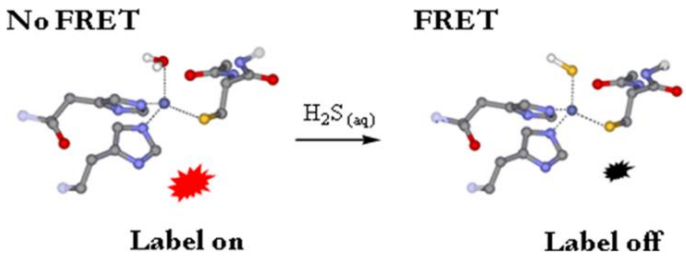


**Figure 3.1.** Mechanism of sensing of Co-PDF.

Recently Tang et al. exploited $H_2S$ binding to metal porphyrins with sensing purposes. More specifically, they reported a $Cu^{II}$-metalated 3D porous nanoscale metal–organic framework (nano-MOF) {CuL-$[AlOH]_2$}*n* [PAC; H6L = *meso*-tetrakis(4-carboxyphenyl)porphyrin] as a heterogeneous fluorescence probe for $H_2S$ detection.[5] Drawing upon these encouraging results and to improve an $H_2S$ sensors I focused on designing a simple copper porphyrin complex, which I reasoned could work by a coordinative-based approach.

## 3.2. Result and Discussion

### 3.2.1. Synthesis of Cu(II) Protoporphyrin IX

The target copper complex (Cu(II) Protoporphyrin IX, CuPPIX) was obtained in good yield by mixing an equimolar amount of

[5] Y. Ma, H. Su, X. Kuang, X. Li, T. Zhang, B. Tang, *Anal. Chem.* **2014**, *86*, 11459.

protoporphyrin IX and $Cu(CH_3COO)_2$ in glacial acetic acid by following a literature procedure (**Scheme 3.1**).[6]

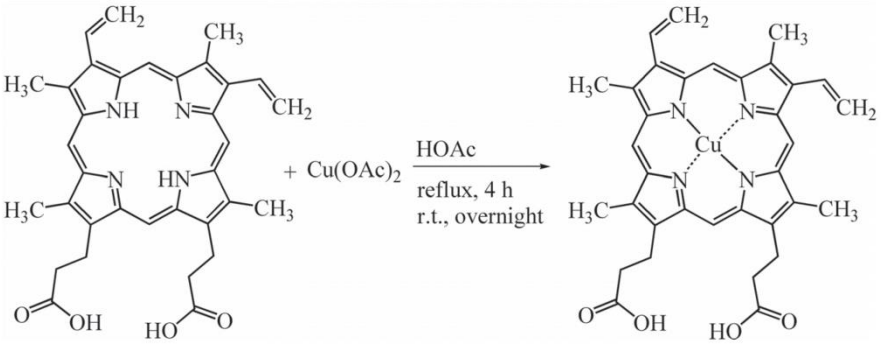


**Scheme 3.1.** Synthesis of CuPPIX.

The stoichiometry was confirmed by ESI-MS where the major peak at 663.1 *m/z* units corresponds to the mononuclear $[(CuPPIX)K]^+$ species. Less intense peaks at 647.2 and 623.7 were visible and were attributed to the species $[(CuPPIX)Na]^+$ and $[CuPPIX]^+$, respectively. No evidence for binuclear species in solution was found. Because of the paramagnetism of the copper center, the $^1H$ NMR spectrum of CuPPIX showed featureless broad resonances. CuPPIX was further characterized by UV/Vis and fluorescence spectroscopy in MilliQ water solutions (see **Figures 3.2** and **3.3**). The UV/Vis spectrum was detected in basic water (pH 12.6) because of the poor solubility of the complex in pure water. Protoporphyrin IX bears two carboxylic moieties, which are deprotoneted in basic solution and, therefore, the related salt was soluble. The UV/Vis spectrum of CuPPIX (which

[6] G. D. Dorough, J. R. Miller, F. M. Huennekens, *J. Am. Chem. Soc.* **1951**, *73*, 4315.

resembles those of similar metal porphyrin complexes[7]) exhibits the B-band (Soret band) at 385 nm with a shoulder at 343 nm. The Q-bands appear collapsed into two transitions at 538 nm and 575 nm, from an increase in symmetry of the molecule upon addition of the metal ion (**Figure 3.3**).

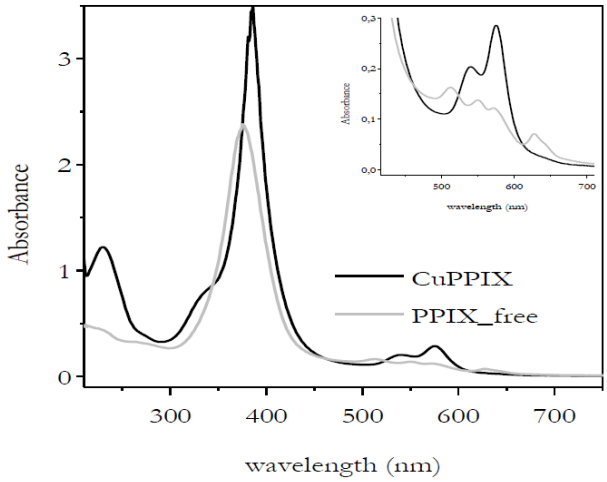


**Figure 3.2.** Electronic absorption spectra of CuPPIX and PPIX free in MilliQ water (pH = 12.6; r.t.). [CuPPIX ] = [PPIX] = $3.5 \cdot 10^{-5}$ M. Insert = enlargement of the 400-700 nm zone.

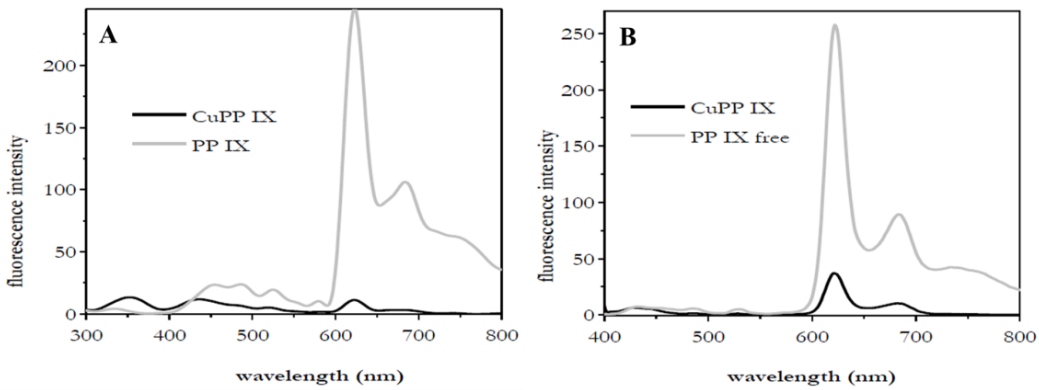


[7] I. T. Oliver, W. A. Rawlinson, *Biochem. J.* **1955**, *61*, 641.

**Figure 3.3. A**. Fluorescence emission spectra ($\lambda_{exc}$ 230 nm) of CuPPIX and PPIX free in MilliQ water (pH = 12.6; r.t.). [CuPPIX ] = [PPIX] = $5.2 \cdot 10^{-5}$ M **B**. Fluorescence emission spectra ($\lambda_{exc}$ 386 nm) of CuPPIX and PPIX free in MilliQ water (pH = 12.6 ; r.t.). [CuPPIX ] = [PPIX] = $5.2 \cdot 10^{-5}$ M.

The fluorescence spectrum displays intense fluorescence originating from the first ($S_1$) excited singlet state (the Q state). The band with two peaks at 623 nm and 682 nm is mirror symmetric to the absorption spectrum in the Q region. The fluorescence originating from the second ($S_2$) excited singlet state (the B state) is generally quenched in copper porphyrins because of an efficient relaxation pathway ending in a triplet state. The fluorescence spectrum of CuPPIX is consistently weaker than that of the free porphyrin ligand (**Figure 3.3**), which is most likely due to the coordination of the free ligand to the paramagnetic $Cu^{2+}$ center.[8]

### 3.2.2. $H_2S$ Sensing

$H_2S$ binding to CuPPIX was first assessed by UV/Vis spectroscopy. When KSH (a commonly employed $H_2S$ donor) was added to a MilliQ water solution of CuPPIX a clear change of the initial spectrum was observed. **Figure 3.4** shows a typical UV/Vis spectrum of a solution containing $2 \cdot 10^{-5}$ M of CuPPIX in which the hyperchromic shift of the Soret band is particularly evident. The system was then studied by fluorescence spectroscopy.

[8] L. E. Santos-Figueroa, C. de la Torre, S. El Sayed, F. Sancenon, R. Martinez-Manez, A. M. Costero, S. Gil, M. Parra, *Eur. J. Inorg. Chem.* **2014**, 41.

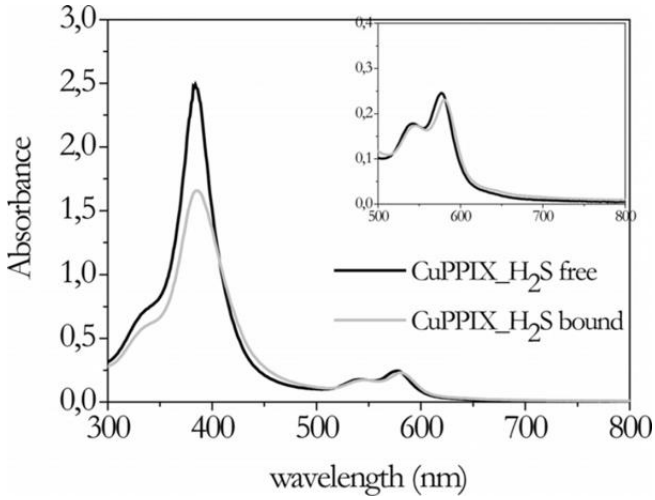


**Figure 3.4.** Electronic absorption spectra of CuPPIX free and upon addition of an excess of KSH (r.t., MQ water, pH = 12.6). [CuPPIX] = $2 \cdot 10^{-5}$ M; [KSH] = $2 \cdot 10^{-4}$ M.

In the presence of KSH, a significant enhancement of the $S_2$ fluorescence emission was observed. **Figure 3.5** shows a typical fluorescence emission spectrum of a solution containing $2 \cdot 10^{-5}$ M of CuPPIX when excited at 386 nm.

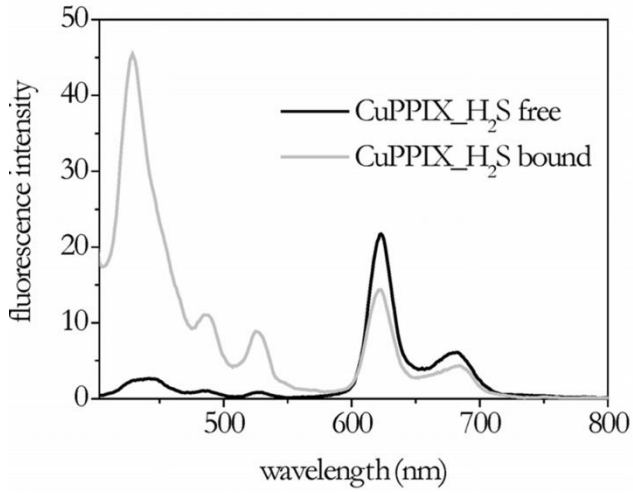


**Figure 3.5.** Emission spectra of CuPPIX free ($\lambda_{ex}$ = 386 nm) and upon addition of an excess of KSH (r.t., MQ water, pH = 12.6). [CuPPIX] = $2 \cdot 10^{-5}$ M; [KSH] = $2 \cdot 10^{-4}$ M.

To assess whether the amount of the fluorescence enhancement of CuPPIX varies with the concentration of the analyte, the fluorescence intensity of the system was monitored after the addition of increasing amounts of KSH solution. **Figure 3.6** shows that there is a clear dependence of the fluorescence intensity displayed by the CuPPIX on the KSH concentration.

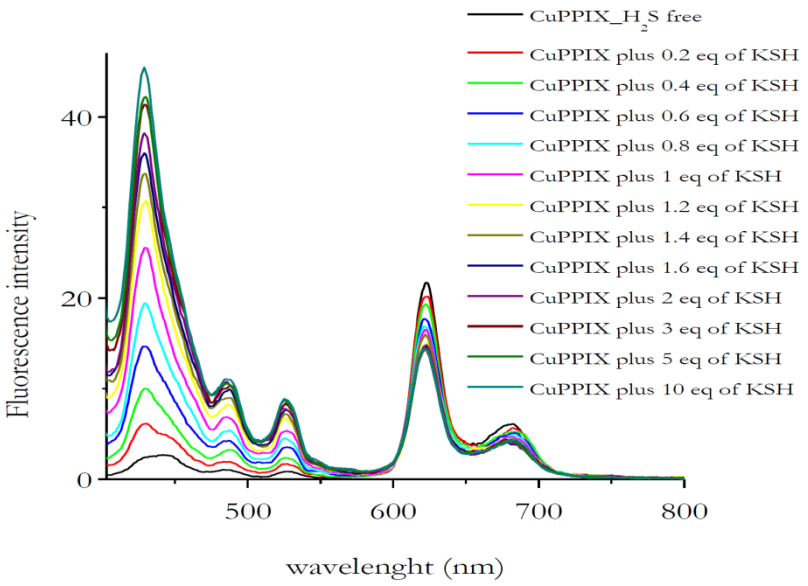


**Figure 3.6.** Emission spectra of CuPPIX (exc 386 nm) when titrated with KSH (rt, MQ water, pH = 12.6). [CuPPIX] = $2 \cdot 10^{-5}$ M; end concentration of KSH varied in the range 4-$200 \cdot 10^{-6}$ M.

To obtain an indication of the selectivity of the construct, the fluorescence intensity of CuPPIX in the presence of biologically relevant and potentially competing thiols [e.g., L-cysteine (L-cys) and glutathione (GSH)] or in the presence of a range of anions or of common oxidants was checked. **Figure 3.7** shows the obtained results. For the species investigated we observed fluorescence trends

completely different from those found with KSH suggesting a good selectivity of our probe under the experimental conditions tested.

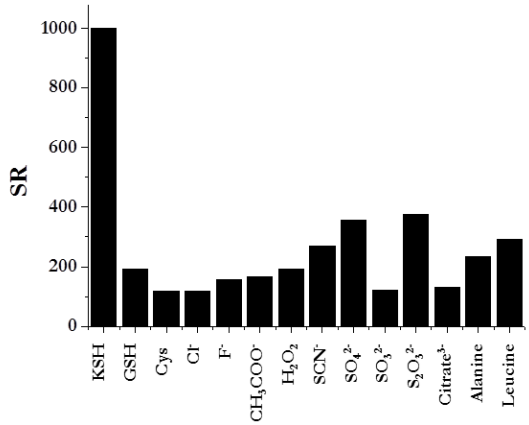


**Figure 3.7.** Relative fluorescence emission at 430 nm ($\lambda_{ex}$ = 386 nm) of CuPPIX ($2.0 \cdot 10^{-5}$ M) in the presence of KSH ($2.0 \cdot 10^{-5}$ M), glutathione (GSH), cysteine, $Cl^{-}$, $F^{-}$, $CH_3COO^{-}$, $H_2O_2$, $SCN^{-}$, $SO_4^{2-}$, $SO_3^{2-}$, $S_2O_3^{2-}$, alanine, and leucine ($1.2 \cdot 10^{-3}$ M) in an aqueous solution. Spectra were registered when the fluorescence reached the threshold value, which corresponds to the saturation point in our case.

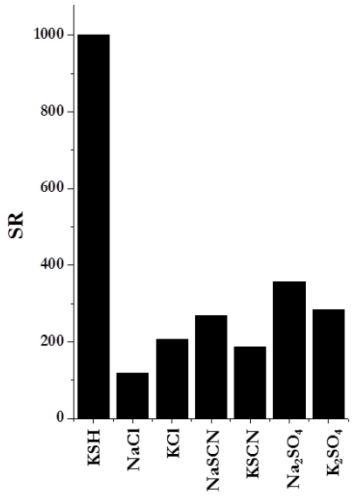


**Figure 3.8.** Relative fluorescence emission at 430 nm ($\lambda_{ex}$= 386 nm) of CuPPIX ($2.0 \cdot 10^{-5}$ M) in the presence of KSH ($2.0 \cdot 10^{-5}$ M), NaCl, KCl, NaSCN, KSCN, $Na_2SO_4$ , $K_2SO_4$ ($1.2 \cdot 10^{-3}$ M) in aqueous solution.

We also studied whether there was any effect when substituting the potassium salts (as a source of anions) with the sodium ones. No significant effects were found (**Figure 3.8**).

To investigate the potential of the implemented devise we determined its sensitivity. We found that the sensor still gives an evident fluorescence enhancement with a concentration of $1 \cdot 10^{-6}$ M of KSH. Thus the detection limit for the implemented devise is in the sub-micromolar range (**Figure 3.9**).

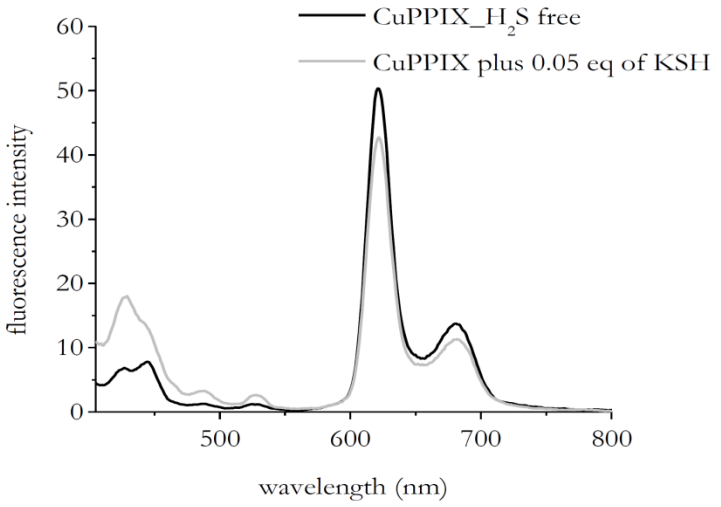


**Figure 3.9.** Emission spectra of CuPPIX_$H_2S$ free (exc 386 nm) and in the presence of KSH (rt, MQ water, pH = 12.6). [CuPPIX] = $2 \cdot 10^{-5}$ M; end concentration of KSH = $1 \cdot 10^{-6}$ M.

In order to gain independent evidence for the binding of $H_2S$ to CuPPIX we examined the reaction by NMR spectroscopy. At first we analyzed the $^1$H NMR spectrum of complex CuPPIX in the presence of excess $H_2S$. No significant change in the initial $^1$H NMR spectrum was observed upon addition of $H_2S$ to a $D_2O$ solution of CuPPIX, excluding the fact that the excess of anion can extract the metal from

the complex causing the release of the porphyrin ligand. It is well known that metals can catalyze the oxidation of $HS^-$ to polysulfides and also that copper easily undergoes redox chemistry. To exclude the possible oxidation of $HS^-$ to HSSH[9] (**Figure 3.10**), we tracked the reaction between the title complex and $H_2S$ by quantitative NMR spectroscopic analysis.

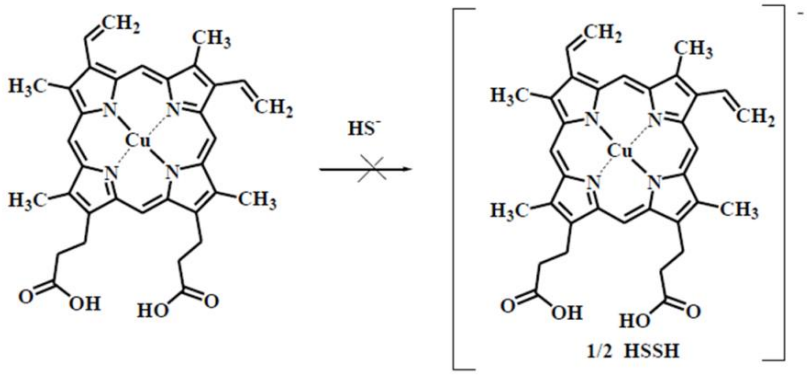


**Figure 3.10.** Possible oxidation CuPPIX-mediate of $HS^-$ to HSSH.

We followed a literature protocol for detecting and determining the possible presence of polysulfide species in solution, which consists of the alkylation of the polysulfide ions with dimethyl sulfate.[10]

The reaction was carried out in water with a complex/KSH molar ratio of 1:20 at room temperature under aerobic conditions. At the same time a control reaction (without complex) was also performed. No peaks ascribable to disulfides or polysulfides could be detected. Perfectly superimposable $^1$H NMR and $^{13}$C NMR spectra for the two

[9] M. D. Hartle, S. K. Sommer, S. R. Dietrich, M. D. Pluth, *Inorg. Chem.* **2014**, *53*, 7800.

[10] (*a*) I. Filpponen, A. Guerra, A. Hai, L. A. Lucia, D. S. Argyropoulos, *Ind. Eng. Chem. Res. 2***006**, *45*, 7388; (*b*) D. S. Argyropoulos, Y. Hou, R. Ganesaratnam, D. N. Harpp, K. Koda, *Holzforschung* **2005**, *59*, 124.

reactions were obtained (**Figure 3.11**). This clearly indicates that $HS^-$ is not oxidated to disulfides/polysulfides by the title complex. Then we studied the reaction between CuPPIX and $H_2S$ by electrospray ionization mass spectrometry in aqueous solution. No peaks ascribable to the free ligand could be detected, which confirms what we had already seen from NMR spectroscopy. The major peak at 679.24 *m*/*z* units is consistent with the mononuclear $[(CuPPIX)NaHS]^-$ species, which suggests analyte binding to the copper complex. To the best of our knowledge, this is the first example of such a reaction. Typically, in the presence of $H_2S$, literature copper complexes undergo a demetalation reaction with concomitant release of the organic ligand.[11] Coordination of organic bases to copper porphyrins have already been observed by Glazkov et al.[12]

[11] L. E. Santos-Figueroa, C. de la Torre, S. El Sayed, F. Sancenon, R. Martinez-Manez, A. M. Costero, S. Gil, M. Parra, *Eur. J. Inorg. Chem.* **2014**, 41.

[12] (*a*) Y. Glazkov, A. I. Vrublevskii, E. K. Kruglik, T. F. Kachura, *J. Appl. Spectrosc.* **1981**, *35*, 1254; (*b*) A. I. Vrublevskii, Y. Glazkov, T. F. Kachura, *J. Appl. Spectrosc.* **1984**, *41*, 1166.

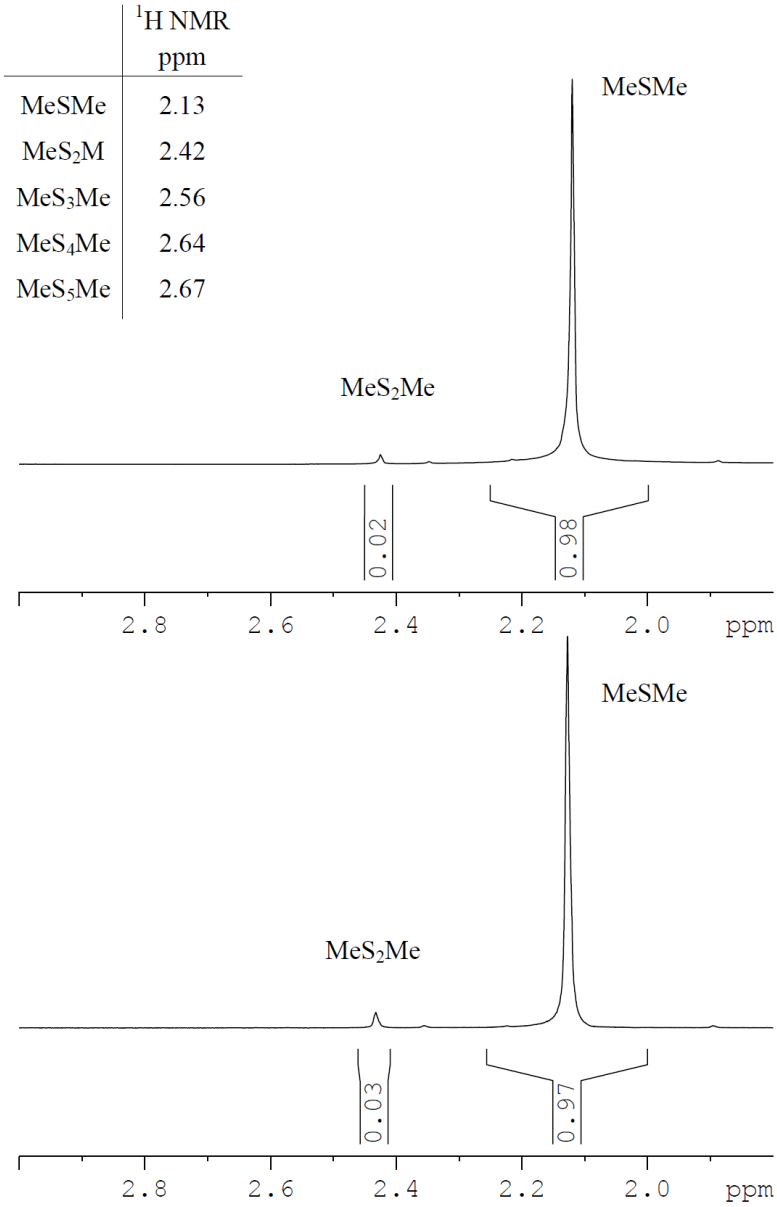


**Figure 3.11.** $^1$H NMR spectra for the polysulfides determination experiment (see experimental part). The upper spectrum shows the sample without CuPPIX (control reaction); the lower spectrum is that of the sample in the presence of CuPPIX. Peaks assignment was made on the basis of reference 9.

### 3.2.3. Conclusions

In conclusion CuPPIX can be successfully used as a "turn on", sensitive and selective fluorescence probe for the detection of $H_2S$ in aqueous environments via a coordinative-based approach. The probe can selectively and sensitively detect $HS^-$ anions in water over other anions, biothiols, and common oxidants such as $H_2O_2$. $^1H$ NMR and ESI-MS experiments provide clear evidence that the turn-on response in the presence of $H_2S$ is ascribed to binding of the target analyte to the copper center. We are currently investigating the mechanism by which the $S_2$ fluorescence in CuPPIX is prompted by the coordination of the hydrogen sulfide to the copper center.

## 3.3. Reference List

1. R. Pietri, A. Lewis, R. G. Leon, G. Casabona, L. Kiger, S. R. Yeh, S. Fernandez-Alberti, M. C. Marden, C. L. Cadilla, J. Lopez-Garriga, *Biochemistry* **2009**, *48*, 4881.

2. M. Strianese, F. De Martino, C. Pellecchia, G. Ruggiero, S. D'Auria, *Protein Pept. Lett.* **2011**, *18*, 282.

3. J. W. Pavlik, B. C. Noll, A. G. Oliver, C. E. Schulz, W. R. Scheidt, *Inorg. Chem.* **2010**, *49*, 1017.

4. M. Strianese, G. J. Palm, S. Milione, O. Kuhl, W. Hinrichs, C. Pellecchia, *Inorg. Chem.* **2012**, *51*, 11220.

5. Y. Ma, H. Su, X. Kuang, X. Li, T. Zhang, B. Tang, *Anal. Chem.* **2014**, *86*, 11459.

6. G. D. Dorough, J. R. Miller, F. M. Huennekens, *J. Am. Chem. Soc.* **1951**, *73*, 4315.

7. L. E. Santos-Figueroa, C. de la Torre, S. El Sayed, F. Sancenon, R. Martinez-Manez, A. M. Costero, S. Gil, M. Parra, *Eur. J. Inorg. Chem.* **2014**, 41.

8. M. D. Hartle, S. K. Sommer, S. R. Dietrich, M. D. Pluth, *Inorg. Chem.* **2014**, *53*, 7800.

9. (*a*) I. Filpponen, A. Guerra, A. Hai, L. A. Lucia, D. S. Argyropoulos, *Ind. Eng. Chem. Res. 2***006**, *45*, 7388; (*b*) D. S. Argyropoulos, Y. Hou, R. Ganesaratnam, D. N. Harpp, K. Koda, *Holzforschung* **2005**, *59*, 124.

10. L. E. Santos-Figueroa, C. de la Torre, S. El Sayed, F. Sancenon, R. Martinez-Manez, A. M. Costero, S. Gil, M. Parra, *Eur. J. Inorg. Chem.* **2014**, 41.

11. (*a*) Y. Glazkov, A. I. Vrublevskii, E. K. Kruglik, T. F. Kachura, *J. Appl. Spectrosc.* **1981**, *35*, 1254; (*b*) A. I. Vrublevskii, Y. Glazkov, T. F. Kachura, *J. Appl. Spectrosc.* **1984**, *41*, 1166.

# Chapter 4: Azurin as a $H_2S$ Sensor.

## 4.1. Introduction

Exploiting the previous experience on the copper complexes as $H_2S$ sensors, I decided to focus my attention on the Azurin. This work has been carried out in collaboration with the group of Professor Canters, of the University of Leiden. Azurin is a copper protein expressed in a very easy way and very stable in nature, two positive characteristics in the implementation of a sensor. Azurin, a 14 kDa protein derived from bacterial species especially from *Pseudomonas aeruginosa* function as a donor in terminal electron transfer process.[1] Azurin is one of the blue copper proteins, so called because of their intense absorption band in the visible part of the spectrum ($\lambda_{max}$ = 600 to 625 nm). The presence of copper ion in the polypeptide chain contributes to the azurin stability.[2] In azurin the metal in the active site is immobilized by three strong ligands (the nitrogen donors $His^{46}$ and $His^{117}$, and the sulfur donor $Cys^{112}$) and a fourth weaker axial ligand (the sulfur donor $Met^{121}$). The carbonyl oxygen of $Gly^{45}$ provides for an additional axial interaction (**Figure 4.1**). The spectroscopic properties of the metal site are dominated by the copper-sulfur ($Cys^{112}$) interaction (14).[3]

[1] I. Pozdnyakova, J. Guidry, P. Wittung-Stafshede, *Archives of Biochemistry and Biophysics* **2001**, *390*, 146.
[2] (*a*) I. Pozdnyakova, J. Guidry, P. Wittung-Stafshede, *Biophysical Journal* **2002**, *82*, 2645; (*b*) I. Pozdnyakova, P. Wittung-Stafshede, *Biochemistry* **2001**, *40*, 13728.
[3] E. I. Solomon, M. D. Lowery, *Science* **1993**, *259*, 1575.

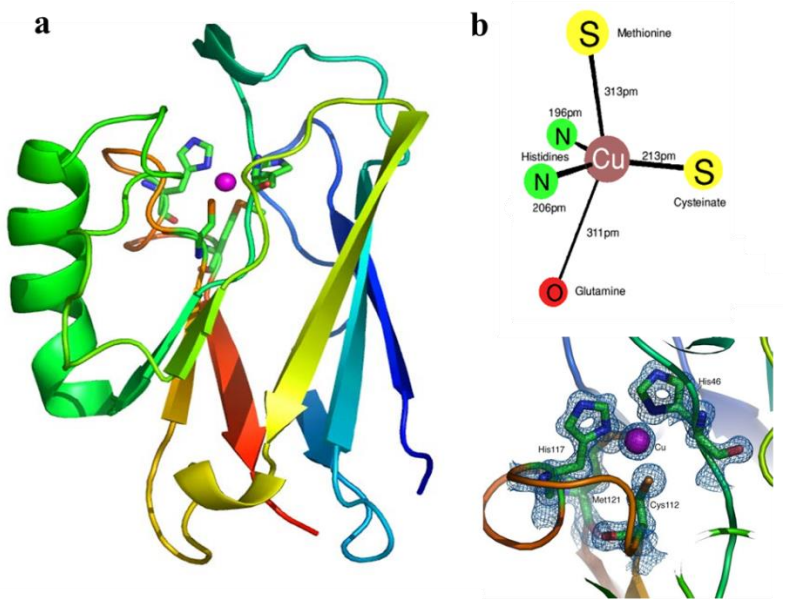


**Figure 4.1. a**) Standard ribbon representation of azurin: active site is on top and $\alpha$-helix on the left (with N-terminus on bottom and C-terminus on top). **b**) Active site atoms.

In the native protein this interaction is responsible, among others, for two sulfur-copper charge transfer transitions in the optical absorption spectrum, a weak one around 400 nm and a strong one around 600 nm, a pattern that is characteristic of a (distorted) tetrahedral “type 1” site. Furthermore, this metal-protein has been previously expressed and purified in various mutants and this opens up a wide range of possibilities to go to functionalize the system in fluorescence in a rather targeted.

The approach I decided to follow for this sensor to be implemented with the azurin is an approach based on a particular technique of fluorescence that takes the name of FRET. Fluorescence resonance energy transfer (FRET) has become widely used in all applications of fluorescence, including medical diagnostics and optical imaging. The

widespread use of FRET is due to the favorable distances for energy transfer, which are typically the size of a protein. Additionally, the extent of FRET is readily predictable from the spectral properties of the fluorophores. If the spectral properties of the fluorophores allow FRET, it will occur and will not be significantly affected by the biomolecules in the sample. These favorable properties allow for the design of experiments based on the known sizes and structural features of the sample.

FRET is an electrodynamic phenomenon that can be explained using classical physics. In the process of FRET, initially a donor fluorophore (D) absorbs the energy due to the excitation of incident light and transfer the excitation energy to a nearby chromophore, the acceptor (A) in the ground state.

$$D + h\nu \rightarrow D^*$$

$$D^* + A \rightarrow D + A^*$$

$$A^* \rightarrow A + h\nu'$$

The donor molecules typically emit at shorter wavelengths that overlap with the absorption spectrum of the acceptor. Energy transfer occurs without the appearance of a photon and is the result of long-range dipole-dipole interactions between the donor and acceptor (**Figure 4.2**).

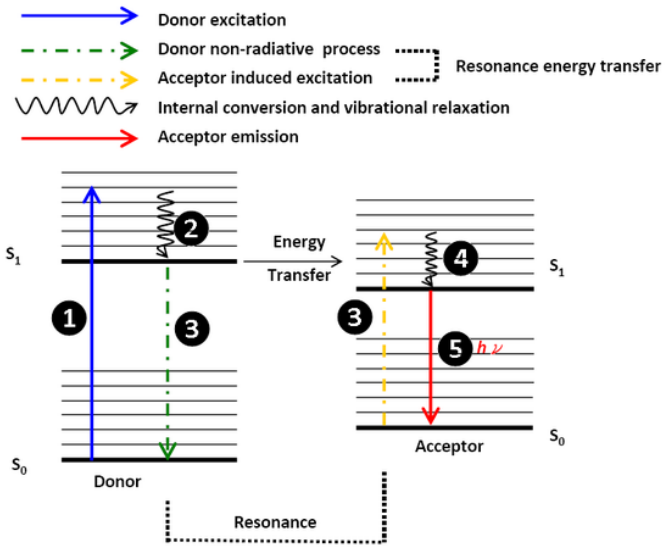


**Figure 4.2.** Schematic Diagram of Förster Resonance Energy Transfer.

The rate of energy transfer depends upon the extent of spectral overlap $J(\lambda)$ of the emission spectrum of the donor with the absorption spectrum of the acceptor (that should be as large as possible, **Figure 4.3**), the quantum yield of the donor, the relative orientation of the donor and acceptor transition dipoles, and the distance R between the donor and acceptor molecules (which also appears to the sixth power FRET efficiency).

$$E_{FRET} = R_0^6/(R^6+R_0^6)$$

Where $R_0$ is the Förster radius at which half of the excitation energy of donor is transferred to the acceptor chromophore. Therefore Förster radius ( $R_0$ ) is referred to as the distance at which the efficiency of energy transfer is 50%. $R_0$ is a function of quantum yield of the donor chromophore $\Phi_D$ , spectral overlap of donor and acceptor

*J(λ)*, directional relationship of transition dipoles $\kappa^2$ and the refractive index of the medium $\eta$.

$$(R_0)^6 \propto \kappa^2 \cdot \Phi_D \cdot J(\lambda) \cdot \eta^{-4}$$

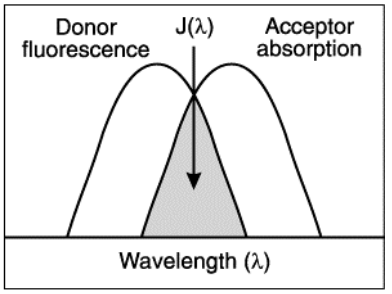


**Figure 4.3.** The schematic diagram of spectral overlap.

## 4.2. Result and Discussion

### 4.2.1. Azurin Wild Type

To test the possible use of the system as fluorescence $H_2S$ biosensor, $H_2S$ binding to azurin was firstly assessed via UV-visible spectroscopy. When adding KSH to a azurin solution, the absorption spectrum significantly changed. KSH addition results in the increase of the 280 nm band and in the quenching of the 630 nm band (**Figure 4.4**).

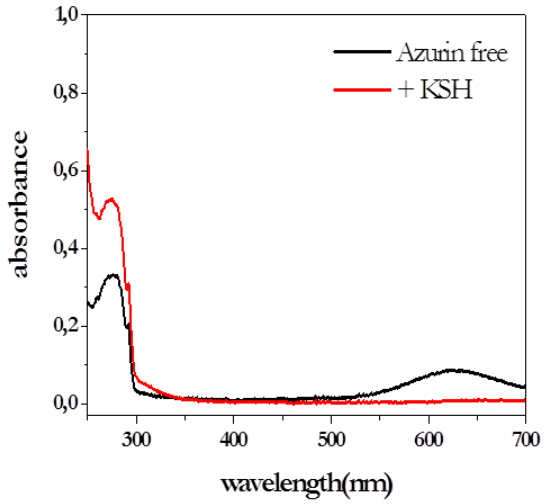


**Figure 4.3.** Electronic absorption spectra of azurine (rt, black line, 4.5 x $10^{-5}$ M in potassium phosphate buffer (100 mM, pH = 6.8)) and after addition of KSH (rt, red line, 2 x $10^{-4}$ M in potassium phosphate buffer (100 mM, pH = 6.8)).

I decided to covalently attach a fluorescent label to the protein whose emission spectrum overlaps with the 630 nm band of the protein in its $HS^-$-free state. The most commonly used amine-reactive dye derivatives are N-hydroxysuccinimidyl(NHS)-esters. NHS-esters readily react with amino groups of proteins, i.e. the ε-amino groups of lysines or the amine terminus, forming a chemically stable amide bond between the dye and the protein.[4] In this way, the label fluorescence will follow the difference in spectral overlap between the $HS^-$-free and $HS^-$-bound states of the azurin via a FRET mechanism (**Figure 4.4**).

[4] Labelling ratios were in the range 0.12-0.83 (dye molecule/protein).

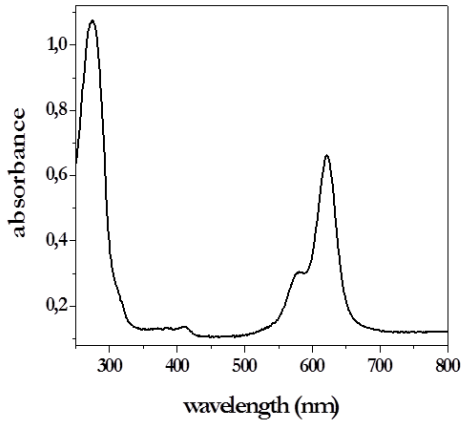


**Figure 4.4.** Electronic absorption spectra of azurine covalently functionalized with the Atto620 dye label on the available amine groups.

That is, when the protein is in the $HS^-$-free state all the energy absorbed by the label is (partially) quenched due to FRET to the 630 nm band. On the other hand, in the $HS^-$-bound state of azurin, the label fluorescence is emitted as fluorescence (**Figure 4.5**).

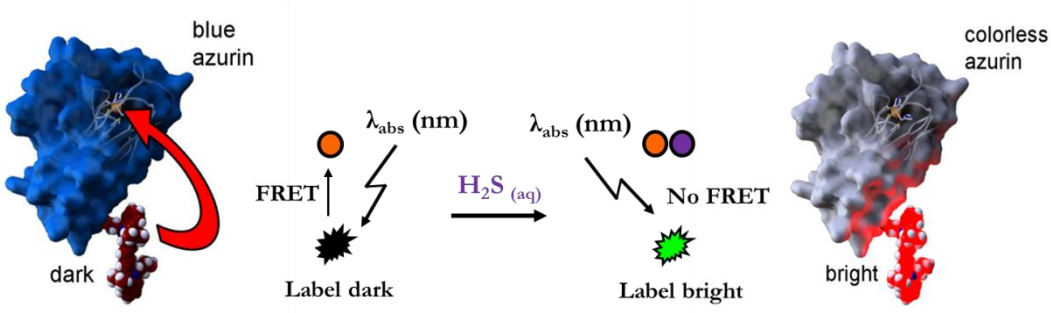


**Figure 4.5.** Schematic mechanism of FRET.

Indeed when monitoring the fluorescence intensity of Atto620 labelled azurin wild type and adding an excess of KSH a clear fluorescence increasing was observed (**Figure 4.6**).

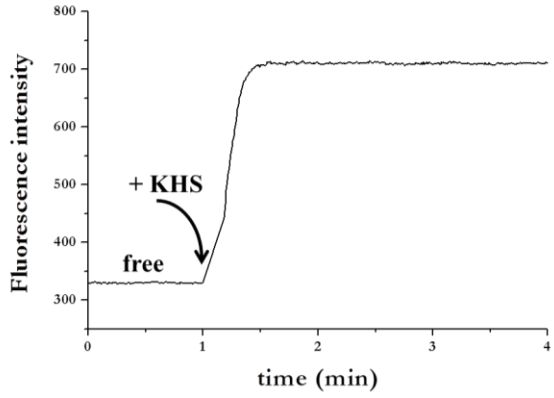


**Figure 4.6.** Fluorescence time trace ( $\lambda_{em}$ = 630 nm) of Atto620 labelled azurin. Azurine (4 x $10^{-5}$ M in potassium phosphate buffer (100 mM, pH = 6.8)) and after addition of KSH (rt, red line, 4 x $10^{-4}$ M in potassium phosphate buffer (100 mM, pH = 6.8)).

However, when adding GSH through the azurin solution, the fluorescence spectrum show a similar change. So, this system has not proved selective (**Figure 4.7**).

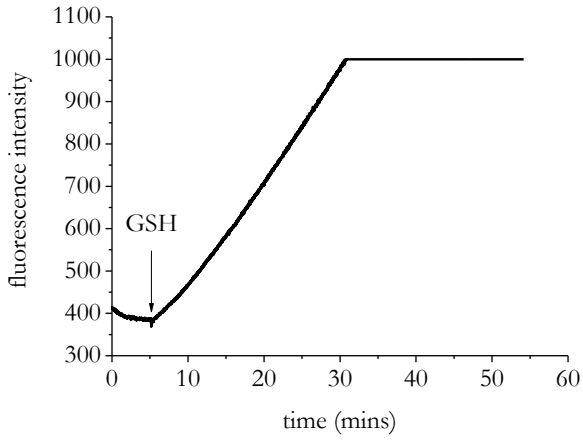


**Figure 4.7.** Fluorescence time trace ( $\lambda_{em}$ = 630 nm) of Atto620 labelled azurin. Azurine (5 x $10^{-5}$ M in potassium phosphate buffer (100 mM, pH = 6.8)) and after addition of GSH (rt, red line, 5 x $10^{-4}$ M in potassium phosphate buffer (100 mM, pH = 6.8)).

Indeed was thought to change the metal in the active site.

### 4.2.2. Cobalt-azurin

It is thought to replace the copper with cobalt, that is known to have a strong affinity for sulfur-containing ligands.[5] Copper was first removed from the oxidized holoprotein by reduction with sodium dithionite and dialysis against 0.1 M KCN. The cobalt(II) metalloderivative was prepared adding 5 equiv. of $CoCl_2 \cdot 6H_2O$ to the apo-protein stock and the excess of metal was removed dialyzing overnight against TRIS/HCl buffer. Also in this case, to test the possible use of the system as fluorescence $H_2S$ biosensor, KSH binding to Cobalt containing azurin was firstly assessed via UV-visible spectroscopy. When adding KSH through a Co-azurin solution, the absorption spectrum significantly changed. Specifically, while the absorption spectrum of Co-azurin exhibits three bands at 280 nm, 330 nm and 375 nm and two less intense bands centred at 523 nm and 640 nm,[6] KSH addition results in the increase of the 330nm band, in the shifting of the 375 nm band to 390 nm and in the quenching of the 523 and 640 nm bands (**Figure 4.8**).

[5] (*a*) A. Earnshw, N. Greenwood, *Chemistry of the Elements; Pergamon Press: Oxford, U.K.*, **1989**, 786; (*b*) C. Elschenbroich, A. Salzer, *Organometallchemie; Teubner BG: Stuttgart, Germany*, **1988**, 438.

[6] (*a*) D. R. McMillin, R. C. Rosenberg, H. B. Gray, *Proc. Nat. Acad. Sci.* **1974**, *71*, 4760; (*b*) J. Salgado, S. J. Kroes, A. Berg, J. M. Moratal, G. W. Canters, *J. Biol. Chem.* **1998**, *273*, 177.

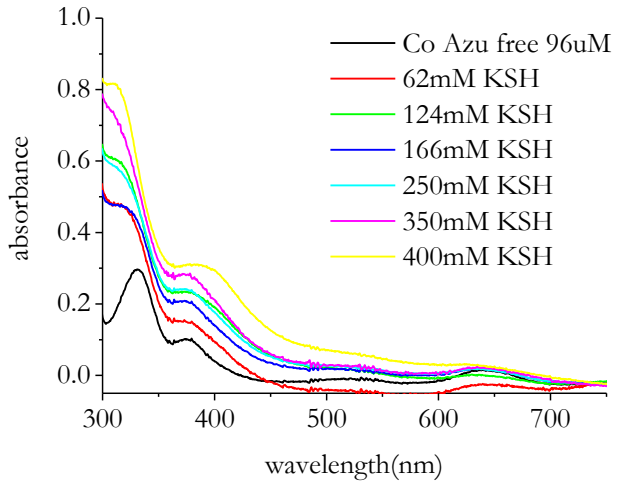


**Figure 4.8.** Electronic absorption spectra of Co-Azurin (rt, 96 μM, potassium phosphate buffer (100 mM, pH = 6.8)) upon addition of increasing concentrations of KHS (from 62 mM to 400 mM).

The protein was functionalized with the Atto620 (a fluorophore that emits at 643 nm; $\lambda_{exc}$ = 619 nm) to increase its yield of fluorescence. The fluorescence spectrum of the Co-Azurin-Atto620 (rt, 96 μM, potassium phosphate buffer (100 mM, pH = 6.8)) not show appreciable changes after addition of an excess of KSH (100 μL 1 M) when excited at 620 nm as one can deduce from the minor changes in the UV spectrum in this spectral region.. But when looking at the UV-vis spectrum of CoAzu after subsequent addition of KSH (see **Figure 4.8**) it is clear that the zone between 300 - 450 nm undergoes major changes. Thus, to gain in sensitivity for our system, we functionalized Co-azurin with Alexa 350 (a dye absorbing at 346 nm and emitting at 442 nm) (**Figure 4.9**). By covalently attaching this fluorescent label to the protein whose emission spectrum overlaps with the 330 nm band of the protein in its $HS^-$-bound state, the label

fluorescence will follow the difference in spectral overlap between the $HS^-$-free and $HS^-$-bound states of the Co-azurin via a FRET mechanism.

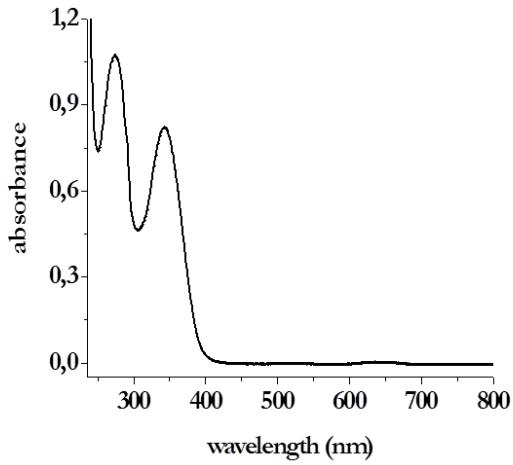


**Figure 4.9.** Electronic absorption spectra of Co-azurine (5.5 μM in potassium phosphate buffer (100 mM pH 6.8, r.t)) covalently functionalized with the Alexa350 dye label on the available amine groups.

That is, when the protein is in the $HS^-$-free state all the energy absorbed by the label is emitted as fluorescence. On the other hand, in the $HS^-$-bound state of Co-azurin, the label fluorescence is (partially) quenched due to FRET to the 330 nm band. The overlap of the Co-azurin absorption bands ($HS^-$-free and $HS^-$-bound forms) with the emission spectrum of Alexa350 ($\lambda_{em}$ = 440 nm), the dye label we selected in this study, is significant. In our first experiments Co-azurin was covalently functionalized with the Alexa350 dye label on the available amine groups (N-terminus and lysines). To test the system, the fluorescence intensity of functionalized Co-azurin was monitored when adding an excess of KSH.

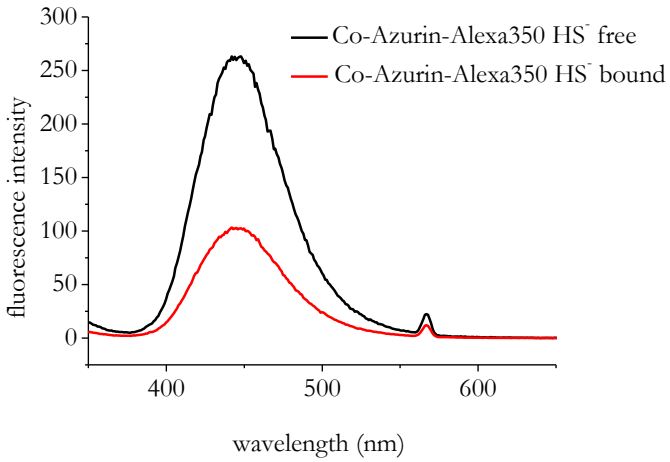


**Figure 4.10.** Emission spectra of Co-azurin-Alexa350 (potassium phosphate buffer, 100 mM pH 6.8, r.t), $\lambda_{exc}$ = 340 nm) before and after addition of an excess of KSH.

**Figure 4.10** shows a typical fluorescence spectrum of a solution containing 100 nM of Co-azurin-Alexa350 when excited at the absorption maximum ($\lambda_{exc}$ = 340 nm) of the dye (Alexa350). A fluorescence quenching of label emission was clearly observed upon KSH additions. Under the experimental conditions tested, the $H_2S$ binding process occurs and results in a clear fluorescence switch, which is crucial for practical sensing applications. To assess whether the amount of FRET mediated quenching of the label fluorescence is dependent on the $HS^-$ concentration the fluorescence intensity of Co-azurin-Alexa350 was monitored after adding increasing amounts of KSH solution. **Figure 4.11** shows there is a dependence of the fluorescence intensity displayed by the Co-azurin- Alexa350 on the KSH concentration. In this case we got a switching ratio of 80%.

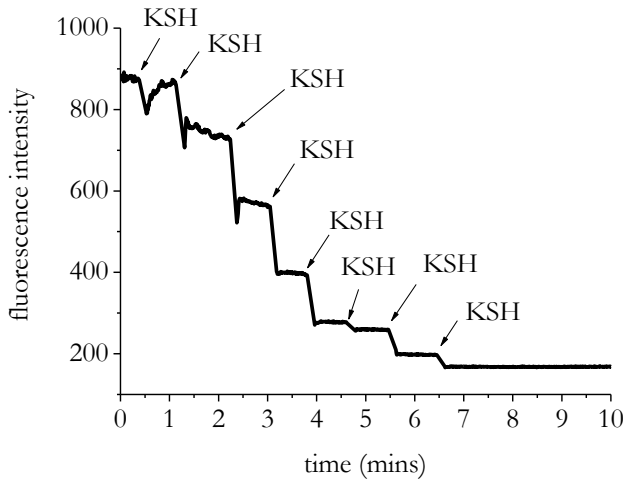


**Figure 4.11.** [CoAzu Alexa 350]= 5.5 μM in potassium phosphate buffer (100 mM pH 6.8, r.t); In this experiment 20 μl aliquots of a KSH solution (1 M) were subsequently added to an initial volume of 650 μl.

The detection limit of the proposed system was found to be in the micromolar range (**Figure 4.12**).

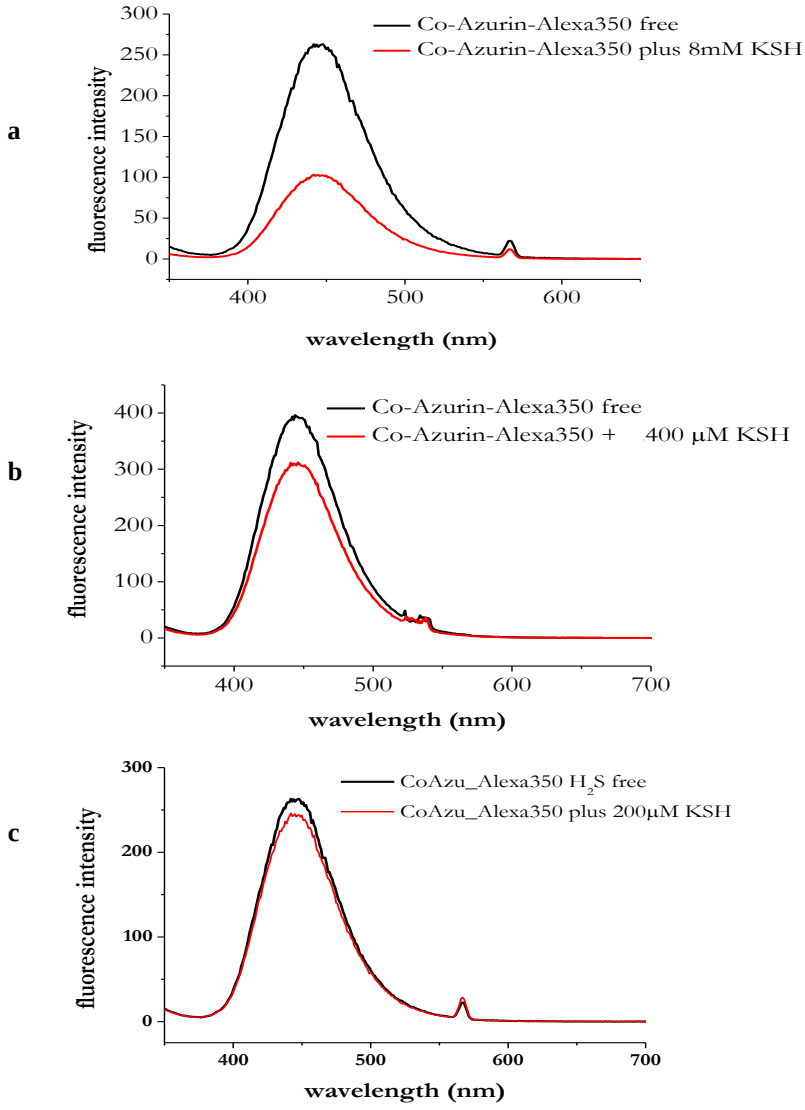


**Figure 4.12.** Emission spectra of Co-azurin-Alexa350 (rt, potassium phosphate buffer 100 mM pH 6.8, r.t, $\lambda_{exc}$ = 340 nm) before and after addition of **(a)** 8 mM, **(b)** 400 µM and **(c)** 200 µM of KSH respectively.

To obtain an indication on the selectivity of the construct the fluorescence intensity of Co-azurin-Alexa350 in the presence of biologically relevant and potentially competing thiols (e.g. L-cysteine

(L-cys) and glutathione (GSH)) was checked. In the presence of GSH (**Figure 4.13**) was observed fluorescence trends significantly different than that we had found with KSH.

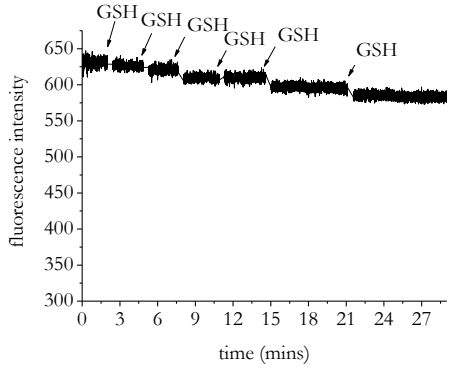


**Figure 4.13.** [CoAzu Alexa350] = 11 μM in in potassium phosphate buffer (100 mM pH 6.8, r.t); in this experiment 50 μl aliquots of a GSH solution (1 M) were subsequently added to an initial volume of 750 μl.

Was performed several control experiments to exclude the possible influence of other factors on the central FRET-experiment. No significant changes in the fluorescence intensity were observed when monitoring Co-azurin-Alexa350 in the absence of $H_2S$. Neither did KSH addition show any effect, when free dyes, Alexa350 functionalized BSA or unfunctionalized Co-azurin were used as sensing material.

### 4.2.3. Conclusions

In summary, Atto620 labelled azurin wild type showed a good fluorescence response but has not shown selectivity and the system was not reversible. The best results has been obtained with Cobalt-

azurin-Alexa 350. This system, nevertheless working by turn-off mechanism, showed a good fluorescence response when adding KSH, a dependence of the fluorescence intensity on the KSH concentration, a detection limit in micromolar range and a good selectivity.

## 4.3. Reference List

1. I. Pozdnyakova, J. Guidry, P. Wittung-Stafshede, *Archives of Biochemistry and Biophysics* **2001**, *390*, 146.

2. (*a*) I. Pozdnyakova, J. Guidry, P. Wittung-Stafshede, *Biophysical Journal* **2002**, *82*, 2645; (*b*) I. Pozdnyakova, P. Wittung-Stafshede, *Biochemistry* **2001**, *40*, 13728.

3. E. I. Solomon, M. D. Lowery, *Science* **1993**, *259*, 1575.

4. Labelling ratios were in the range 0.12-0.83 (dye molecule/protein).

5. (*a*) A. Earnshw, N. Greenwood, *Chemistry of the Elements; Pergamon Press: Oxford, U.K.*, **1989**, 786; (*b*) C. Elschenbroich, A. Salzer, *Organometallchemie; Teubner BG: Stuttgart, Germany*, **1988**, 438.

6. (*a*) D. R. McMillin, R. C. Rosenberg, H. B. Gray, *Proc. Nat. Acad. Sci.* **1974**, *71*, 4760; (*b*) J. Salgado, S. J. Kroes, A. Berg, J. M. Moratal, G. W. Canters, *J. Biol. Chem.* **1998**, *273*, 177.

# Chapter 5: Cyclam derivative for sensing hydrogen sulfide.

## 5.1. Introduction

In the last years have been reported few $H_2S$ fluorescent sensor developed on the method of copper sulfide precipitation utilizing dyes-functionalized cyclam-copper(II) complexes.[1] Despite showing good sensibility and excellent selectivity, this sensors work as simple chemodosimeter and are not reusable, since the recognition process is not reversible. My aim is to use a coordinative-based approach owing to a reversible binding process. This would be advantageous for practical sensing applications allowing reusability of the sensing device and for in vivo monitoring of $H_2S$ concentration changes. To obtain this purpose, I have idealized a cyclam-based fluorescent sensor in which a dimethylpyridine moiety allows a further coordination and a greater steric hindrance to the copper ion (**Figure 5.1**).

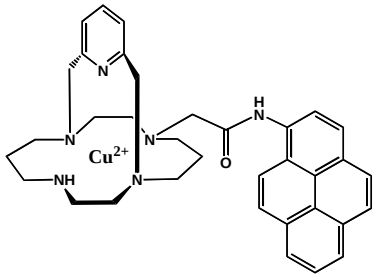


**Figure 5.1.** Structure of pycup derivative **7**.

[1] (*a*) L. E. Santos-Figueroa, C. de la Torre, S. El Sayed, F. Sancenón, R. Martínez-Máñez, A. M. Costero, s. Gil, M. Parra, *Eur. J. Inorg. Chem.* **2014**, 41; (*b*) K. Sakasura, K. Hanaoka, N. Shibuya, Y. Mikami, Y. Kimura, T. Komatsu, T. Ueno, T. Terai, H. Kimura, T. Nagano, *J. Am. Chem. Soc.***2011**, *133*, 18003.

## 5.2. Results and Discussion

The synthesis was carries out according to rif. 2 in one step by intramolecular cross-bridging using 2,6-bis(bromomethyl)-pyridine (**Scheme 5.1**). A low yield of only 17% for intramolecular cyclization was obtained, likely owing to competing intermolecular reactions that were observed even under high dilution conditions.

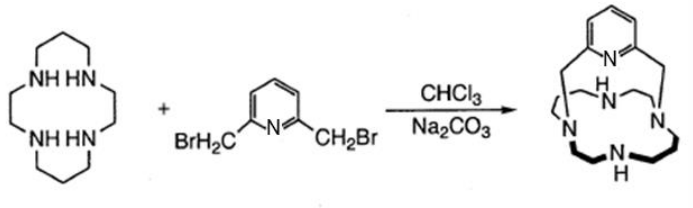


**Scheme 5.1.** Synthesis of pycup.

Pyrenilacetamide derivative **6** was prepared by the alkylation of pycup whit 2-chloro-*N*-pyren-1-yl-acetamide **8** ($K_2CO_3$, $CH_3CN$, 60°C, 7 days), which was preparated by the reaction of 1-aminopyrene with chloroacetyl chloride ($NEt_3/CH_2Cl_2$)[3] as shown in **Scheme 5.2**.

[2] S. Brandès, S. Lacour, F. Denat, P. Pullumbi, R. Guilard, *J. Chem. Soc., Perkin Trans.* **1998**, *1*, 639.
[3] J. H. Kim, A. R. Hwang, S. K. Chang, *Tetrahedron Letters* **2004**, *45*, 7557.

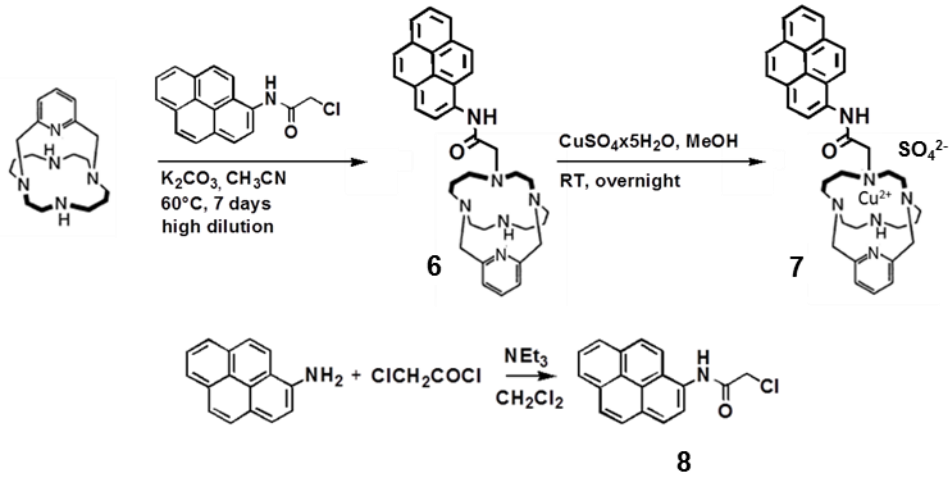


**Scheme 5.2.** Synthesis of derivatives **7** and **8**.

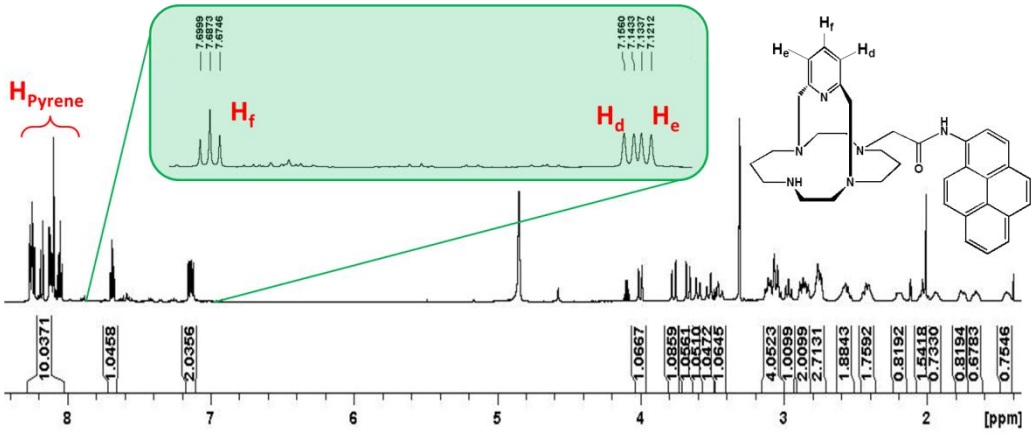


**Figure 5.2.** $^{1}$H-NMR spectra of derivative **1** (600 MHz, $CD_3OD$, 298 K).

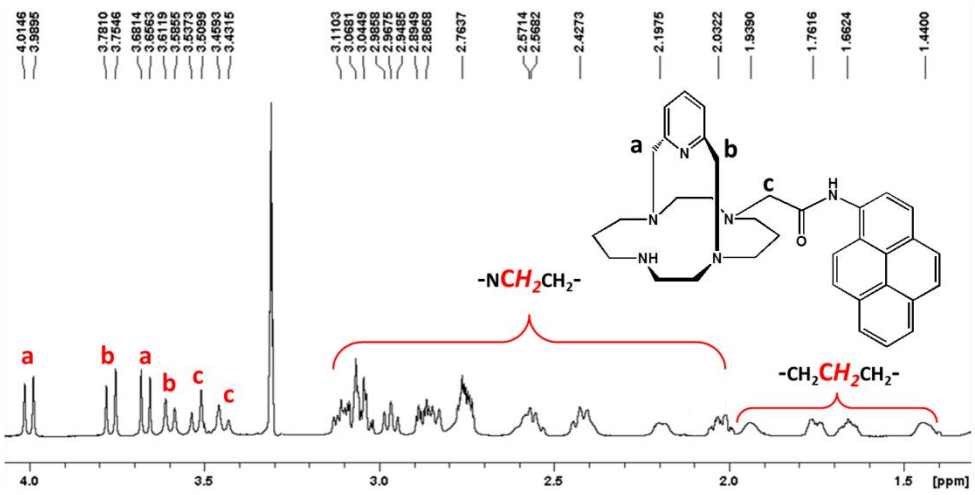


**Figure 5.3.** Expansion of $^{1}$H-NMR spectra of derivative **1** (600 MHz, $CD_3OD$, 298 K).

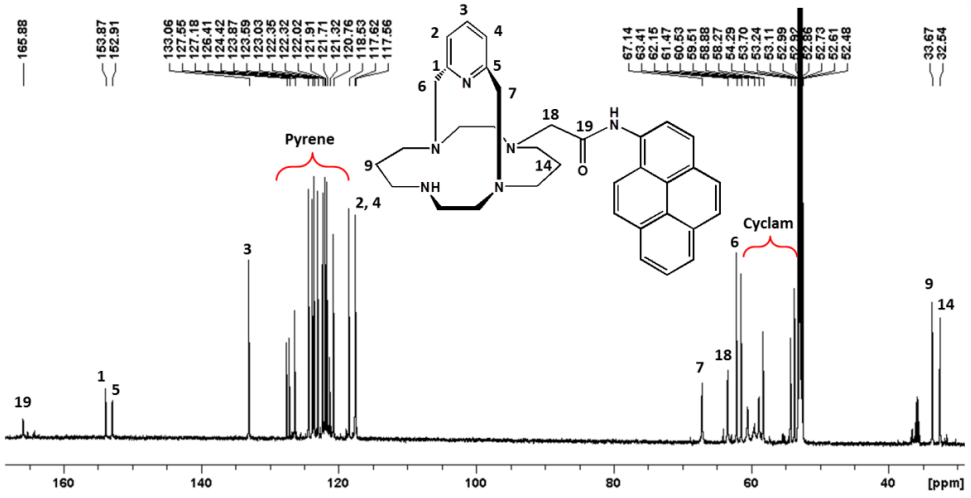


**Figure 5.4.** $^{13}$C-NMR spectra of derivative **1** (600 MHz, $CD_3OD$, 298 K).

The reactions of pycup with $CuSO_4 \cdot 5H_2O$ in methanol were reported to give metal complex (**Figure 2.5**).[4] Accordingly, reaction of **6** under similar conditions afforded complex **7**.

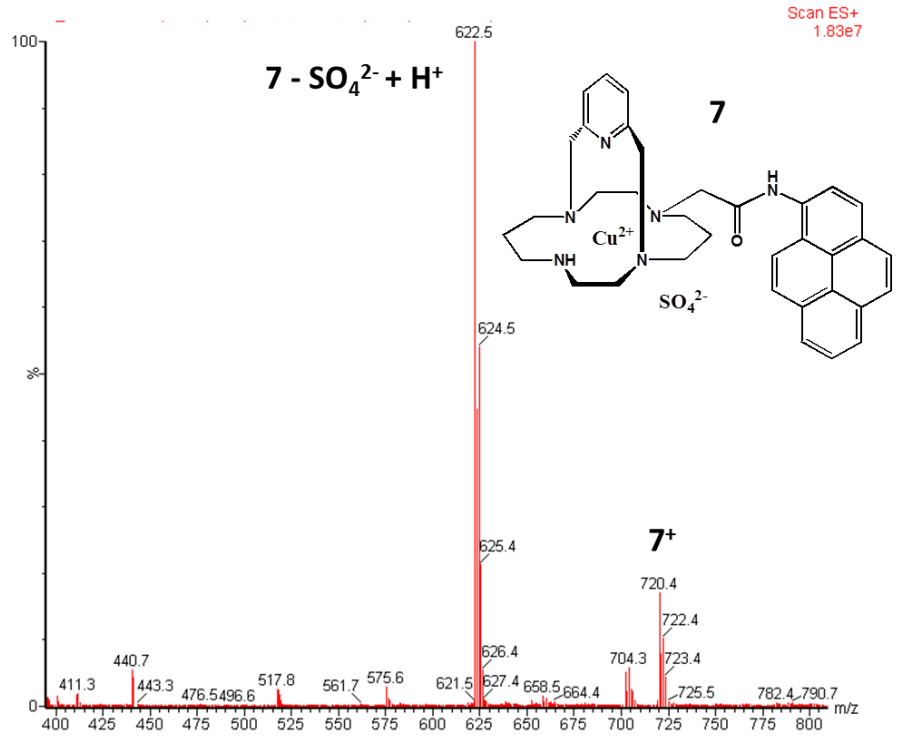


**Figure 5.5.** ESI(+) MS spectra of complex **7**.

Free ligand **6** showed an absorption and a fluorescence spectrum typical of pyrene derivatives in MeOH.

[4] L. G. Alves, M. Souto, F. Madeira, P. Adão, R. F. Munhá, A. M. Martins, *Journal of Organometallic Chemistry* 2014, *760*, 130.

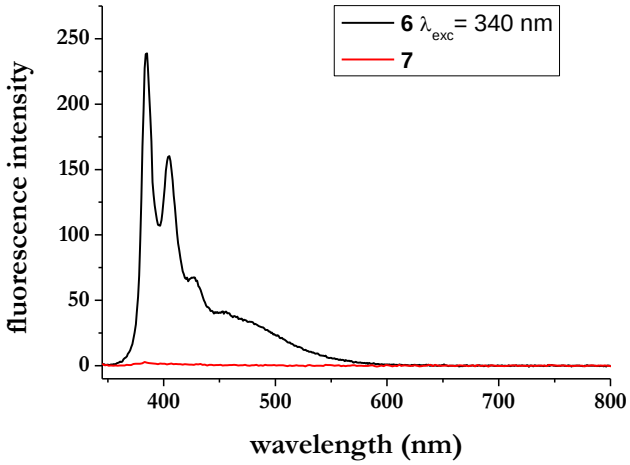


**Figure 5.6.** Emission spectra of ligand **6** (black, $\lambda_{exc}$ = 340 nm) and of complex **7** (red) in MeOH. [**6**] = [**7**] = $1 \cdot 10^{-5}$ M.

On the contrary, in the fluorescence spectrum of complex **7** a structured emission band consistently weaker than that of the free ligand **6**, was observed likely owing to the coordination of the free ligand to the paramagnetic $Cu^{2+}$ centre (**Figure 2.5**).

The design concept for derivative **7** is to create a more pronounced sterical hinderance around the copper ion. The dimethylpyridine unit on the one side and the pyrenil moiety on the other have the function of prevent the access at metal ion from the surrounding environment. The fluorescence of pyrenil moiety is quenched by the presence of copper ion through the phenomenon of PET (**Figure 5.7**)

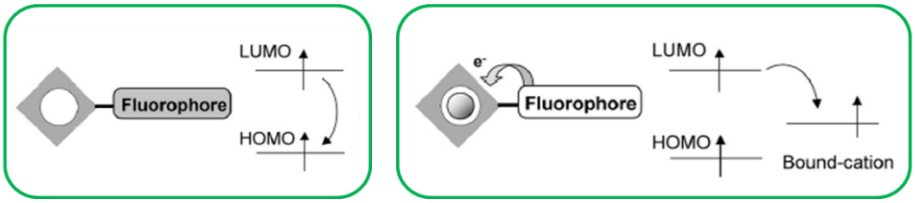


**Figure 5.7.** Schematic diagram illustrating the mechanism of PET effect.

Upon reaction with $H_2S$ (KSH was used as a hydrogen sulfide source in this work), the fluorescence of the pyrenyl moiety, which is moved away from copper ion, is restored (**Figure 5.8**)

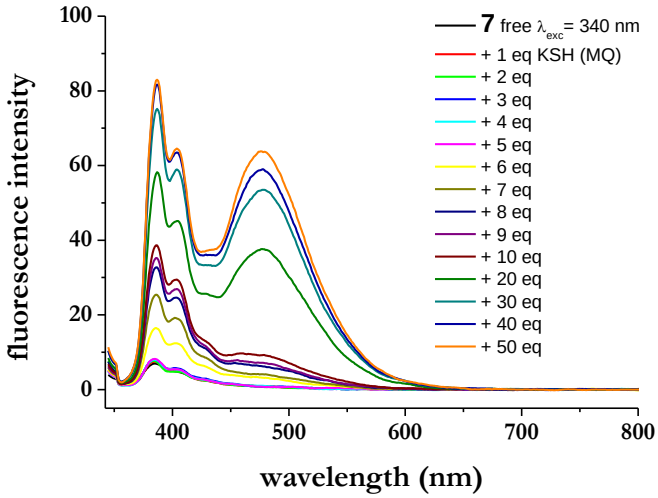


**Figura 5.8.** Emission spectra of complex **7** ($\lambda_{exc}$ = 340 nm, MeOH) when titrated with KSH (rt, MQ water). [**7**] = $1 \cdot 10^{-5}$ M; end concentration of KSH varied in the range 10-500 μM.

However, the complexation of hydrogen sulfide to metal complex **7** does not seem to take place instantaneously, as can be seen from **Figure 5.9**.

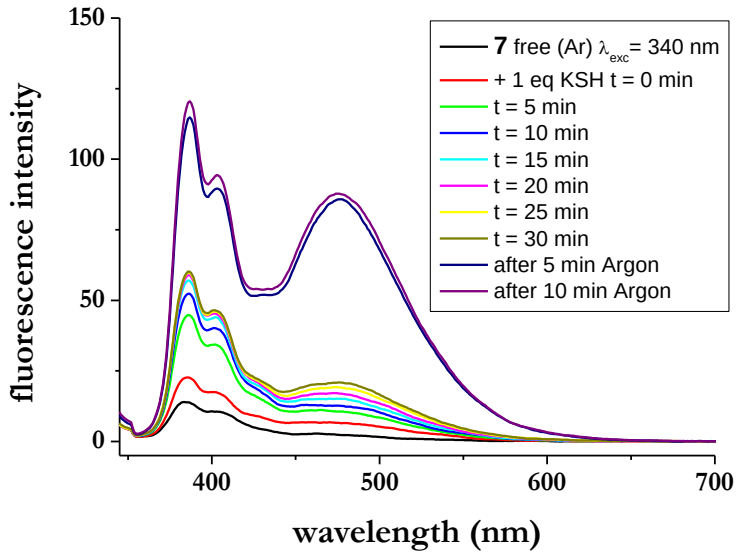


**Figura 5.9.** Emission spectra of complex **7** ($\lambda_{exc}$ = 340 nm, MeOH) whit 1 equivalent of KSH (rt, MQ water) on time. [**7**] = [KSH] = $1 \cdot 10^{-5}$ M.

ESI MS experiment shows that the addition of KSH (10 equiv.) to a methanolic solution of **7** does not lead to removal of copper from the binding site (**Figure 5.10**).

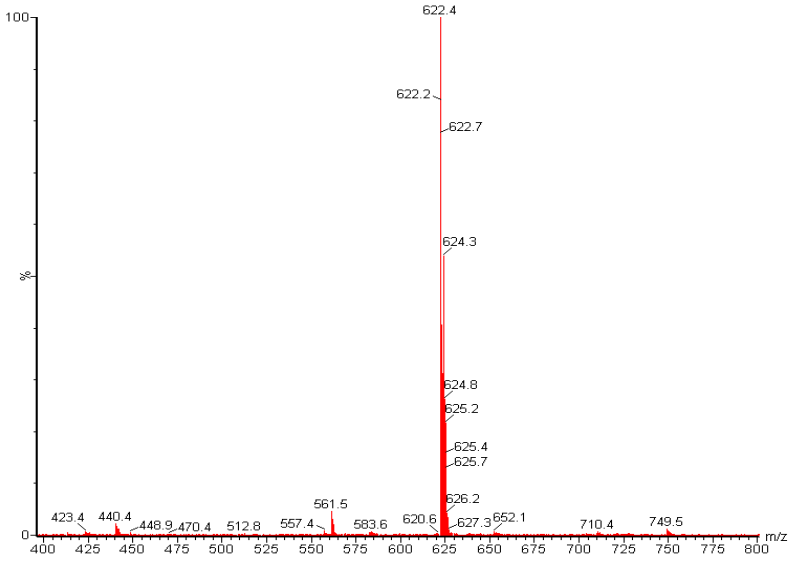


**Figure 5.10.** ESI(+) MS spectra of complex **7** after addition of 10 equivalent of KSH.

To test the selectivity of the complex **7** has been examined the fluorescence spectra in the presence of a biologically relevant and potentially competing glutathione (GSH) (**Figure 5.11**).

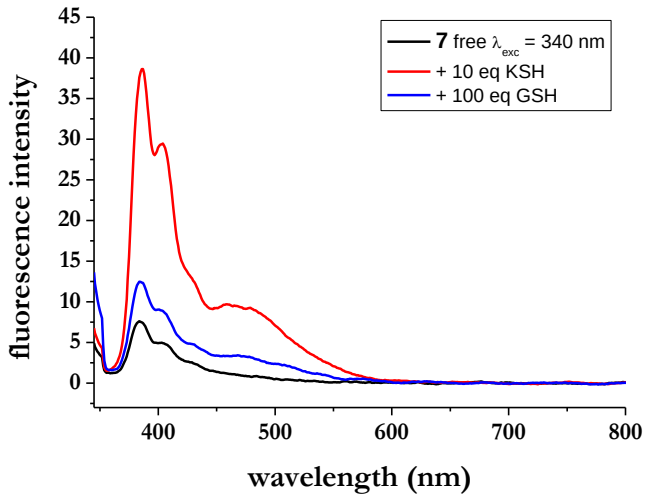


**Figure 5.11.** Emission spectra of complex **7** ($\lambda_{exc}$ = 340 nm, MeOH) whit no addition (black) or addition of 10 equivalent of KSH (red, rt, MQ water), or 100 equivalent of GSH (blue, rt, MQ water). [**7**] = $1 \cdot 10^{-5}$ M; [KSH] = 100 μM; [GSH] = 1 mM.

From the fluorescence titration experiment in water (**Figure 5.12**), a slightly less significant increase of the fluorescence intensity were observed.

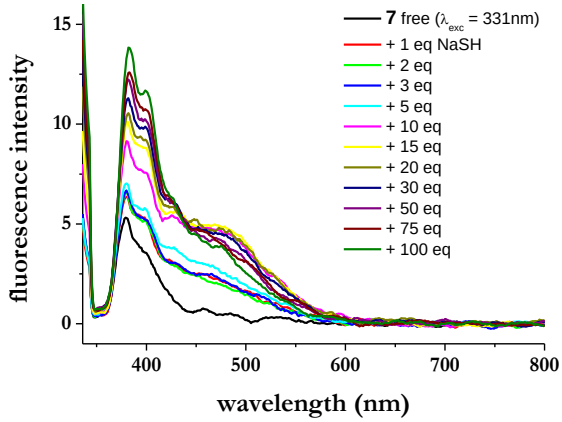


**Figure 5.12.** Emission spectra of complex **7** ($\lambda_{exc}$ = 340 nm, MQ water) when titrated with KSH (rt, MQ water). [**7**] = $1 \cdot 10^{-5}$ M; end concentration of KSH varied in the range 10-500 μM.

## 5.3. Conclusions

In summary, a new coordinative-based approach fluorescence probe **7** for $H_2S$ was reported. Sensor **7** showed a 4.5-fold fluorescence enhancement with 10 equivalents of KSH in methanol. The probe can highly selectively detect $H_2S$ even in the presence of millimolar concentrations of glutathione. To gain insights in the mechanism of recognition of $H_2S$ ESI-MS and mono-dimensional NMR experiments were performed. However, the main limit of the complex **7** is the poor solubility in water.

## 5.4. Reference List

1. (a) L. E. Santos-Figueroa, C. de la Torre, S. El Sayed, F. Sancenón, R. Martínez-Máñez, A. M. Costero, s. Gil, M. Parra, Eur. J. Inorg. Chem. 2014, 41; (b) K. Sakasura, K. Hanaoka, N. Shibuya, Y. Mikami, Y. Kimura, T. Komatsu, T. Ueno, T. Terai, H. Kimura, T. Nagano, J. Am. Chem. Soc.2011, 133, 18003.
2. S. Brandès, S. Lacour, F. Denat, P. Pullumbi, R. Guilard, J. Chem. Soc., Perkin Trans. 1998, 1, 639.
3. J. H. Kim, A. R. Hwang, S. K. Chang, Tetrahedron Letters 2004, 45, 7557.
4. L. G. Alves, M. Souto, F. Madeira, P. Adão, R. F. Munhá, A. M. Martins, Journal of Organometallic Chemistry 2014, 760, 130.

# Chapter 6: Concluding Remarks

In the last years, several reviews on $H_2S$ biology have declared the great need for fluorescence imaging probes. The probes designed until now can detect $H_2S$ in aqueous solution with high sensitivity and selectivity. Nevertheless all these existing probes are reaction-based fluorescent probes. In my opinion a limitation of these fluorescent sensors is the irreversibility of the reaction by which $H_2S$ recognition occurs, which renders the devices not reusable. In my thesis work I have designed probes which works with a coordinative-based approach. In this way one may, in principle, be able to remove $H_2S$ from the metal center of the sensor and ensure a reversible $H_2S$ binding process. This would be advantageous for practical sensing applications allowing reusability of the sensing device.

# Chapter 6: Experimental Section

## 6.1. General Comment

All chemicals used for the synthetic work were obtained from Sigma-Aldrich or Strem Chemicals and were of reagent grade. They were used without further purification. Bis(dimethylglyoximate)ethylpyridinecobalt(III) (**1**) and bis-dimethylglyoximate)phenylpyridinecobalt(III) (**5**) were prepared as previously reported.[1] Wild type azurin (*Pseudomonas aeruginosa*) was expressed in *E. coli* and purified according to literature procedures.[2] Atto620 NHS-ester and Alexa350 NHS-ester were purchased from ATTO-TEC Biolabeling and Ultraanalytics (Siegen, Germany) and Thermo Fisher Scientific (Waltham, Massachusetts, United States) respectively. NaSH anhydrous was bought from Alfa Aesar (Lancashire, United Kingdom) and stored in glove-box. L-Glutathione reduced (GSH) and L-cysteine were obtained from Sigma Aldrich. PD-10 Desalting Columns contain Sephadex G-25 Medium (GE Healthcare) was used for chromatography. The dialyses were carried out using regenerated cellulose dialysis tubing Spectra/Por 1 (Molecular Weight Cut-Off's: 6 – 8 kD). Derivatives pycup (1,8-(2,6-Pyridinedimethylene)-1,4,8,11-tetraazacyclotetradecane, rif. 2) and **8** (2-chloro-*N*-pyren-1-yl-acetamide, rif. 3) were synthesized according to literature procedures.

---

[1] (*a*) P. J. Toscano, L. G. Marzilli, *Prog. Inorg. Chem.* **1984**, *31*, 105. (*b*) N. Bresciani-Pahor, M. Forcolin, L. G. Marzilli, L. Randaccio, M. F. Summers, P. J. Toscano, *Coord. Chem. Rev.* **1985**, *63*, 1.

[2] M. Vandekamp, F. C. Hali, N. Rosato, A. F. Agro, G. W. Canters, *Biochim. Biophys. Acta* **1990**, *1019*, 283.

Anhydrous solvents were purchased from Aldrich. Reaction temperatures were measured externally. Elemental analyses were performed with a Perkin–Elmer 240-C. Flash chromatography was performed on Merck silica gel (60, 40-63 μm). Reactions were monitored by TLC on Merck silica gel plates (0.25 mm) and visualized by UV light. They were used without further purification. Room temperature 1D and 2D NMR spectra were recorded on a Bruker Avance-600 spectrometer [600 ($^{1}$H) and 150 MHz ($^{13}$C)], Bruker Avance-400 spectrometer [400 ($^{1}$H) and 100 MHz ($^{13}$C)], or Bruker Avance-300 spectrometer [300 ($^{1}$H) and 75 MHz ($^{13}$C)]; chemical shifts are reported relative to the residual solvent peak (C*H*$Cl_3$: δ 7.26, *C*D$Cl_3$: δ 77.23; $CD_3O$*H*: δ 4.87, *C*$D_3$OD: δ 49.0). All spectra were recorded in 5 mm o.d. NMR tubes. Chemical shifts (δ) are listed in parts per million referenced to $SiMe_4$. Typically, 5 mg of the complex in 0.5 mL of solvent was used for each experiment. For the NMR experiments in $D_2O$ a presaturation pulse sequence was used to suppress the water signal.

Absorption spectra were recorded on a Cary-50 Spectrophotometer, using a 1 cm quartz cuvette (Hellma Benelux bv, Rijswijk, Netherlands) and a slit-width equivalent to a bandwidth of 5 nm. All measurements were performed at room temperature. Fluorescence spectra were measured on a Cary Eclipse Spectrophotometer in a $10\times10mm^2$ airtight quartz fluorescence cuvette (Hellma Benelux bv, Rijswijk, Netherlands) with an emission band-pass of 10 nm and an excitation band-pass of 5 nm. Both absorption and fluorescence measurements were performed at room temperature. The titration experiments were performed as follows: the cuvette was filled with

sample solutions. Then µL amounts of KSH solutions (to the end concentrations specified in the figure captions) were injected via a gas-tight syringe. For azurin measurement were performed in potassium phosphate buffer (100 mM, pH 6.8) at room temperature. Mass spectrometry analyses were carried out using a Micromass Quattro micro API triple quadrupole mass spectrometer equipped with an electrospray ion source operating in the negative ion mode (Waters, Milford, MA). For CuPPIX ESI experiments were performed in $H_2O/CH_3CN$ (50:50) with 0.5% formic acid. For the in situ experiments between CuPPIX and KSH the reaction was performed in MilliQ water in a 1:10 molar ratio and then an aliquot of the mixture was diluted in $H_2O/CH_3CN$ (50:50) with 0.5% formic acid.

## 6.2. Cobaloximes

### *6.2.1. Synthesis of K[Co(dmgH)$_2$(CH$_2$CH$_3$)(SH)] (**2**):*

$[Co(dmgH)_2(CH_2CH_3)(py)]$ (0,060 g; $1.51\cdot10^{-4}$ mol) was dissolved in 400 µl of MeOH. Then KSH (0,109 g; $1.51\cdot10^{-3}$ mol), previously dissolved in water (900 µl), was added. The reaction was left under stirring for 5 minutes. Then was filtered and left at -20 °C for five days. The product was isolated as a light orange powder by filtration and dried under vacuum. Yield: 0.032 g (55%). Anal. Calcd. for $C_{10}H_{20}CoKN_4O_4S$: C, 30.77; H, 5.16; O, 16.39. Found: C, 31.25; H, 5.31; O, 16.23. **$^1$H NMR** (400 MHz, MeOD, 25 °C): δ -2.59 (br s, 1H, *H*S), 0.32 (t, J = 7.7 Hz, 3H, $CoCH_2CH_3$), 1.46 (q, J = 7.7 Hz, 2H, $CoCH_2CH_3$), 2.16 (s, 12H, $CH_3$-C=N). **ESI-MS** (methanol,

negative-ion mode): *m/z* calcd (%) for $C_{10}H_{20}CoN_4O_4S$, 351,05; found, 351.5 (15) $[M]^-$, 322.4 (40) $[M\text{-}Et]^-$, 288.5 (100) $[M\text{-}Et\text{-}HS]^-$.

### 6.2.2. *Synthesis of [Co(dfgH)$_2$(CH$_2$CH$_3$)(py)] (**4**):*

$CoCl_2.6\ H_2O$ (2,4 g; $1\cdot10^{-2}$ mol) and diphenylglyoxime (4,8 g; $2\cdot10^{-2}$ mol) were mixed in acetone (130 ml) and left under reflux for about 4 hours. The reaction mixture was left under stirring overnight at room temperature. Pyridine (0,9 g; $1,1\cdot10^{-2}$ mol) was added and the system was left under stirring for about thirty minutes. Then NaOH (1,6 g; $4\cdot10^{-2}$ mol) previously dissolved in MilliQ water (5 mL) and degassed was added. At this point the reaction mixture turned brown. $CH_3CH_2I$ (0,4 mL; $5\cdot10^{-3}$ mol) in MeOH (5 mL) was then added via dropping funnel. The reaction mixture was left under stirring for about 1 hour. A crystalline brown-red powder was isolated after removing the solvents under pressure. The powder was washed with a mixture of ice and MilliQ water, and dried under vacuum. Yield: 4.8 g (71%). Anal. Calcd. for $C_{37}H_{38}N_5O_4Co$: C 65.77, H 5.67, N 10.37; found C 65.82, H 5.72, N 10.43. $^1$H NMR (400 MHz, $CDCl_3$, 25 °C): $\delta$ = 8.9 (d, 1H, C*H*$_{pyr}$), 7.8 (t, 1 H, C*H*$_{pyr}$), 7.4 (t, 1H, C*H*$_{pyr}$), 2.35 (q, 2H, C*H*$_2$CH$_3$), 1.2 (t, 3H, CH$_2$C*H*$_3$). **ESI-MS** (methanol, negative-ion mode): *m/z* calcd (%) for $C_{10}H_{20}CoN_4O_4S$, 351,05; found, 351.5 (15) $[M]^-$, 322.4 (40) $[M\text{-}Et]^-$, 288.5 (100) $[M\text{-}Et\text{-}HS]^-$.

### 6.2.3. *Fluorescence Quantum Yields*

Fluorescence quantum yields ($\Phi_F$) were determined by comparative method using the equation:

$$\Phi_F = \Phi_{F(Std)} (F \cdot A_{Std} \cdot n^2/F_{Std} \cdot A \cdot n_{Std}^2)$$

where F and $F_{Std}$ are the areas under the fluorescence curves of cobaloximes derivatives and the reference, respectively. A and $A_{Std}$ are the absorbances of the sample and reference at the excitation wavelength, and $n^2$ and $n_{Std}^2$ are the refractive indices of solvents used for the sample and standard, respectively. All of the samples and the standard were excited at the same relevant wavelength. Quantum yield determinations were studied in water and methanol. The emission spectra were also compared under the same conditions. The yields in solvents are $1.6 \cdot 10^{-4}$ for **1** in water ($\lambda_{exc}$ = 450 nm), $9.1 \cdot 10^{-3}$ for **4** in methanol ($\lambda_{exc}$ = 280 nm) and $7.8 \cdot 10^{-3}$ for **5** in water ($\lambda_{exc}$ = 250 nm).

### 6.2.4. *Determination of Polysulfide*

$[Co(dmgH)_2(CH_2CH_3)(py)]$ (0.005 g; $1.26 \cdot 10^{-5}$ mol) and KSH (0.020 g; $2.52 \cdot 10^{-4}$ mol) were dissolved in 1.0 mL of $D_2O$ under aerobic conditions at room temperature. The reaction wa left under stirring for five minutes then NaOH (0.080 g; $2.01 \cdot 10^{-3}$ mol) was added. Subsequently $(CH_3O)_2SO_2$ (0.130 g; $1.01 \cdot 10^{-3}$ mol) dissolved in $CDCl_3$ (500 μl) was added. The reaction mixture was stirred for another 90 minutes. The organic phase was the separated and collected in a NMR tube to register the NMR spectra. The $^1H$ and $^{13}C$ NMR spectra clearly indicated the presence of dimethylsulphane and dimethyldisulphane (arising from the alkylation of $S^{2-}$ and $S_2^{2-}$, respectively) in a 94/6 molar ratio. The reaction between **1** and KSH was repeated with the following reaction time: 5 hours, 24 hours, 4 days and 10 days. After four days the $S^{2-}/S_2^{2-}/S_3^{2-}$ distribution in the product miwture was 84/15/1, after ten days the $S^{2-}/S_2^{2-}/S_3^{2-}$

distribution was 78/20/2. As a control, a sample without $[Co(dmgH)_2(CH_2CH_3)(py)]$ was prepared in each experiment, using the same quantities as specified above. The same distributions of polysulfide anions were found.

### 6.2.5. *Computational Details*

Molecular structures and electronic energies of all molecules discussed here were calculated using the Gaussian 09 packages.[3] All geometries were optimized without constraints at the BP86 level of theory, that is, by employing the exchange and correlation functionals of Becke[4] and Perdew,[5] respectively. The basis set consisted of 6-31G(d) basis sets for all atoms. No constraints were imposed during the optimizations. Default geometric and SCF convergence criteria were used. Stationary point geometries were characterized as local minima on the potential energy surfaces. The absence of imaginary frequency demonstrated that the structures were true minima as their

[3] M. Frisch, G. W. Trucks, H. B. Schlegel, G. E. Scuseria, M. A. Robb, J. R. Cheeseman, G. Scalmani, V. Barone, B. Mennucci, G. A. Petersson, H. Nakatsuji, M. Caricato, X. Li, H. P. Hratchian, A. F. Izmaylov, J. Bloino, G. Zheng, J. L. Sonnenberg, M. Hada, M. Ehara, K. Toyota, R. Fukuda, J. Hasegawa, M. Ishida, T. Nakajima, Y. Honda, O. Kitao, H. Nakai, T. Vreven, J. A. Montgomery Jr., J. E. Peralta, F. Ogliaro, M. Berpark, J. J. Heyd, E. Brothers, K. N. Kudin, V. N. Staroverov, R. Kobayashi, J. Normand, K. Raghavachari, A. Rendell, J. C. Burant, S. S. Iyengar, J. Tomasi, M. Cossi, N. Rega, J. M. Millam, M. Klene, J. E. Knox, J. B. Cross, V. Bakken, C. Adamo, J. Jaramillo, R. Gomperts, R. E. Stratmann, O. Yazyev, A. J. Austin, R. Cammi, C. Pomelli, J. W. Ochterski, R. L. Martin, K. Morokuma, V. G. Zakrzewski, G. A. Voth, P. Salvador, J. J. Dannenberg, S. Dapprich, A. D. Daniels, O. Farkas, J. B. Foresman, J. V. Ortiz, J. Cioslowski, D. J. Fox, *Gaussian 09, revision A.02*, Gaussian, Inc., Wallingford, CT, **2009**.

[4] A. D. Becke, *Phys. Rev. A: At., Mol., Opt. Phys.* **1988**, *38*, 3098.

[5] (*a*) J. P. Perdew, *Phys. Rev. B: Condens. Matter, Mater. Phys.* **1986**, *33*, 8822; (*b*) J. P. Perdew, *Phys. Rev. B: Condens. Matter Mater. Phys.* **1986**, *34*, 7406.

respective levels of theory. The $Co^{3+}$ ion has the [Ar] $3d^6$ electron configuration, the low-spin state (S = 0) was assumed for all the species considered in this work. Solvent effects (water) have been estimated in single-point calculations on the gas phase optimized structures, based on the polarizable continuous solvation model PCM[6] as implemented in Gaussian 09 (keyword: scrf = (pcm, solvent = water)). The gas-phase free energies at 298 K were corrected by the solvation term.[7]

### 6.2.6. *Crystal Structure Determination*

The crystal data for compound $K_2[Co_2(dmgH)_2(CH_2CH_3)_2(\mu\text{-}S_3)]$ (**3**) were collected at room temperature using a Nonius Kappa CCD diffreactometer with graphite monochromated Mo-Kα radiation. The data sets were integrated with the Denzo-SMN package [8] and corrected for Lorentz, polarization and absorption effects (SORTAV).[9] The structures were solved by direct methods using SIR97 [10] system of programs and refined using full-matrix least-squares with all non-hydrogen atoms anisotropically and hydrogens included on calculated positions, riding on their carrier atoms, except those linked to the oxygen atoms of glioximato ligands which were

[6] J. Tomasi, B. Mennucci, R. Cammi, *Chem. Rev.* **2005**, *105*, 2999.
[7] The solvent-corrected Gibbs free energies = gas-phase Gibbs free enrgies + (solvent-phase electronic energies – gas-phase electronic energies).
[8] Z. Otwinowski, W. Minor, in *Methods in Enzymology, Part A*, ed. C. W. Carter and R. M. Sweet, Academic Press, London, **1997**, *276*, 307.
[9] R. H. Blessing, *Acta Crystallogr., Sect. A: Found. Crystallogr.* **1995**, *51*, 33.
[10] A. Altomare, M. C. Burla, M. Camalli, G. L. Cascarano, C. Giacovazzo, A. Guagliardi, A. G. Moliterni, G. Polidori, R. Spagna, *J. Appl. Crystallogr.* **1999**, *32*, 115.

refined isotropically. All calculations were performed using SHELXL-97[11] and PARST[12] implemented in WINGX[13] system of programs. The crystal data are given in **Table 2.1**.

**Table 2.1.** Crystallographic data.

| Compound | **$K_2[Co_2(dmgH)_2(CH_2CH_3)_2(\mu\text{-}S_3)]$** |
|---|---|
| Formula | $[C_{20}H_{38}Co_2N_8O_8S_3]^{=} \bullet 2K^{+} \bullet 4H_2O$ |
| M | 882.89 |
| Space group | *P-1* |
| Crystal system | Triclinic |
| *a*/Å | 10.7251(2) |
| *b*/Å | 11.4534(2) |
| *c*/Å | 16.0740(3) |
| α/° | 95.3842(7) |
| β/° | 108.6656(7) |
| γ/° | 97.8766(8) |
| U/Å$^3$ | 1832.95(6) |
| *Z* | 2 |
| T/K | 295 |
| $D_c$/g cm$^{-3}$ | 1.600 |
| F(000) | 916 |
| μ(Mo-Kα)/cm$^{-1}$ | 13.66 |
| Measured Reflections | 27696 |
| Unique Reflections | 10526 |
| $R_{int}$ | 0.0370 |
| Obs. Refl.ns [I≥2σ(I)] | 8614 |
| $\theta_{min}$- $\theta_{max}$/° | 3.30 – 30.00 |
| hkl ranges | -15,14;-16,16;-21,22 |
| R($F^2$) (Obs.Refl.ns) | 0.0355 |
| wR($F^2$) (All Refl.ns) | 0.0971 |
| No. Variables | 466 |
| Goodness of fit | 1.047 |

[11] G. M. Sheldrick, SHELX-97, *Program for Crystal Structure Refinement*, University of Gottingen, Germany, **1997**.
[12] M. Nardelli, *J. Appl. Crystallogr.* **1995**, *28*, 659.
[13] L. J. Farrugia, *J. Appl. Crystallogr.* **1999**, *32*, 837.

| | |
|---|---|
| $\Delta\rho_{max}$; $\Delta\rho_{min}$ /e Å$^{-3}$ | 0.743; -0.690 |
| CCDC Deposition N. | 1000024 |

Single crystal of **3** were grown using the following procedure: $[Co(dmgH)_2(CH_2CH_3)(py)]$ (0.030 g; $7.55\cdot10^{-5}$ mol) and KSH (0.054 g; $7.55\cdot10^{-4}$ mol) were dissolved in 300 μl of MeOH. The reaction was left inder stirring for 15 minutes and then filteres. The solution was put in a small vial that in turn was placed in a larger one containing $Et_2O$. the system was closed and stored in the dark for two weeks. Yiels: 0.021 g (31%).

**Table 2.1.** Selected bond distances and angles (Å and degrees) for $K_2[Co_2(dmgH)_2(CH_2CH_3)_2(\mu\text{-}S_3)]$.

| $[\mu\text{-}S_3\{(dmgH)_2Co(Et)\}_2]K_2$ | | | |
|---|---|---|---|
| **Distances** | | | |
| Co1-N1 | 1.859(1) | Co2-N5 | 1.884(2) |
| Co1-N2 | 1.874(2) | Co2-N6 | 1.870(2) |
| Co1-N3 | 1.879(1) | Co2-N7 | 1.874(2) |
| Co1-N4 | 1.880(2) | Co2-N8 | 1.873(2) |
| Co1-S1 | 2.3902(5) | Co2-S3 | 2.3757(5) |
| Co1-C9 | 2.046(2) | Co2-C19 | 2.052(2) |
| S1-S2 | 2.0643(6) | S2-S3 | 2.0475(6) |
| O1…O3 | 2.489(2) | O5…O7 | 2.516(3) |
| O2…O4 | 2.508(2) | O6…O8 | 2.474(2) |
| K1…S1 | 3.3148(7) | K2…S2 | 3.4018(7) |
| K1…S3 | 3.1730(7) | K2…O1 | 2.801(2) |
| K1…O2 | 2.806(2) | K2…O1w | 2.866(2) |
| K1…O6 | 2.931(2) | K2…O2w | 2.689(2) |
| K1…O3w | 2.789(2) | K2…O3(1-x,1-y,2-z) | 2.780(2) |
| K1…O6(-x,-y,1-z) | 2.702(2) | K2…O1w(1-x,1-y,2-z) | 2.751(2) |
| **Angles** | | | |
| N1-Co1-N2 | 82.07(7) | N5-Co2-N6 | 81.61(7) |
| N1-Co1-N3 | 98.84(7) | N5-Co2-N7 | 99.60(7) |
| N1-Co1-N4 | 179.07(7) | N5-Co2-N8 | 176.77(7) |

| | | | |
|---|---|---|---|
| N1-Co1-S1 | 91.09(5) | N5-Co2-S3 | 89.92(5) |
| N1-Co1-C9 | 89.92(7) | N5-Co2-C19 | 87.29(8) |
| N2-Co1-N3 | 177.84(7) | N6-Co2-N7 | 178.63(7) |
| N2-Co1-N4 | 98.41(7) | N6-Co2-N8 | 98.14(7) |
| N2-Co1-S1 | 90.95(5) | N6-Co2-S3 | 91.16(5) |
| N2-Co1-C9 | 89.95(8) | N6-Co2-C19 | 92.76(9) |
| N3-Co1-N4 | 80.64(7) | N7-Co2-N8 | 80.61(7) |
| N3-Co1-S1 | 90.98(5) | N7-Co2-S3 | 89.48(5) |
| N3-Co1-C9 | 88.09(8) | N7-Co2-C19 | 86.68(9) |
| N4-Co1-S1 | 89.70(5) | N8-Co2-S3 | 93.30(5) |
| N4-Co1-C9 | 89.29(7) | N8-Co2-C19 | 89.51(8) |
| S1-Co1-C9 | 178.73(6) | S3-Co2-C19 | 174.82(7) |
| Co1-S1-S2 | 109.63(2) | Co2-S2-S3 | 109.11(2) |
| S1-S2-S3 | 112.49(3) | | |
| O3-H…O1 | 166(3) | O7-H…O5 | 171(3) |
| O4-H…O2 | 167(3) | O8-H…O6 | 171(4) |

## Cartesian coordinates and energies of calculated structures

**[Co(dmgH)$_2$(CH$_2$CH$_3$)(py)]**

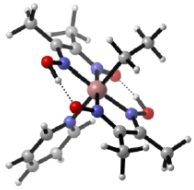

*Charge* = 0
*Multiplicity* = 1

| | | | |
|---|---|---|---|
| C | 2.627213 | -0.304535 | 0.908184 |
| C | 2.668482 | -0.540257 | -0.528392 |
| N | 1.396233 | -0.232112 | 1.378961 |
| N | 1.452372 | -0.675589 | -1.061438 |
| O | 1.288818 | -0.854085 | -2.357530 |
| O | 1.233966 | -0.029603 | 2.720153 |
| H | 0.170218 | 0.000358 | 2.804856 |
| O | -1.296535 | 0.086352 | 2.620121 |
| N | -1.455816 | -0.248137 | 1.355001 |
| C | -2.671608 | -0.396626 | 0.824582 |
| C | -2.630001 | -0.722921 | -0.594686 |
| N | -1.400604 | -0.785047 | -1.071212 |
| O | -1.240249 | -1.072673 | -2.398438 |
| H | -0.176219 | -1.046635 | -2.492215 |
| Co | -0.002270 | -0.461825 | 0.143774 |
| C | 0.149901 | 1.998266 | -1.520124 |
| C | -0.248678 | 2.439041 | 0.732694 |
| C | 0.130147 | 3.362260 | -1.831068 |
| H | 0.334360 | 1.234879 | -2.283698 |
| C | -0.282007 | 3.817691 | 0.497822 |
| H | -0.410370 | 2.018867 | 1.731319 |
| C | -0.089301 | 4.294139 | -0.806837 |
| H | 0.287266 | 3.678787 | -2.866892 |
| H | -0.458288 | 4.500620 | 1.334677 |
| H | -0.109853 | 5.368268 | -1.020605 |
| N | -0.036419 | 1.536374 | -0.257980 |
| C | -3.829936 | -0.967506 | -1.463541 |
| H | -4.765360 | -0.880515 | -0.889992 |
| H | -3.857794 | -0.248198 | -2.302187 |
| H | -3.780646 | -1.974859 | -1.915175 |
| C | -3.928488 | -0.236193 | 1.630416 |
| H | -4.523306 | -1.168692 | 1.651988 |
| H | -3.652780 | 0.026760 | 2.662959 |
| H | -4.578784 | 0.560870 | 1.223738 |
| C | 3.826465 | -0.159569 | 1.800001 |
| H | 4.763676 | -0.223422 | 1.226298 |
| H | 3.799438 | 0.806596 | 2.335496 |
| H | 3.829266 | -0.947926 | 2.574750 |
| C | 3.922881 | -0.624663 | -1.349401 |
| H | 3.643611 | -0.734334 | -2.408341 |
| H | 4.547292 | 0.281240 | -1.238295 |
| H | 4.545771 | -1.492441 | -1.060467 |
| C | -0.021589 | -2.431278 | 0.577879 |
| H | -1.053779 | -2.637213 | 0.914425 |
| H | 0.643157 | -2.562555 | 1.450163 |
| C | 0.361502 | -3.405333 | -0.533350 |
| H | 0.220775 | -4.448448 | -0.180850 |
| H | -0.261309 | -3.280079 | -1.435851 |
| H | 1.416686 | -3.306106 | -0.840826 |

*E* = -2543.51328373 a.u.
*G* = -2543.189522 a.u.
*E*(H$_2$O) = -2543.52467182 a.u.
*G*(H$_2$O) =-2543.200910 a.u.

**[Co(dmgH)$_2$(CH$_2$CH$_3$)(SH)]$^-$**

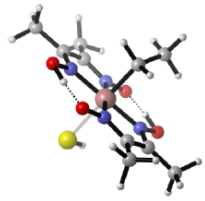

*Charge* = -1
*Multiplicity* = 1

| | | | |
|---|---|---|---|
| C | -2.670360 | 0.614820 | -0.169135 |
| C | -2.626665 | -0.833497 | -0.121841 |
| N | -1.467527 | 1.161081 | -0.193215 |
| N | -1.377467 | -1.311601 | -0.121314 |
| O | -1.154229 | -2.612740 | -0.061951 |
| O | -1.388087 | 2.524343 | -0.255620 |
| H | -0.320201 | 2.670670 | -0.220576 |
| O | 1.128234 | 2.607874 | -0.178624 |
| N | 1.348995 | 1.307711 | -0.171254 |
| C | 2.598930 | 0.829573 | -0.167459 |
| C | 2.646194 | -0.619207 | -0.154253 |
| N | 1.445891 | -1.170798 | -0.158303 |
| O | 1.367917 | -2.539360 | -0.142540 |
| H | 0.297763 | -2.680242 | -0.115804 |
| Co | -0.013030 | -0.005041 | -0.167627 |
| C | 0.035925 | -0.020745 | -2.184449 |
| H | 1.035335 | 0.367513 | -2.460470 |
| H | -0.714249 | 0.714406 | -2.533039 |
| S | -0.011999 | 0.024183 | 2.236804 |
| H | -0.157071 | -1.322340 | 2.409074 |
| C | -0.195473 | -1.366063 | -2.873625 |
| H | -0.042489 | -1.282341 | -3.972647 |
| H | 0.495613 | -2.144154 | -2.503127 |
| H | -1.220785 | -1.744940 | -2.714525 |
| C | -3.916844 | 1.453591 | -0.156185 |

| | | | |
|---|---|---|---|
| H | -4.821680 | 0.824632 | -0.130493 |
| H | -3.923544 | 2.120026 | 0.726513 |
| H | -3.963616 | 2.108755 | -1.046157 |
| C | -3.823152 | -1.737559 | -0.038763 |
| H | -3.485832 | -2.770745 | -0.220536 |
| H | -4.302046 | -1.706456 | 0.960951 |
| H | -4.597419 | -1.473918 | -0.784222 |
| C | 3.795809 | 1.736506 | -0.143039 |
| H | 4.309902 | 1.722731 | 0.838981 |
| H | 4.543606 | 1.463605 | -0.912367 |
| H | 3.447668 | 2.764995 | -0.330434 |
| C | 3.896599 | -1.450667 | -0.100908 |
| H | 3.956522 | -2.002500 | 0.856591 |
| H | 3.896846 | -2.209971 | -0.904060 |
| H | 4.798113 | -0.824151 | -0.199486 |

*E* = -2694.10034835 a.u.
*G* = -2693.855246 a.u.
*E*($H_2O$) = -2694.17925497 a.u.
*G*($H_2O$) = -2693,93415262 a.u.

**[Co(dmgH)$_2$(CH$_2$CH$_3$)(H$_2$S)]**

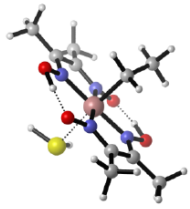

*Charge* = 0
*Multiplicity* = 1

| | | | |
|---|---|---|---|
| C | 2.677431 | -0.658877 | -0.180674 |
| C | 2.665799 | 0.791999 | -0.051617 |
| N | 1.465621 | -1.183241 | -0.231332 |
| N | 1.428989 | 1.299383 | -0.027078 |
| O | 1.222378 | 2.586294 | 0.119684 |
| O | 1.354519 | -2.543050 | -0.359542 |
| H | 0.300402 | -2.672104 | -0.289491 |
| O | -1.178736 | -2.547174 | -0.081466 |
| N | -1.386105 | -1.251186 | -0.177536 |
| C | -2.622032 | -0.743424 | -0.170525 |
| C | -2.627191 | 0.713251 | -0.169022 |
| N | -1.409949 | 1.230482 | -0.124975 |
| O | -1.285499 | 2.587833 | -0.165713 |
| H | -0.224227 | 2.710091 | -0.053668 |
| Co | 0.023586 | 0.023345 | -0.147409 |
| C | 0.106138 | 0.174592 | -2.136099 |
| H | 1.153919 | 0.451212 | -2.351521 |
| H | -0.533526 | 1.032444 | -2.408437 |
| S | 0.031826 | -0.271807 | 2.282117 |
| H | -1.185138 | 0.213263 | 2.660061 |
| H | -0.413183 | -1.562315 | 2.278893 |
| C | -3.845280 | -1.612960 | -0.135495 |
| H | -4.336815 | -1.605946 | 0.857273 |
| H | -4.596654 | -1.286406 | -0.876459 |
| H | -3.547126 | -2.649384 | -0.357557 |
| C | -3.856517 | 1.573079 | -0.221290 |
| H | -3.752705 | 2.432187 | 0.462864 |
| H | -4.000727 | 1.991005 | -1.235794 |
| H | -4.758127 | 0.999980 | 0.046059 |
| C | 3.889627 | 1.653379 | 0.064357 |
| H | 4.430095 | 1.476301 | 1.013972 |
| H | 4.600418 | 1.467220 | -0.761483 |
| H | 3.579857 | 2.709202 | 0.036407 |
| C | 3.911808 | -1.509952 | -0.250556 |
| H | 3.850861 | -2.336466 | 0.479254 |
| H | 4.007197 | -1.977237 | -1.248221 |
| H | 4.818516 | -0.918949 | -0.051221 |
| C | -0.284255 | -1.066614 | -2.929627 |
| H | 0.294361 | -1.956336 | -2.627870 |
| H | -1.355553 | -1.311659 | -2.830883 |
| H | -0.085537 | -0.894935 | -4.007976 |

*E* = -2694.61404193 a.u.
*G* = -2694.358957 a.u.
*E*($H_2O$) = -2694.62608577 a.u.
*G*($H_2O$) = -2694,37100084 a.u.

**[Co(dmgH)$_2$(CH$_2$CH$_3$)(H$_2$O)]**

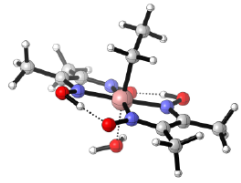

*Charge* = 0
*Multiplicity* = 1

| | | | |
|---|---|---|---|
| C | -2.66410300 | -0.64987000 | -0.05738000 |
| C | -2.66629200 | 0.80698800 | -0.13546800 |
| N | -1.44971900 | -1.16071500 | -0.00069600 |
| N | -1.43705000 | 1.32579300 | -0.13482200 |
| O | -1.24053000 | 2.61781800 | -0.24384000 |
| O | -1.31400600 | -2.52611500 | 0.08429200 |
| H | -0.29703900 | -2.63861200 | -0.14956500 |
| O | 1.16616400 | -2.41106400 | -0.62416700 |
| N | 1.40457900 | -1.17443100 | -0.20340500 |
| C | 2.63335800 | -0.65780200 | -0.21934400 |
| C | 2.62093400 | 0.78932400 | -0.03591500 |
| N | 1.39244200 | 1.28826200 | -0.03919300 |
| O | 1.24763700 | 2.62808400 | 0.15007400 |
| H | 0.18486600 | 2.74994000 | 0.00134100 |
| Co | -0.02446200 | 0.06639400 | -0.05815000 |
| C | -0.08646800 | 0.17727200 | 1.92209000 |
| H | 0.45024000 | 1.09959000 | 2.20764800 |
| H | -1.15431400 | 0.31702600 | 2.17015700 |

| | | | |
|---|---|---|---|
| O | -0.05390700 | -0.29422400 | -2.18138200 |
| H | 0.67414300 | 0.21018800 | -2.60433300 |
| H | 0.28135900 | -1.22910300 | -2.12923100 |
| C | 3.85362100 | -1.48328900 | -0.50782000 |
| H | 4.31020600 | -1.22554000 | -1.48308000 |
| H | 4.63087100 | -1.34213300 | 0.26512900 |
| H | 3.56327200 | -2.54487000 | -0.53492800 |
| C | 3.83264400 | 1.66036000 | 0.11545500 |
| H | 3.75155700 | 2.55018400 | -0.53251400 |
| H | 3.91671600 | 2.03345900 | 1.15377700 |
| H | 4.75489800 | 1.11185800 | -0.13154700 |
| C | -3.89641400 | 1.66026200 | -0.23658500 |
| H | -4.33067600 | 1.63976800 | -1.25524400 |
| H | -4.68050300 | 1.32851600 | 0.46677100 |
| H | -3.62385000 | 2.70274500 | -0.00945300 |
| C | -3.89886700 | -1.50298700 | -0.04413400 |
| H | -3.70335300 | -2.45380400 | -0.56619300 |
| H | -4.19588800 | -1.75508200 | 0.99180300 |
| H | -4.74510500 | -0.98644800 | -0.52425200 |
| C | 0.47328400 | -1.03189800 | 2.66290700 |
| H | -0.01915000 | -1.97066000 | 2.35489300 |
| H | 1.55956400 | -1.15227400 | 2.50863200 |
| H | 0.30782900 | -0.91590600 | 3.75438000 |

*E* = -2371.62811861 a.u.
*G* = -2371.64120687 a.u.
*E*($H_2O$) = -2371.364008 a.u.
*G*($H_2O$) = -2371.377096 a.u.

**Pyridine**

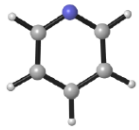

*Charge* = 0
*Multiplicity* = 1

| | | | |
|---|---|---|---|
| C | -3.550078 | -1.224570 | 0.000030 |
| C | -2.145571 | -1.230836 | -0.000067 |
| C | -1.473096 | 0.000074 | -0.000270 |
| C | -2.233468 | 1.178705 | -0.000402 |
| C | -3.633784 | 1.070102 | -0.000323 |
| N | -4.299594 | -0.103053 | -0.000085 |
| H | -0.377824 | 0.040012 | -0.000359 |
| H | -4.108106 | -2.170912 | 0.000184 |
| H | -1.596174 | -2.178520 | 0.000037 |
| H | -1.754619 | 2.163921 | -0.000554 |
| H | -4.259290 | 1.973259 | -0.000379 |

*E* = -248.28027283 a.u.
*G* = -248.221476 a.u.
*E*($H_2O$)= -248.28505789 a.u.
*G*($H_2O$) = -248.22626106 a.u.

**$HS^-$**

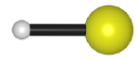

*Charge* = -1
*Multiplicity* = 1

| | | | |
|---|---|---|---|
| S | 0.000000 | 0.000000 | 0.080753 |
| H | 0.000000 | 0.000000 | -1.292049 |

*E* = -398.83041162 a.u.
*G* = -398.842571 a.u.
*E*($H_2O$) = -398.94551057 a.u.
*G*($H_2O$) = -398.95766995 a.u.

**$H_2S$**

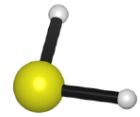

*Charge* = 0
*Multiplicity* = 1

| | | | |
|---|---|---|---|
| S | 0.000000 | 0.000000 | 0.104757 |
| H | 0.000000 | 0.980167 | -0.838057 |
| H | 0.000000 | -0.980167 | -0.838057 |

*E* = -399.40827076 a.u.
*G* = - 399.413118 a.u.
*E*($H_2O$)= -399.41236246 a.u.
*G*($H_2O$) = -399.41720970 a.u.

**$H_2O$**

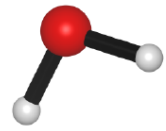

*Charge* = 0
*Multiplicity* = 1

| | | | |
|---|---|---|---|
| O | 0.509291 | -0.181246 | 0.000000 |
| H | 1.485301 | -0.125690 | 0.000000 |
| H | 0.235862 | 0.757326 | 0.000000 |

*E* = -76.40919764 a.u.
*G* = -76.41646378 a.u.
*E*($H_2O$)= -76.406309 a.u.
*G*($H_2O$) = -76.413575 a.u.

## 6.3. Porphyrin

### 6.3.1. *Synthesis of CuPPIX*

Protoporphyrin IX (0.5 g, 0.89 mmol) in glacial acetic acid (300 mL) was boiled gently with copper(II) acetate (1.5 g, 8.9 mmol). The solution was stirred at reflux for 4 h and then overnight at ambient temperature. After conversion to the $Cu^{II}$–protoporphyrin is complete, as indicated by the absence of free base absorption bands in a visual spectrum, the solution is transferred to a separating funnel with about 400 mL of benzene. Water is added to the separating funnel, and the resulting benzene layer is washed several times with water to completely remove the reaction solvent and inorganic salts. The resulting benzene solution is evaporated to dryness under vacuum to yield the purple-brown solid, yield 84%. $C_{34}H_{32}CuN_4O_4$ (624.20): calcd. C 65.42, H 5.17, N 8.98; found C 65.52, H 5.22, N 8.78. MS (ESI acetonitrile): *m*/*z* (%) = 663.1 (100) $[CuPPIX\text{-}K]^+$, 647.2 (80) $[CuPPIX\text{-}Na]^+$, 623.7 (50) $[CuPPIX]^+$.

Quantum yield, $\Phi_F$ ($H_2O$, $\lambda_{exc}$ = 386 nm): $9.5 \cdot 10^{-4}$.

### 6.3.2. *Fluorescence Quantum Yield*

The fluorescence quantum yield ($\Phi$F) value was measured in optically diluted solutions using phenol ($\Phi$F = 0.014 in MilliQ water) as the standard, according to the equation shown below.

$$\Phi_F = \Phi_{F(Std)} (F \cdot A_{Std} \cdot n^2 / F_{Std} \cdot A \cdot n_{Std}^2)$$

Index Std denote the reference. F stands for the integrated emission intensity, A is the absorbance at the excitation wavelength, and n is the refractive index of the solvent.

### 6.3.3. *Polysulfides Determination*

CuPPIX (0.006 g; 0.01 mmol) and KSH (0.014 g; 0.2 mmol) were dissolved in $D_2O$ (1 mL) under aerobic conditions at room temperature and NaOH (0.064 g; 1.6 mmol) was added. The reaction was left whilst stirring for 30 min. Subsequently $(CH_3O)_2SO_2$ (76 μL; 0.8 mmol) dissolved in $CDCl_3$ (500 μL) was added. The reaction mixture was stirred for another 90 min. The organic phase was then separated and collected in a NMR tube to record the NMR spectrum. As a control, a sample without CuPPIX was prepared for each experiment, using the same quantities as specified above.

## 6.4. Azurin

### 6.4.1. *Preparation of Azurin Metalloderivatives*

Copper was removed from the oxidized holoprotein by several steps.[14] First, reducing a 800 μL ($4.4 \cdot 10^{-4}$ M) azurin sample at 20 °C against 1 mL of a 20 mM TRIS/HCl solution (pH 8.3) with a slight excess (5 μL) of 0.1 M sodium dithionite solution in 0.1 M NaOH (5 μL), for reducing copper. Then, was performed the dialysis the resulting colorless solution overnight at 4°C against 0.1 M KCN in 0.15 M TRIS/HCl buffer, pH 8.3. The excess of KCN was removed by a 4-h dialysis against 50 mM TRIS/HCl buffer, at room

[14] C. M. Hutnik, A. G. Szabo, *Biochemistry* **1989**, *28*, 3923.

temperature. The last dialysis is done against 50 mM ammonium acetate buffer, pH 6.1, at 4°C. The obtical absorption at 628 nm was monitored to confirm the absence of residual copper. The nickel(II) and cobalt(II) metalloderivatives were prepared adding 5 equiv. of $MCl_2 \cdot 6H_2O$ to the apo-protein stock in 50 mM ammonium acetate buffer, pH 6.1 at room temperature for one day. The excess of metal was removed dialyzing overnight against 25 mM TRIS/HCl buffer, pH 8.3. Then, was performed a dialysis against 100 mM KPi buffer, pH 6.8. These solutions were then equilibrated at room temperature and monitored by absorption and fluorescence spectroscopy for reconstitution after various times. The concentrations of the azurin metalloderivatives were measured spectrophotometrically, using the extinction coefficients $\varepsilon_{440} = 3.3 \times 10^3\ M^{-1}\ cm^{-1}$ for Ni(II)-azurin and $\varepsilon_{650} = 1.7 \cdot 10^4\ M^{-1}\ cm^{-1}$ for Co(II)-azurin.[15]

### 6.4.2. *Fluorescent Labeling of Proteins and Chromatography of Labeled Species*

Proteins labeling was performed using a modified version of a already known protocol.[16] 8 For amino labelling, proteins was incubated with 0.5 equiv. of the NHS-ester of the fluorescent label in 20 mM HEPES buffer, pH 8.3 for 120 min. The unreacted label was removed using a PD-10 Desalting Columns contain Sephadex G-25 Medium (GE Healthcare). Labelling ratios were in the range 0.12-

[15] D. L. Tennent, D. R. McMillin, *J. Am. Chem. Soc.* **1979**, *101*, 2307.
[16] S. Kuznetsova, G. Zauner, R. Schmauder, O. A. Mayboroda, A. M. Deelder, T. J. Aartsma, G. W. Canters, *Anal. Biochem.* **2006**, *350*, 52.

0.83 (dye molecule/protein), as determined from the absorption spectra of the labelled proteins.

### 6.4.3. *Control Experiments*

Control experiments has been taken and no significant changes in the fluorescence intensity were observed when monitoring the labelled proteins in the absence of KSH. Neither KSH addition to the free fluorescent dyes Atto620 and Alexa350 show any effect.

## 6.5. Cyclam

### 6.5.1. *Synthesis of Derivate **6***

1,-(2,6-Pyridinedimethylene)-4(2-*N*-pyren-1-yl-acetamide)-1,4,8,11-tetraazacyclotetradecane (**6**). 1,8-(2,6-Pyridinedimethylene)-1,4,8,11-tetraazacyclotetradecane (0.300g, 0.99 mmol) was dissolved in MeCN (170 mL). $K_2CO_3$ (0.205 g, 1.48 mmol) and **3** (0.130 g, 0.44 mmol) were added to the solution, and the reaction mixture was stirred at 60°C for one week. Subsequently, the solid components were filtered off, and the solvent was partially removed *in vacuo*. The crude product was subjected to flash chromatography on silica gel ($CH_2Cl_2$/MeOH, 90/10, *v/v*), to give derivative **6** as a yellow solid (0.081 g, 29%). **ESI-MS$^+$**: *m*/*z* = 561 ($MH^+$); **$^1$H NMR** ($CD_3OD$, 600 MHz, 298 K, ppm): 8.26-8.03 (m, 9H, $(ArH)_{pyrene}$), 7.68 (t, 1H, $(H_\gamma)_{Pyridine}$), 7.14 (dd, 2H, $(H_\beta)_{Pyridine}$), 4.01 and 3.68 [AX, ($ArCH_2N$), 2H], 3.78 and 3.61 [AX, ($ArCH_2N$), 2H], 3.53 and 3.45 [AX, -$C(O)CH_2N$-, 2H], 3.09 (m, 4H, -$CH_2N$-), 2.96 (m, 1H, -$CH_2N$-) 2.88 (m, 2H, -$CH_2N$-), 2.76 (m, 3H, -$CH_2N$-), 2.56 (m, 2H, -$CH_2N$-), 2.42 (m, 2H, -$CH_2N$-), 2.20 (m, 1H, -$CH_2N$-), 2.03 (m, 1H, $CH_2$), 1.94 (m,

1H, $CH_2$), 1.76 (m, 1H, $CH_2$), 1.44 (m, 1H, $CH_2$). $^{13}C$ NMR ($CD_3OD$, 150 MHz, 298 K, ppm): 162.0, 150.0, 149.0, 129.2, 123.6, 123.3, 122.5, 120.5, 120.0, 119.7, 119.1, 119.0, 118.5, 118.4, 118.1, 118.0, 117.8, 117.4, 116.9, 114.6, 113.8, 113.7, 63.2, 59.5, 58.2, 57.6, 56.6, 55.6, 55.0, 54.4, 50.4, 49.8, 49.0, 29.8, 28.6. Anal. Calcd for $C_{35}H_{40}N_6O$: C, 74.97; H, 7.19; N, 14.99; O, 2.85. Found: C, 74.83; H, 7.23; N, 14.93; O, 2.91.

### 6.5.2. *Synthesis of Complex **7***

Derivate **6** (0.081 g, 0.14 mmol) was dissolved in 40 mL of MeOH and one equiv. of $CuSO_4 \cdot 5H_2O$ (0.036 g, 0.14 mmol) was added at room temperature. The yellow solution turned blue-green and it was left stirring overnight. After filtration and evaporation of the solvent to dryness, the compound was obtained as a dark green solid in 70% yield (0.070 g, 0.097 mmol). **ESI-MS$^+$**: *m*/*z* = 623 (M - $SO_4^{2-}$ - $H^+$); Anal. calcd for $C_{35}H_{40}CuN_6O_5S$: C, 58.36; H, 5.60; Cu, 8.82; N, 11.67; O, 11.11; S, 4.45. Found: C, 58.93; H, 5.37; Cu, 8.20; N, 11.42; O, 10.73; S, 4.64.

## 6.6. Reference List

1. (*a*) P. J. Toscano, L. G. Marzilli, *Prog. Inorg. Chem.* **1984**, *31*, 105. (*b*) N. Bresciani-Pahor, M. Forcolin, L. G. Marzilli, L. Randaccio, M. F. Summers, P. J. Toscano, *Coord. Chem. Rev.* **1985**, *63*, 1.J. R. Reiffenstein, W. C. Hulbert, S. H. Roth, *Annu. Rev. Pharmacol. Toxicol.* **1992**, *32*, 109.

2. M. Vandekamp, F. C. Hali, N. Rosato, A. F. Agro, G. W. Canters, *Biochim. Biophys. Acta* **1990**, *1019*, 283.

3. M. Frisch, G. W. Trucks, H. B. Schlegel, G. E. Scuseria, M. A. Robb, J. R. Cheeseman, G. Scalmani, V. Barone, B. Mennucci, G. A. Petersson, H. Nakatsuji, M. Caricato, X. Li, H. P. Hratchian, A. F. Izmaylov, J. Bloino, G. Zheng, J. L. Sonnenberg, M. Hada, M. Ehara, K. Toyota, R. Fukuda, J. Hasegawa, M. Ishida, T. Nakajima, Y. Honda, O. Kitao, H. Nakai, T. Vreven, J. A. Montgomery Jr., J. E. Peralta, F. Ogliaro, M. Berpark, J. J. Heyd, E. Brothers, K. N. Kudin, V. N. Staroverov, R. Kobayashi, J. Normand, K. Raghavachari, A. Rendell, J. C. Burant, S. S. Iyengar, J. Tomasi, M. Cossi, N. Rega, J. M. Millam, M. Klene, J. E. Knox, J. B. Cross, V. Bakken, C. Adamo, J. Jaramillo, R. Gomperts, R. E. Stratmann, O. Yazyev, A. J. Austin, R. Cammi, C. Pomelli, J. W. Ochterski, R. L. Martin, K. Morokuma, V. G. Zakrzewski, G. A. Voth, P. Salvador, J. J. Dannenberg, S. Dapprich, A. D. Daniels, O. Farkas, J. B. Foresman, J. V. Ortiz, J. Cioslowski, D. J. Fox, *Gaussian 09, revision A.02*, Gaussian, Inc., Wallingford, CT, **2009**.

4. A. D. Becke, *Phys. Rev. A: At., Mol., Opt. Phys.* **1988**, *38*, 3098.

5. (*a*) J. P. Perdew, *Phys. Rev. B: Condens. Matter, Mater. Phys.* **1986**, *33*, 8822; (*b*) J. P. Perdew, *Phys. Rev. B: Condens. Matter Mater. Phys.* **1986**, *34*, 7406.

6. J. Tomasi, B. Mennucci, R. Cammi, *Chem. Rev.* **2005**, *105*, 2999.

7. The solvent-corrected Gibbs free energies = gas-phase Gibbs free enrgies + (solvent-phase electronic energies – gas-phase electronic energies).

8. Z. Otwinowski, W. Minor, in *Methods in Enzymology, Part A*, ed. C. W. Carter and R. M. Sweet, Academic Press, London, **1997**, *276*, 307.

9. R. H. Blessing, *Acta Crystallogr., Sect. A: Found. Crystallogr.* **1995**, *51*, 33.

10. A. Altomare, M. C. Burla, M. Camalli, G. L. Cascarano, C. Giacovazzo, A. Guagliardi, A. G. Moliterni, G. Polidori, R. Spagna, *J. Appl. Crystallogr.* **1999**, *32*, 115.

11. G. M. Sheldrick, SHELX-97, *Program for Crystal Structure Refinement*, University of Gottingen, Germany, **1997**.

12. M. Nardelli, *J. Appl. Crystallogr.* **1995**, *28*, 659.

13. L. J. Farrugia, *J. Appl. Crystallogr.* **1999**, *32*, 837.

14. C. M. Hutnik, A. G. Szabo, *Biochemistry* **1989**, *28*, 3923.

15. D. L. Tennent, D. R. McMillin, *J. Am. Chem. Soc.* **1979**, *101*, 2307.

16. S. Kuznetsova, G. Zauner, R. Schmauder, O. A. Mayboroda, A. M. Deelder, T. J. Aartsma, G. W. Canters, *Anal. Biochem.* **2006**, *350*, 52.